Characterization of

Aberrant c-Myc Phosphorylation and Stability

in Acute Myeloid and Lymphoblastic Leukemia

by Deanne Carol Tibbitts

A DISSERTATION

Presented to the Department of Molecular and Medical Genetics

and Oregon Health and Science University

School of Medicine

in partial fulfillment of the requirement for the degree of

Doctor of Philosophy

Approved by the Oral Examination Committee

September 2011

School of Medicine
Oregon Health & Science University

CERTIFICATE OF APPROVAL

This is to certify that the Ph.D. dissertation of

Deanne Tibbitts

has been approved

Chair: Phillip Stork, M.D.

Member: Rosalie Sears, Ph.D.

Member: Matt Thayer, Ph.D.

Member: Grover Bagby, M.D.

Member: Peter Kurre, M.D.

Member: R. Michael Liskay, Ph.D.

Table of contents

Table of contents

List of figures

List of tables

List of abbreviations

AKT	v-akt murine thymoma viral oncogene homolog
ALL	acute lymphoblastic leukemia
AML	acute myeloid leukemia
B ALL	B cell acute lymphoblastic leukemia
B-Myc	brain Myc
CIP2A	cancerous inhibitor of PP2A
CDK	cyclin-dependent kinase
DAPI	4',6-diamidino-2-phenylindole
dMyc	*Drosophila* Myc
DNA	deoxyribonucleic acid
DTT	dithiothreitol
EBV	Epstein Barr Virus
ERK	Extracellular signal-regulated kinase
FBS	fetal bovine serum
Fbw7	F-box and WD repeat domain containing 7
FISH	fluorescence in situ hybridization
FLT3	FMS-like tyrosine kinase 3
FLT3-ITD	FLT3 internal tandem duplication
GFP	green fluorescent protein
GSK3	glycogen synthase kinase 3
H-RAS	v-Ha-ras Harvey rat sarcoma viral oncogene homolog

IDH1/2   isocitrate dehydrogenase 1/2

IP   immunoprecipitation

JNK   c-Jun kinase

K-RAS   v-Ki-ras2 Kirsten rat sarcoma viral oncogene homolog

L-Myc   v-myc avian myelocytomatosis viral oncogene

         homolog 1, lung carcinoma-derived

LSK $Lin^-/Sca1^+/c\text{-}Kit^+$

MAPK   mitogen-activated protein kinase

MBI   Myc homology box I

MBII   Myc homology box II

miRNA   microRNA

mRNA   messenger RNA

MYC   v-myc myelocytomatosis viral oncogene homolog

         (avian)

NBM   normal bone marrow

N-Myc   v-myc avian myelocytomatosis viral-related

         oncogene, neuroblastoma-derived

NPM1   nucleophosmin 1

N-RAS   neuroblastoma RAS viral oncogene homolog

P57   proline 57

PBMC   peripheral blood mononuclear cells

PBS   phosphate buffered saline

PCR   polymerase chain reaction

PI3K	phosphoinositide-3-kinase
PMN	polymorphonuclear cells
Pol	polymerase
PP2A	protein phosphatase 2A
pS62	phosphoserine 62
pT58	phosphothreonine 58
qPCR	quantitative PCR
RAS	rat sarcoma
RBC	red blood cell
RNA	ribonucleic acid
RPMI	Roswell Park Memorial Institute
rRNA	ribosomal RNA
RT-PCR	reverse transcription PCR
S62	serine 62
SB	sample buffer
SCF	Skp1/Cul1/F-box protein
SET	SET nuclear oncogene
T58	threonine 58
T ALL	T cell Acute Lymphoblastic Leukemia
TET	tetracycline
tRNA	transfer RNA
tTa	tetracycline-transactivator
UTR	untranslated region

Acknowledgments

The road to finishing my PhD has not been without its ups and downs, and I have many people I would like to thank. First, I give my heartfelt appreciation to my mentor, Dr. Rosalie Sears. During my tenure in her lab, she has been supportive beyond my expectations, and I am truly grateful to have trained under such a dedicated, enthusiastic, and gifted scientist. Her love for what she does is both palpable and infectious. Rosie, thank you for all you have done for me.

I would like to thank the members of my thesis advisory committee, Drs. Grover Bagby, Peter Kurre, Phil Stork, and Matt Thayer. Their guidance through this process has been invaluable, and I thank them for the time spent reading and critiquing this dissertation. I also thank Dr. Mike Liskay for serving on my oral examination committee.

I extend a multitude of thanks to the many members of the Sears lab, both current and former, who have been a joy to work with over these last several years. Special thanks go to Drs. Hugh Arnold, Sarah Byers, Julie Escamilla-Powers, and Xiaoli Zhang, as well as Karyn Taylor and Colin Daniel for extensive technical and emotional support. Additional thanks for technical support go to Arun Kumar Krishnamoorthy and Xiaoyan Wang in the Sears lab and to Keaney Rathbun and Winifred Keeble in the Bagby lab. Likewise, thanks go out to the many friends at OHSU who have both encouraged me and consoled me during this process, specifically Dr. Brenda Polster, Dr. Jayme Gallegos, Dr. Chantelle

Rein, Dr. Brenda Marsh, Dr. Eric Stoffregen, Dr. Jodi Johnson, Dr. Ashleigh Miller, and the future Dr. Katy Van Hook, as well as outside friends, specifically my oldest and dearest friend Anika Mahoney and fellow grad student-in-the-trenches Sara Anderson. I also thank all of my parents for their love and support.

I would like to thank the administrative staff of the Molecular and Medical Genetics Department – Glenda Benton, Autumn Linde, Marisa Crowe, Shawna Rinne, and Anne Huntzicker – for their assistance with grant applications, graduation requirements, and all other administrative matters. Their help has been greatly appreciated.

I would like to thank our internal and external collaborators for providing mouse strains, cell lines, patient material, or other reagents: Dr. Harv Fleming, OHSU; Dr. Guang Fan, OHSU; Dr. Anupriya Agarwal, OHSU; Dr. Dean Felsher, Stanford University; Dr. Frank Costantini, Columbia University; Dr. Thomas Look, Dana Farber Cancer Institute; Dr. Lawrence Lum, UT Southwestern. Additional thanks go to Dr. Chantelle Rein and Kristine Alexander in the Farrell lab for expertly performing phlebotomy so I could have normal blood samples for this work.

I must extend a special thanks to my classmates – of the inimitable PMCB Class of 2004 – who have stood alongside me on this journey. From classes to quals to crises of confidence and from funding to first papers to defending, we have been

there for each other – crying, cheering, encouraging, laughing, listening. As difficult as this process has been, it would've been unbearable if not for the unwavering support of my classmates, colleagues, and dear friends: Drs. Abhinav Sinha, Damian Curtis, Chang Liu, Kristin Diez Sauter, Paul Wille, and Tom Keck, and especially my girls – Drs. Christina Lorentz, Bridget Robinson, Annie Powell, Kirsten Blensly Verhein, and Carole Kuehl. I wouldn't trade our time together for anything.

Finally to my husband Jonathan, who has been amazing not only through our many years together, but especially during this PhD experience – for enduring my innumerable late nights in lab, emotional turmoil, and mental exhaustion, and for providing open arms, patient attention, and wise words, you have my gratitude forever.

Abstract

c-Myc is a pleiotropic transcription factor that regulates hematopoiesis, and high levels of c-Myc are frequently found in human leukemia. c-Myc protein levels are controlled in part by the phosphorylation of two N-terminal residues, serine 62 (S62) and threonine 58 (T58), and phosphorylation of these residues controls c-Myc protein stability. Based on these findings, I hypothesized that increased c-Myc protein stability is partly responsible for high c-Myc levels in leukemia. In this dissertation, I describe the discovery of increased c-Myc protein stability in both lymphoid and myeloid leukemia coupled to altered phosphorylation of c-Myc at S62 and T58. In addition, I have found that this altered protein stability and phosphorylation can occur through multiple mechanisms, including the constitutive activation of upstream signaling pathways and the deregulation of proteins that promote c-Myc degradation. Lastly, I investigated the effects of overexpressing one of these proteins, AXIN1, in a mouse model of c-Myc-driven lymphoma to determine whether promoting c-Myc degradation could delay the onset of tumor development and to provide a proof of principle to support the idea that promoting c-Myc degradation could be an effective cancer therapy. Together, these results establish aberrant stabilization and phosphorylation of c-Myc as a common mechanism underlying high c-Myc levels in myeloid and lymphoblastic leukemia and may provide new avenues for targeting c-Myc in cancer through the modulation of pathways that control its stability.

Chapter 1. Background

c-Myc structure and function

c-Myc is the founding member of the Myc family of transcription factors that includes N-Myc, L-Myc, and B-Myc. c-Myc was originally identified as the cellular homolog of the viral oncogene *v-myc* (Vennstrom et al, 1982) and is both ubiquitously expressed and highly conserved. c-Myc is widely expressed during development and in proliferating tissues in adult organisms (Downs et al, 1989; Malynn et al, 2000; Stanton et al, 1992). c-Myc is also highly conserved between humans and lower organisms, and much of c-Myc's structure is shared across Myc family members. This conservation is both structural and functional, as *Drosophila* Myc (dMyc) is able to functionally substitute for c-Myc in murine fibroblasts (Trumpp et al, 2001) and human c-Myc can rescue lethal *dmyc* mutations in *Drosophila* (Benassayag et al, 2005).

Like many transcription factors, the structure of c-Myc can be divided into two main components, a C-terminal DNA binding domain and an N-terminal transactivation domain (Figure 1.1). The DNA binding domain of c-Myc contains a basic region that directly facilitates DNA binding and a helix-loop-helix/leucine zipper (HLH/LZ) domain that is required for heterodimerization with the small HLH/LZ protein Max (Meyer & Penn, 2008). The transactivation domain contains two elements, termed Myc Homology Box I and II (MBI and MBII), that are highly conserved between Myc family members and across a wide range of species (Sarid et al, 1987). MBI is important for post-translational regulation of c-Myc,

while MBII is important for the recruitment of cofactors to c-Myc. Both MBI and

MBII are essential for c-Myc's transforming activity (Sarid et al, 1987).
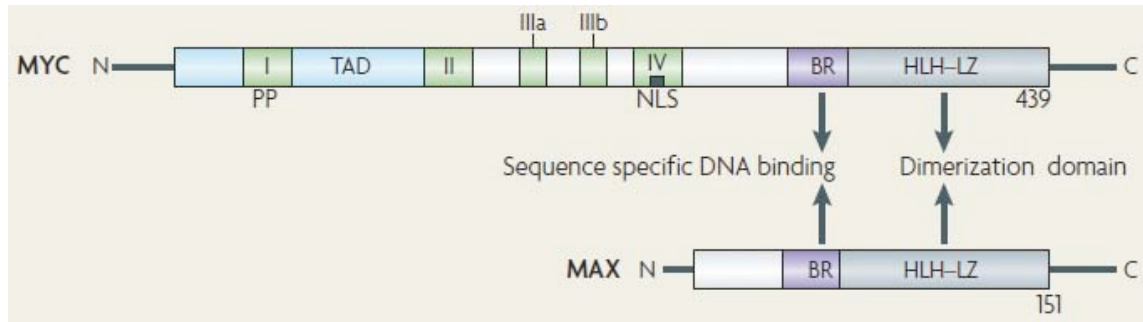
Figure 1.1. Structure of the c-Myc protein and its dimerization partner Max.

Domains of c-Myc and Max are denoted by color: transactivation domain (TAD), blue; basic region (BR), purple; helix-loop-helix/leucine zipper (HLH-LZ), grey. Myc homology boxes (MB) I-IV are shown in green. (From Meyer and Penn, 2008; used with permission.)

Initial investigation of c-Myc transcriptional activity revealed that dimerization with Max was required for c-Myc to transactivate genes. c-Myc:Max heterodimers directly bind to specific DNA elements called E-boxes, with the canonical sequence CACGTG, which are typically found in the promoters of c-Myc transactivated genes (Blackwell et al, 1990; Blackwood & Eisenman, 1991) (Figure 1.2A). When bound to E-boxes, c-Myc recruits histone acetyltransferases such as TIP60, GCN5, and TRRAP, and these acetylate histone H3 and H4, promoting an open chromatin conformation (Bouchard et al, 2001; Frank et al, 2003; Frank et al, 2001; McMahon et al, 2000). Transactivation of c-Myc target genes is opposed by the Mxd (formerly Mad) family of repressor proteins, which compete with c-Myc for binding to Max (Ayer et al, 1993). The Mxd family includes Mxd1-4, Mnt, and Mga (Hurlin & Huang, 2006), and these proteins require dimerization with Max in order to bind DNA (Ayer et al, 1993). Like c-Myc:Max heterodimers, Mxd:Max heterodimers also bind to E-boxes but instead repress transcription by recruiting co-repressors and histone deacetylases (Ayer et al, 1995; Li et al, 2002; Schreiber-Agus et al, 1995) (Figure 1.2B). Mxd family members generally have opposite expression patterns from c-Myc and are highly expressed in differentiated cell types (Ayer & Eisenman, 1993; Larsson et al, 1994).

c-Myc can also function as a transcriptional repressor when bound to Max. However, this function is poorly characterized and probably occurs through multiple distinct mechanisms. The best-characterized mechanism is the

interaction of the c-Myc:Max heterodimer with the transcription factor Miz1.

These three proteins form a ternary complex that results in the repression of the

Miz1 target genes *p15INK4b* and *p21CIP1* (Peukert et al, 1997; Seoane et al,

2001; Staller et al, 2001; Wu et al, 2003) (Figure1.2C). Though c-Myc:Max and

Miz1 form a ternary complex, repression of Miz1 target genes does not require

direct binding of c-Myc:Max to DNA (Wu et al, 2003). Other genes, such as

GADD45, are also repressed by c-Myc (Marhin et al, 1997), but the mechanism

is unknown.

While c-Myc:Max heterodimer formation is required for many of c-Myc's

transcriptional functions, it is not required for all of c-Myc's transcriptional

functions. c-Myc regulates the transcription of both rRNA precursors transcribed

by RNA Polymerase I (Pol I) (Grandori et al, 2005) and many protein-coding

genes transcribed by RNA Pol II, but c-Myc also regulates the transcription of

tRNA and rRNA genes transcribed by RNA Pol III, and this activity is E-box-

independent (Gomez-Roman et al, 2003) (Figure 1.2D). In addition, dMyc can

induce Pol III targets in *max*-null flies, supporting the idea that Max and E-box

binding are not required for all of Myc's transcriptional functions (Steiger et al,

2008). This is further supported by the milder phenotype of *max*-null flies when

compared to *dmyc*-null flies (Steiger et al, 2008).
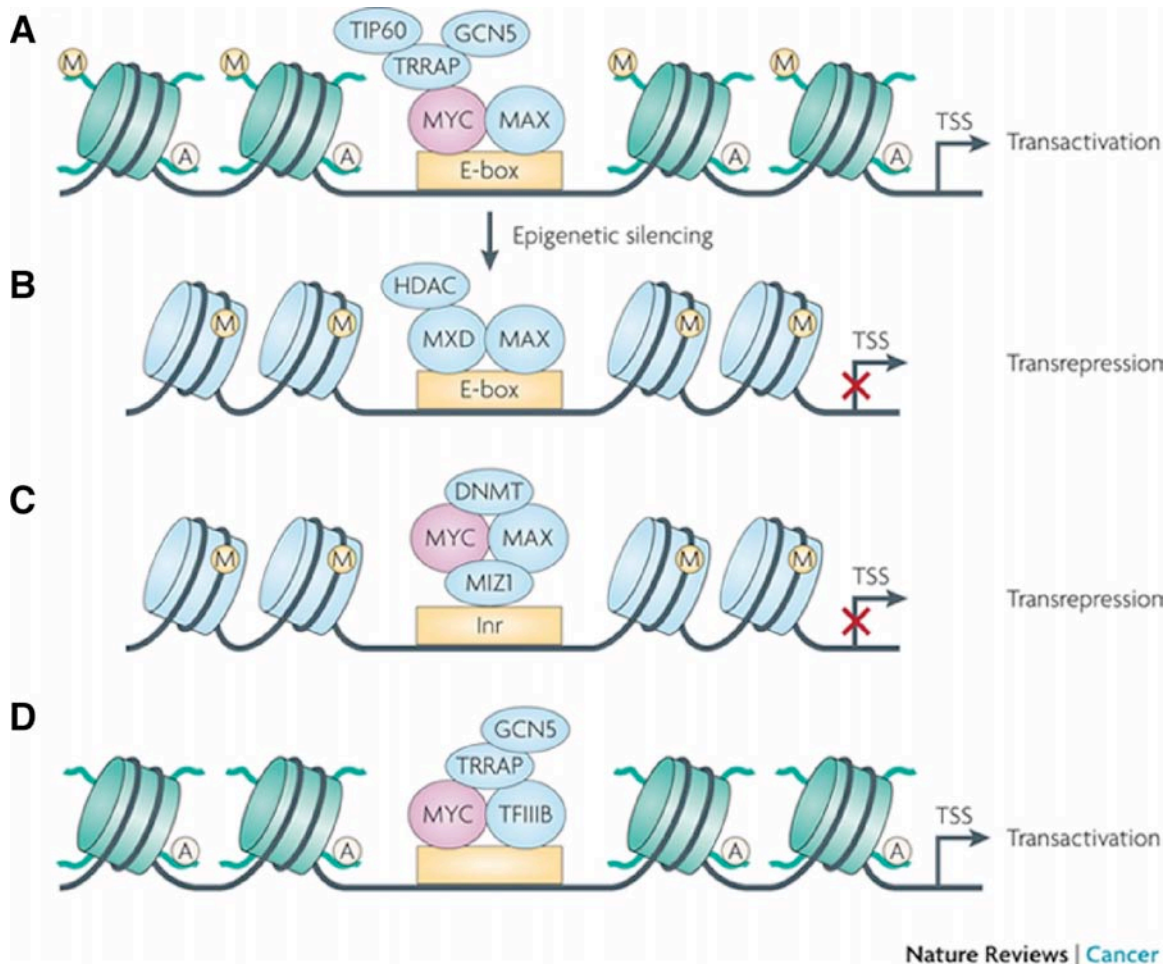
Figure 1.2. Gene regulation by c-Myc.

A. c-Myc activates transcription though dimerization with Max, E-box binding, and the recruitment of histone acetyltransferases (TIP60, GCN5, TRRAP). **B.** Mxd family members repress transcription through dimerization with Max, E-box binding, and recruitment of histone deacetylases (HDAC). **C.** c-Myc can repress transcription through a ternary complex with Max and Miz1 that recruits DNA methyltransferases (DNMT). **D.** c-Myc can activate transcription of Pol III target genes by binding to TFIIIB and recruiting histone acetyltransferases. Transactivation of Pol III target genes is independent of c-Myc binding to Max. (From van Riggelen and Felsher, 2010; used with permission.)

Though many c-Myc target genes have been characterized one at a time, we now know through genome-wide DNA binding studies that c-Myc binds to 10-15% of genes (Fernandez et al, 2003; Li et al, 2003; Orian et al, 2003; Zeller et al, 2006). As expected, the majority of these binding sites contain canonical or non-canonical E-boxes, but many of these sites do not contain any E-boxes and do not appear to coincide with Max binding (Orian et al, 2003; Zeller et al, 2006). Besides the Max-independent functions described above, some of these binding sites may represent replication origins, as c-Myc has been shown to promote DNA replication independent of both Max-binding and transcriptional activity (Dominguez-Sola et al, 2007; Gusse et al, 1989). Clearly, c-Myc's activity is more complex than previously thought and remains to be fully understood.

c-Myc controls many cellular processes

If c-Myc functions primarily as a transcription factor, then one would assume that understanding the impact of c-Myc expression would be as simple as defining its target genes. However, c-Myc target genes are numerous and span many functional categories. Some of these functions, like cell cycle progression, apply to a wide variety of cell types, while others, like differentiation, may be apparent only in specific cellular contexts. Below, I will highlight a selection of c-Myc functions that are relevant for this dissertation.

Cell cycle

One of the best-characterized effects of c-Myc expression is its ability to promote cell cycle entry. As an immediate early gene, c-Myc expression is induced downstream of growth stimulation. c-Myc then acts to promote the G1/S transition through the transcriptional upregulation of major cell cycle regulators, including cyclin D2 (Bouchard et al, 2001), cyclin E (Perez-Roger et al, 1997), CDK4 (Hermeking et al, 2000), and E2F1, 2, and 3a (Adams et al, 2000; Leone et al, 1997; Sears et al, 1997), and repression of cell cycle inhibitors like p15 and p21 (Staller et al, 2001; Wu et al, 2003). Phenotypically, ectopic expression of *Myc* in quiescent cells can induce cell cycle entry and progression (Eilers et al, 1991), and *Myc*-null cells have a greatly prolonged cell cycle (Mateyak et al, 1997). Interestingly, a genetic screen for genes that could rescue the "slow growth" phenotype of *Myc*-null cells only revealed *myc* family members, demonstrating the inability of a single *Myc* target gene to substitute for *Myc* expression (Berns et al, 2000).

Cell growth

An increase in cell mass ("cell growth") is intrinsically coupled to cell cycle progression, and ribosome biogenesis is the cornerstone of this process. c-Myc upregulates both ribosomal RNAs and ribosomal proteins for the assembly of new ribosomes (Gomez-Roman et al, 2003; Grandori et al, 2005; Kim et al, 2000; Schlosser et al, 2003). c-Myc also upregulates translation initiation factors and tRNAs to increase protein synthesis (Gomez-Roman et al, 2003; Kim et al, 2000;

Schlosser et al, 2003; Schuhmacher et al, 2001). In addition, c-Myc upregulates factors like nucleolin and nucleophosmin that help with rRNA processing and shuttling of ribosomal subunits (Ginisty et al, 1998; Maggi et al, 2008; Schlosser et al, 2003; Zeller et al, 2001). Overexpression of c-Myc has been shown to increase both cell size and the rate of total protein synthesis (Iritani & Eisenman, 1999; Schuhmacher et al, 1999).

Differentiation

The ability of c-Myc to negatively regulate terminal differentiation has been demonstrated by a multitude of studies. c-Myc is downregulated in both normal myeloid cells (Gowda et al, 1986) and in leukemic myeloid cells (Larsson et al, 1994) when terminal differentiation is induced *in vitro*. Conversely, forced expression of c-Myc (or *v-myc*) both in normal bone marrow cells (Amanullah et al, 2000) and in leukemic cell lines (Coppola & Cole, 1986; Larsson et al, 1988; Wall et al, 2008; Wu et al, 2003) can block terminal differentiation. In some cases, inhibiting *Myc* with anti-sense RNA is sufficient to induce differentiation (Holt et al, 1988; Nguyen et al, 1995), further highlighting the inverse relationship between c-Myc and terminal differentiation. *In vivo*, downregulation of c-Myc is critical for the terminal differentiation of multiple hematopoietic lineages, including megakaryocytes (Takayama et al, 2010) and erythrocytes (Jayapal et al, 2010). Together, these results show that c-Myc downregulation is both necessary and, in some cases, sufficient for terminal differentiation and suggest that c-Myc

functions as a switch in the induction of terminal differentiation in most hematopoietic lineages.

Apoptosis

In addition to promoting proliferation and growth, c-Myc also increases the cellular sensitivity to apoptosis. This coupling of proliferation to apoptosis was at first confounding but is now viewed as a fail-safe mechanism for preventing aberrant c-Myc activity. c-Myc's ability to induce apoptosis has been characterized both *in vitro* and *in vivo*. *In vitro* studies of c-Myc overexpression have shown that c-Myc induces apoptosis when cells lack survival signals (Askew et al, 1991; Evan et al, 1992). In vivo, studies of transgenic mice overexpressing c-Myc in B cells have shown both increased proliferation and apoptosis of B cells prior to the clonal outgrowth of tumors (Jacobsen et al, 1994). This increased sensitivity to apoptosis has been confirmed by many studies showing that increased expression of anti-apoptotic genes (e.g. BCL2, BCL-XL) or decreased expression of pro-apoptotic genes (e.g. Bim) cooperates w/ c-Myc in tumorigenesis (Eischen et al, 2001; Hemann et al, 2005; Strasser et al, 1990).

Adhesion/stem cell self renewal

A more recently described function of c-Myc is its role in controlling the expression of adhesion molecules and how this is related to stem cell function, both in the skin and the hematopoietic system (Murphy et al, 2005). Specifically,

studies of c-Myc's function in long-term hematopoietic stem cells (LT-HSCs) have uncovered an ability of c-Myc to regulate the stem cell state. In normal LT-HSCs, which are quiescent, c-Myc expression is low and increases as these cells receive signals to migrate out of the stem cell niche and differentiate (Murphy et al, 2005; Wilson et al, 2004). When *Myc* is deleted in LT-HSCs, these cells do not leave the niche, resulting instead in an accumulation of LT-HSCs, a reduction in multipotent progenitor cells (MPPs), and the eventual loss of differentiated hematopoietic lineages (Wilson et al, 2004). This phenotype results from the inappropriate expression of adhesion molecules, including N-cadherin and integrins, that are normally downregulated by c-Myc to promote the transition from LT-HSC to MPP. Illustrating this, forced expression of c-Myc in LT-HSCs results in downregulation of these adhesion molecules and, eventually, stem cell depletion as the LT-HSC compartment is converted to non-self renewing MPPs (Murphy et al, 2005; Wilson et al, 2004). This study elegantly demonstrates the importance of c-Myc in regulating the balance between stem and progenitor cells in the hematopoietic system through the control of adhesion molecules.

Regulation of c-Myc expression

Considering that c-Myc affects a large number of target genes and, by extension, a variety of cellular processes, it is perhaps not surprising that expression of c-Myc is tightly controlled. In fact, c-Myc is subject to a heavy degree of regulation so that cells can quickly tailor the amount of c-Myc expression to changes in cellular conditions. While this dissertation is primarily concerned with the

regulation of c-Myc protein stability, I will also highlight other modes of c-Myc regulation.

Transcription

Control of *MYC* transcription is complex and responds to signals from a wide range of signaling pathways, including those that regulate proliferation and differentiation. *MYC* gene expression is induced by a dizzying array of transcription factors, including β-catenin/TCF4, E2F1-3, STAT3, STAT4, and Notch, all of which are activated downstream of mitogen stimulation or other extracellular signals. *MYC* is also repressed by an array of factors including SMAD2/3, repressive E2Fs, and differentiation factors like BLIMP-1, CEBPα, and CEBPβ. Besides the interplay between transcriptional activators and repressors that control transcription initiation, *MYC* transcription is also controlled at the level of transcription elongation. Elongation is controlled by fine-tuning the transcriptional activity of RNA Pol II, such as through phosphorylation of the Pol II C-terminal domain by P-TEFb. Elongation control provides another sensitive and rapid way for *MYC* expression to be tailored to changing cellular conditions; in fact several studies have shown that changes in elongation precede changes in transcription initiation ((Wierstra & Alves, 2008) and references therein).

mRNA stability and translation control

The *MYC* mRNA is regulated at several levels. Early studies uncovered a very short half-life for *MYC* mRNA (~30 min) (Dani et al, 1984), suggesting that *MYC*

mRNA is rapidly degraded. This was found to occur by at least two mechanisms. Turnover of *MYC* mRNA is regulated in a translation-independent fashion by an AU-rich region of the 3' UTR that controls shortening of the *MYC* poly (A) tail (Brewer & Ross, 1988; Jones & Cole, 1987). In addition, turnover of *MYC* mRNA is regulated in a translation-dependent fashion by a polysome-associated protein, coding region determinant-binding protein (CRD-BP), that binds the "coding region determinant" of *MYC* mRNA and protects *MYC* mRNA from cleavage by the endonuclease APE1 (Barnes et al, 2009; Bernstein et al, 1992; Doyle et al, 1998).

Translation of *Myc* mRNA can also be regulated. For example, translation initiation can change in response to altered nutrient availability. In the face of nutrient deprivation, particularly methionine deprivation, cells will switch from expression of p64 Myc2 to expression of p68 Myc1 through the use of an upstream non-AUG translation start site (Hann et al, 1992). In addition, translation of *Myc* can be suppressed by microRNAs (miRNAs) such as let-7 (Kim et al, 2009; Kumar et al, 2007).

Post-translational modifications and protein stability
Like *Myc* mRNA, c-Myc protein is also extremely unstable (~30min half-life, (Hann & Eisenman, 1984)), representing another way for the cell to quickly modulate the level of c-Myc. c-Myc is continuously synthesized and destroyed, and this continuous destruction is facilitated by the coordination of multiple

posttranslational modifications of c-Myc followed by proteolysis via the 26S proteasome. These modifications, such as phosphorylation or ubiquitination of certain residues, can either delay or promote c-Myc proteasomal destruction. In particular, phosphorylation of two N-terminal residues has a particularly important role in regulating c-Myc protein stability and degradation following cell stimulation. These N-terminal residues, serine 62 (S62) and threonine 58 (T58), are located in MBI (Figure 1.1) and have opposing effects on c-Myc protein stability. Phosphorylation at S62 increases c-Myc half-life, while phosphorylation at T58 destabilizes c-Myc by promoting its degradation (Sears et al, 2000).

Phosphorylation at these sites is important for the stimulation of quiescent cells into the cell cycle and was defined in studies using rat embryo fibroblasts. Growth factor signaling through receptor tyrosine kinases (RTKs) activates two Ras effector pathways, the MAPK and PI3K pathways, which transiently stabilize c-Myc through phosphorylation at S62 (Sears et al, 1999; Sears et al, 2000) (Figure 1.3). Signaling through the MAPK pathway activates ERK, which directly phosphorylates c-Myc at S62, while signaling through PI3K inactivates GSK3, preventing phosphorylation of c-Myc at T58. Phosphorylation at S62 increases c-Myc half-life and is necessary for the accumulation of c-Myc protein in G1 (Sears et al, 1999; Sears et al, 2000). The reduction in c-Myc levels that occurs as the cell cycle proceeds is dependent on phosphorylation of T58 by GSK3 (Sears et al, 2000) and is facilitated by the scaffolding protein Axin1 (Arnold et al, 2009). Phosphorylation at T58 provides a recognition site for the prolyl isomerase Pin1,

which isomerizes proline 63 from cis to trans and allows the trans-specific

phosphatase protein phosphatase 2A (PP2A) to dephosphorylate S62 (Arnold &

Sears, 2006; Yeh et al, 2004). This T58-phosphorylated form of c-Myc is then

targeted for proteasomal degradation by the SCF ubiquitin ligase complex with

the phosphorylation-directed Fbox protein Fbw7 as the recognition component of

the E3 ligase (Welcker et al, 2004; Yada et al, 2004). This complex sequence of

interactions is critical for the fine control of c-Myc levels in early G1.
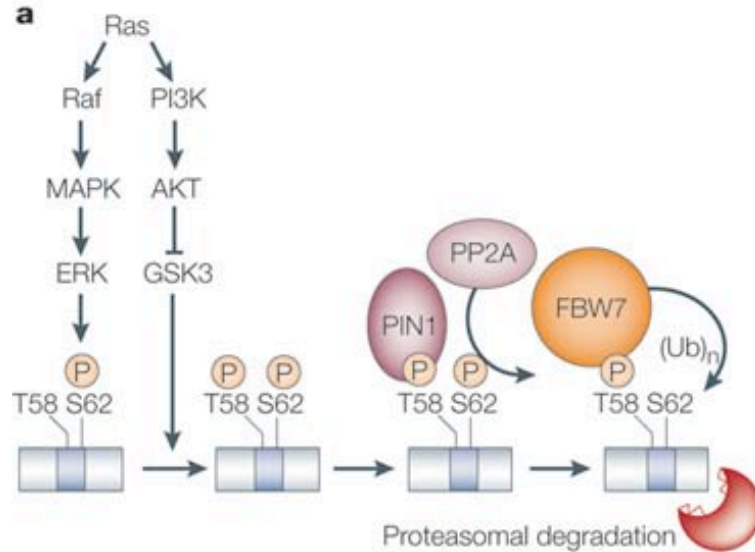
Figure 1.3. Regulation of c-Myc phosphorylation and stability by Ras effector pathways.

c-Myc protein stability is controlled by the sequential phosphorylation of S62 and T58 downstream of two Ras effector pathways, Raf-MAPK-ERK and PI3K-AKT-GSK3. After the activation of receptor tyrosine kinases, these two pathways are activated and ERK phosphorylates S62, stabilizing c-Myc protein. Simultaneously, the PI3K pathway inhibits GSK3, preventing c-Myc degradation. Reduced PI3K activity results in active GSK3, which phosphorylates T58. c-Myc is then recognized by the Pin1 prolyl isomerase that isomerizes P63 from cis to trans, which promotes dephosphorylation of S62 by the PP2A-B56α phosphatase. c-Myc is then recognized by the phosphorylation-dependent E3 ubiquitin ligase Fbw7, which poly-ubiquitinates c-Myc, leading to proteasomal degradation. GSK3, Pin1, and PP2A form a complex with c-Myc through association with the scaffolding protein Axin1 (not shown). (From (Adhikary & Eilers, 2005); used with permission.)

While S62 can also be phosphorylated by other kinases and in other cellular contexts, including by Cdk1 in G2/M, ERK in response to oxidative stress, and JNK in response to DNA damage (Hann, 2006), whether S62 phosphorylation results in the same cycle of c-Myc stabilization and degradation described above has not been determined. In addition, other mechanisms of modulating c-Myc stability exist, such as phosphorylation of c-Myc at C-terminal sites by the Pim kinases (Zhang et al, 2008).

c-Myc is also targeted by other ubiquitin ligases that likely operate independent of the pS62/pT58-dependent degradation pathway described above. One such E3, Skp2, not only promotes c-Myc degradation but also acts as a transcriptional cofactor, enhancing c-Myc's transcriptional activity through its interaction with the MBII region of c-Myc (Kim et al, 2003; von der Lehr et al, 2003). This is consistent with SKP2's role as an oncogene (Gstaiger et al, 2001; Latres et al, 2001). Another E3, TRUSS, promotes c-Myc degradation, though the specific cellular context of this interaction has not been described (Choi et al, 2010). In contrast, the E3 ligase β-TRCP and the ubiquitin-specific protease USP28 have been shown to oppose c-Myc degradation by Fbw7 (Popov et al, 2010; Popov et al, 2007). Another E3 ligase, HECTH9, has not been shown to affect c-Myc stability but instead modulates its transcriptional activity through ubiquitination (Adhikary et al, 2005).

c-Myc is essential for hematopoiesis

c-Myc is clearly important for proliferation, cell growth, and other cellular processes, and due to this, c-Myc expression is regulated at multiple levels to give the cell fine control over c-Myc levels in response to a changing environment. As a central regulator of these processes and a hub for integrating diverse signals, c-Myc is important for the development and homeostasis of many tissues. The hematopoietic system is a well-studied example.

c-Myc regulates hematopoietic development

c-Myc is critical for the establishment of the hematopoietic system. This has been clearly shown through the study of *Myc*-null mice, which die at E12 from a failure of both primitive yolk-sac hematopoiesis and definitive embryonal hematopoiesis (Dubois et al, 2008). In these embryos, the absence of *Myc* expression causes apoptosis of the erythroblasts that populate the yolk sac. In addition, hematopoietic stem cells that populate the fetal liver are greatly increased in number but do not give rise to differentiated lineages *in vitro* or *in vivo*. Supporting these results, the phenotype of epiblast-restricted *Myc*-null mice is recapitulated in mice where deletion of *Myc* is restricted to the hematopoietic and vascular systems (Dubois et al, 2008; He et al, 2008). Interestingly, these hematopoietic defects were not noted in the original description of *Myc*-null mice, which displayed a generalized developmental delay and died by E10.5 (Davis et al, 1993). This earlier lethality is likely due to a requirement for Myc in the placenta, since restricting *Myc* deletion to the epiblast rescued the generalized

developmental delay seen in the full *Myc* knockout and allowed for the

characterization of the hematopoietic defect (Dubois et al, 2008).

c-Myc is not only essential for the establishment of the hematopoietic system but

also for angiogenesis. Several groups have shown that *Myc* deletion in the

hematopoietic compartment compromises vascular development through

paracrine effects, including loss of angiogenic growth factor secretion by

hematopoietic cells (Baudino et al, 2002; He et al, 2008). Deletion of *Myc* in the

hematopoietic compartment also impairs the development of the fetal liver, an

early reservoir of hematopoiesis in the embryo (Dubois et al, 2008). These

results suggest that not only is *Myc* critical for the establishment of

hematopoiesis during embryonic development, but loss of *Myc* expression in the

hematopoietic compartment can impair the development of other tissues.

c-Myc regulates bone marrow homeostasis

Besides c-Myc's important role in establishing hematopoiesis during

embryogenesis, c-Myc is also critically important for bone marrow homeostasis in

the adult. As described above, deletion of c-Myc from hematopoietic stem cells

results in a loss of differentiated hematopoietic cells due to the accumulation of

non-functional HSCs. Conversely, overexpression of c-Myc in this compartment

also causes a loss of differentiated hematopoietic cells but through a different

mechanism, namely the downregulation of integrins and other adhesion

molecules important for maintaining HSCs in the osteoblast bone marrow niche

(Wilson et al, 2004). Together these data support a model in which the level of c-Myc controls the maintenance of HSCs in the niche. Recent results have extended this model to show that this process is regulated by the activity of the E3 ligase Fbw7 (Reavie et al, 2010). Since Fbw7 controls c-Myc levels by targeting c-Myc for proteasomal degradation, this result suggests that stem cell maintenance is controlled at the level of c-Myc protein stability. This is supported by data showing that *Myc* mRNA is maintained at a constant level between HSCs and multipotent progenitors (Reavie et al, 2010).

Since Fbw7 targets c-Myc for degradation when c-Myc is phosphorylated at T58, these results provocatively suggest that the pS62/pT58-regulated degradation pathway described above may play a role in the transition of LT-HSCs to multipotent progenitors. In addition, the conditional deletion of Fbw7 increases c-Myc protein levels not only in LT-HSCs, but also in multipotent progenitors and more restricted progenitors like myeloerythroid progenitors and double negative (CD4$^-$ CD8$^-$) thymocytes (Reavie et al, 2010), suggesting that pT58-dependent degradation may control c-Myc protein levels in all of these populations. However, since these populations are rare, expression of *Myc* in these populations has mostly been studied at the mRNA level (Laurenti et al, 2008; Reavie et al, 2010), leaving open the question of whether S62/T58 phosphorylation regulates c-Myc expression levels in these populations. Based on this data, I hypothesized that S62/T58 phosphorylation regulates c-Myc

protein levels in hematopoietic progenitors. Results from the investigation of this question will be presented in chapter 3.

c-Myc promotes hematopoietic tumors in mice

Studies examining *Myc* deletion clearly reveal a requirement for c-Myc expression in the hematopoietic compartment. Likewise, studies of c-Myc overexpression reveal c-Myc's oncogenic capability, and c-Myc has been well studied for its ability to drive hematopoietic tumors in mice. The first mouse model of c-Myc overexpression was a model of Burkitt's lymphoma, a B cell malignancy defined by the translocation of the *MYC* locus to one of three immunoglobulin loci. In this transgenic mouse, *Myc* expression is driven by the Eμ heavy chain enhancer, and these mice develop clonal pre-B cell lymphomas with a highly variable latency (Adams et al, 1985). Further studies have revealed that these tumors contain a deregulated p53 pathway, rendering them insensitive to apoptosis (Eischen et al, 1999; Schmitt et al, 1999). The need for a "second hit" to disable apoptosis provided an explanation for the clonality and variable latency of these tumors and is now appreciated as a recurring feature of *Myc*-driven tumor models (Meyer & Penn, 2008).

Despite the need for a "second hit", tumors driven by *Myc* often remain dependent on c-Myc expression. This was first demonstrated in a model where *Myc* expression in T cells could be toggled on and off at the transcriptional level. When *Myc* is expressed in this model, most mice develop an aggressive clonal T

cell lymphoma, but these tumors regress when doxycycline is used to repress *Myc* expression (Felsher & Bishop, 1999). Though the mechanism of tumor regression varies by tissue (Felsher, 2010), this model was the first to demonstrate "oncogene addiction", where a complex tumor remains dependent on the initiating oncogenic lesion.

From the study of many mouse models (reviewed in (Delgado & Leon, 2010)), we know that *Myc* is potently tumorigenic in the hematopoietic system. However, a provocative study has suggested that not all forms of *Myc* are equally potent at driving the formation of tumors. In this study, mutant forms of *Myc* (P57S or T58A) promoted lymphoma development at a greatly accelerated rate compared to wildtype *Myc* (Hemann et al, 2005). However, when wildtype *Myc* was expressed in a Bim$^{-/-}$ or a Bcl2-overexpressing background, all forms of *Myc* promoted lymphoma development at the same rate. This study demonstrated that these mutant forms of *Myc* are deficient for inducing apoptosis, which allows tumors to form without the need for a "second hit" in an apoptotic pathway. Likewise, wildtype *Myc*, when combined with an apoptotic block, was just as efficient at promoting lymphoma development as the *Myc* mutants. This study also supported many *in vitro* studies showing that these two mutations both impair the ability of c-Myc to induce apoptosis and also increase its transforming activity (Hoang et al, 1995).

While this study provides an example of a qualitative difference between wildtype and certain mutant forms of *Myc*, these results are complicated by the use of gross *Myc* overexpression. In order to address the question of whether mutant and wildtype forms of *Myc* are qualitatively different when *Myc* is expressed at low and roughly equivalent levels, our lab has generated both wildtype and T58A *Myc* knock-in mice. These mice express *Myc* from the ROSA locus dependent on co-expression of Lck-Cre, resulting in low-level constitutive expression of *Myc* in T cells. When we followed cohorts of *Myc^{WT/WT}* and *Myc^{T58A/T58A}* for lymphoma development, we found that *Myc^{T58A/T58A}* mice developed lymphoma with a median onset of 149 days, while *Myc^{WT/WT}* mice remained tumor-free for >16 months (S. Byers, unpublished data). However, despite equal mRNA expression, these mice do not express equal levels of ectopic c-Myc protein because the T58A mutation disrupts c-Myc degradation, resulting in higher c-Myc expression in *Myc^{T58A/T58A}* mice than *Myc^{WT/WT}* mice. In contrast, mice expressing only one copy of the T58A mutant (*Myc^{T58A/+}*) express a level of c-Myc protein roughly equivalent to that of *Myc^{WT/WT}* mice. When *Myc^{T58A/+}* mice were followed for lymphoma development, we found that these mice develop T cell lymphoma with a median onset of 466 days (S. Byers, unpublished data), again in contrast to *Myc^{WT/WT}* mice that remain tumor-free during that time despite expressing roughly equivalent levels of c-Myc protein.

While these results support those of Hemann et al, our ability to compare the *Myc^{WT/WT}* and *Myc^{T58A/+}* mice based on c-Myc expression level provides us with

24

unique information. Because T58A c-Myc is highly S62-phosphorylated (Lutterbach & Hann, 1994; Sears et al, 2000), our results suggest that c-Myc phosphorylated at S62 is functionally different than wildtype c-Myc. These results also suggest that promoting a highly S62-phosphorylated form of c-Myc deregulates c-Myc function in a way that promotes tumor formation and is separable from its effect on c-Myc protein levels. Critically, whether S62-phosphorylated c-Myc is prevalent in human leukemia is currently unknown.

c-Myc is commonly deregulated in human leukemia

In light of c-Myc's role in promoting growth and proliferation and its ability to drive tumors in mice, it is perhaps not surprising that c-Myc is deregulated in a wide variety of human cancers. In fact, Myc was originally discovered for its role in leukemia, long before its function was known. c-Myc was discovered based on its homology to a viral gene, *v-myc*, that is present in a virus that causes myeloid leukemia in birds, the avian myelocytomatosis virus (Vennstrom et al, 1982). Further study of c-Myc has since revealed that c-Myc is commonly deregulated in human leukemias of both myeloid and lymphoid lineages. This deregulation can occur through a variety of mechanisms, as shown in Figure 1.4 and described below.
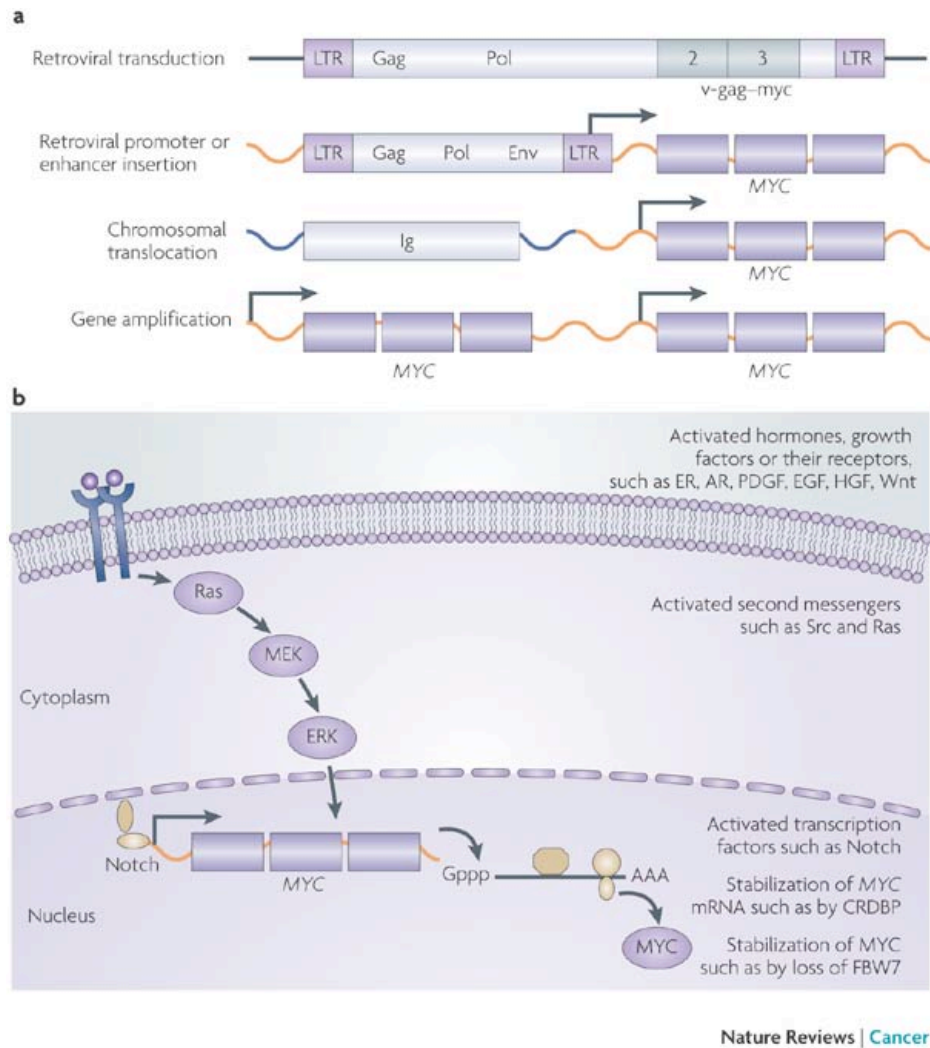
Figure 1.4. Mechanisms of MYC deregulation in cancer.

A. Genetic mechanisms of *MYC* deregulation. **B.** Additional mechanisms of c-Myc deregulation. (From (Meyer & Penn, 2008); used with permission.)

Translocation

The first human malignancy reported to be associated with c-Myc overexpression was Burkitt's lymphoma, a neoplasm of germinal center B cells. In this disease, the *MYC* locus is translocated to one of three immunoglobulin loci (IgH, Igκ, Igλ). While the breakpoints are complex and not consistent, these translocations ultimately juxtapose the entire *MYC* coding region against an immunoglobulin enhancer. This results in constitutive transcription of *MYC*, and these lymphomas often have a very high mitotic index (Boxer & Dang, 2001).

While translocation of *MYC* is a defining feature of Burkitt's lymphoma, other lymphomas and leukemias also show *MYC* translocations, though at a much lower frequency. Two other B cell lymphomas, diffuse large B cell lymphoma (DLBCL) and multiple myeloma, have recurring *MYC* translocations in ~15% of cases (Vita & Henriksson, 2006). Rarely, T cell acute lymphoblastic leukemias (T ALLs) also have *MYC* translocations, which fuse *MYC* to the T cell receptor alpha (TCRα) locus (Erikson et al, 1986; Shima et al, 1986).

Gene amplification

While *MYC* gene amplifications are more common in solid tumors than hematopoietic malignancies (Vita & Henriksson, 2006), some instances of gene amplification in leukemia have been reported. One report shows that modest *MYC* gene amplification can occur in up to 38% of DLBCL cases (Stasik et al, 2010). In these studies, *MYC* gene amplification was associated with advanced

stage disease or lower survival (Rao et al, 1998; Stasik et al, 2010). In contrast, *MYC* gene amplification is rare in acute myeloid leukemia (AML), but has been reported in the form of double minute chromosomes (Bruyere et al, 2010; Lee et al, 2009; Mathew et al, 2000). However, the significance of this is not clear, as *MYC* amplification in AML does not always result in increased *MYC* expression (Gowda et al, 1986; Paulsson et al, 2003; Storlazzi et al, 2006).

Mutation

While oncogenes like *RAS* are often activated by mutations in cancer, *MYC* is only rarely mutated in cancer (Lee et al, 2006). The exception to this is in Burkitt's lymphoma and some AIDS-associated lymphomas, where mutations in *MYC* are frequent (Bhatia et al, 1993; Clark et al, 1994). These mutations can be found throughout the *MYC* locus but cluster in MBI around T58 (Bahram et al, 2000). Interestingly, T58 mutations are also found in isolates of *v-myc*, and both the viral- and Burkitt's-derived mutations have increased transforming activity (Henriksson et al, 1993; Hoang et al, 1995; Pulverer et al, 1994; Symonds et al, 1989).

Transcriptional upregulation

MYC is a transcriptional target for oncogenic transcription factors in both acute myeloid and lymphoid leukemia. In AML, many recurring translocations result in oncogenic fusion proteins. Several of these, such as PML-RARα, AML1-ETO, and PLZF-RARα, have been shown to induce *MYC* expression (Muller-Tidow et

al, 2004; Rice et al, 2009). Another common mutation in AML, that of the FLT3 tyrosine kinase receptor, induces constitutive activation of FLT3 and results in transcriptional upregulation of *MYC* (Kim et al, 2005). In addition, *MYC* overexpression at the mRNA level has been reported in many instances of AML (Delgado & Leon, 2010). In T ALL, *MYC* expression can be induced by the NOTCH transcription factor, which is activated by mutation in 50% of T ALL cases (Weng et al, 2004).

Protein stabilization

The mechanisms of *MYC* deregulation that have been reported are primarily genetic and have been described above. In contrast, there are very few studies examining c-Myc protein stability as a mechanism of elevated c-Myc expression in leukemia and lymphoma. Two studies of Burkitt's lymphoma cell lines have shown that c-Myc protein is stabilized when *MYC* is mutated at proline 57 or threonine 58 (Bahram et al, 2000; Gregory & Hann, 2000), consistent with the role of T58 mutations in disrupting c-Myc degradation. However, in some cell lines, c-Myc was stabilized in the absence of these mutations (Gregory & Hann, 2000), suggesting that mutations are not required to stabilize c-Myc in Burkitt's lymphoma. Whether c-Myc is stabilized in other hematopoietic malignancies is not known, but the investigation of this question will be presented in this dissertation.

Statement of thesis

Clearly, proper regulation of c-Myc is important not only for the establishment and maintenance of the hematopoietic system but also for the prevention of cancer in this complex tissue. Based on what is currently known about the post-translational regulation of c-Myc and the important role c-Myc plays in driving tumor development, I hypothesized that disrupted c-Myc degradation is a mechanism of c-Myc overexpression in leukemia. In chapter 2, I focus on how c-Myc is both aberrantly stabilized and aberrantly phosphorylated at S62 and T58 in acute lymphoblastic leukemia and what pathways may be responsible for this aberrant stabilization and phosphorylation. In chapter 3, I focus on how c-Myc S62/T58 phosphorylation changes during myeloid differentiation and how c-Myc is aberrantly S62-phosphorylated in acute myeloid leukemia and is associated with upstream activating mutations in receptor tyrosine kinases and Ras. In chapter 4, I focus on whether the AXIN1 scaffolding protein functions as a tumor suppressor in leukemia both by examining its deregulation in human leukemia and by testing its ability to oppose the development of c-Myc-driven lymphoma in a mouse model.

Chapter 2: Aberrant stabilization and phosphorylation of c-Myc in lymphoblastic leukemia

Abstract

c-Myc is a pleiotropic transcription factor that is frequently overexpressed in leukemia. Previous studies have shown that this overexpression can be due to translocation or mutation of the *MYC* locus; however, in many cases these genetic changes are absent. To determine whether non-genetic mechanisms control c-Myc abundance in acute lymphoblastic leukemia (ALL), we assessed c-Myc protein half-life and phosphorylation status in B and T cell ALL cell lines and patient samples. We find that c-Myc overexpression in ALL is frequently due to aberrant stabilization of c-Myc protein from altered phosphorylation at serine 62 and threonine 58. Further we find that activation of PI3K and inhibition of PP2A may contribute to this phenotype. These results establish aberrant stabilization and phosphorylation of c-Myc as a common mechanism of c-Myc overexpression in lymphoblastic leukemia and may provide new avenues for targeting c-Myc in cancer through the modulation of pathways that control its stability.

Introduction

c-Myc is a transcription factor that is important for controlling many cellular processes, including proliferation, growth, metabolism, differentiation, and apoptosis (Meyer & Penn, 2008). Deletion of *Myc* during mouse development results in embryonic lethality (Davis et al, 1993), while constitutive overexpression of c-*my*c promotes the development of tumors (Meyer & Penn, 2008), suggesting that proper regulation of c-Myc expression is critical for preventing cancer.

c-Myc is commonly overexpressed in human cancers, including leukemia and lymphoma. Thus far, the mechanisms of c-Myc overexpression reported in these hematopoietic cancers have been largely confined to changes affecting the *MYC* locus. These changes include translocations, gene amplification, and, to a lesser extent, mutation of the *MYC* gene. Translocations have been reported in a number of hematopoietic cancers, including multiple myeloma, T cell acute lymphoblastic leukemia (T ALL), and Burkitt's lymphoma. These translocations cause *MYC* activation by juxtaposing the *MYC* locus with a new enhancer element, such as those of the immunoglobulin family, which results in constitutive transcription of *MYC*. Amplification of the *MYC* locus has also been reported in some leukemia cell lines (Dalla-Favera et al, 1982), and mutation of *MYC* has been reported in Burkitt's lymphoma and AIDS-associated lymphomas but not in other blood cancers (Boxer & Dang, 2001). While these genetic mechanisms of c-Myc overexpression have broadened our understanding of c-Myc's involvement

in blood cancers, they are not as common as c-Myc overexpression observed in leukemias and lymphomas, suggesting that there may be additional mechanisms that account for high c-Myc levels in these cancers.

Since deregulated expression of c-Myc can have profound consequences, cells have evolved multiple layers of regulation to fine-tune c-Myc expression. This regulation includes transcriptional, post-transcriptional, and post-translational controls. For example, when a quiescent cell is stimulated into the cell cycle, c-Myc rapidly accumulates both from increased *MYC* transcription and from increased protein stability (Kelly et al, 1983; Sears et al, 1999). The subsequent decrease in c-Myc abundance, as well as the low level of c-Myc present in quiescent cells, is largely due to the clearing of c-Myc via ubiquitin-dependent proteolysis (Flinn et al, 1998; Salghetti et al, 1999; Sears et al, 1999).

What controls c-Myc stability and degradation? Work from our lab has described a role for two conserved N terminal phosphorylation sites, serine 62 (S62) and threonine 58 (T58), in controlling c-Myc stability and degradation. Phosphorylation of these sites is hierarchical, with T58 phosphorylation requiring prior S62 phosphorylation (Lutterbach & Hann, 1994). Importantly, phosphorylation of these sites has opposing effects on c-Myc stability; S62 phosphorylation increases c-Myc stability, while T58 phosphorylation decreases c-Myc stability and promotes c-Myc ubiquitin-dependent proteolysis (Sears et al,

2000). Additionally, we have shown that dephosphorylation of S62 facilitates c-Myc degradation (Yeh et al, 2004).

Phosphorylation of S62 and T58 is important for controlling c-Myc protein stability as quiescent cells enter the cell cycle. When quiescent cells are stimulated by growth factors, two Ras-dependent pathways are activated that together increase c-Myc stability. Activation of the MAPK pathway results in the phosphorylation of S62 by ERK, while activation of the PI3K pathway inhibits the phosphorylation of T58 by GSK3 (Sears et al, 2000). Simultaneous activation of these pathways results in S62 phosphorylation and an increase in c-Myc stability. As cells progress through the cell cycle, reduced signaling through PI3K leads to an increase in GSK3 activity and phosphorylation of c-Myc at T58 (Sears et al, 2000). Phosphorylation of T58 enhances the dephosphorylation of S62 by PP2A, and this leads to the ubiquitination of c-Myc by the E3 ligase SCF^{Fbw7} and subsequent proteasomal degradation of c-Myc (Welcker et al, 2004; Yada et al, 2004; Yeh et al, 2004). This complex regulation of c-Myc stability through the post-translational modification of c-Myc is important for the controlled accumulation of c-Myc in early G1.

The discovery of this mode of c-Myc regulation suggests that stabilizing c-Myc by elevating S62 phosphorylation represents a potential non-genetic mechanism for elevated c-Myc levels in cancer. In fact, some evidence for this possibility already exists. In vitro, mutation of T58 to alanine (T58A) both increases c-Myc stability

and facilitates cell transformation (Sears et al, 2000; Yeh et al, 2004). In vivo, expression of c-Myc T58A accelerates lymphoma development compared to the expression of wildtype c-Myc, both in the context of retroviral overexpression (Hemann et al, 2005) and in the context of low constitutive expression from the ROSA locus (S. Byers and R. Sears, unpublished data). Additionally, mutations found in Burkitt's lymphoma cluster around T58 and frequently result in both reduced T58 phosphorylation and increased c-Myc stability (Bahram et al, 2000; Gregory & Hann, 2000). However, whether c-Myc is stabilized in other types of leukemia in the absence of mutations has not been investigated.

Here we describe c-Myc protein stabilization in the absence of *MYC* mutations in acute lymphoblastic leukemia. We find that in cell lines and primary patient samples, c-Myc stability is increased. We also find that in cell lines this stabilization correlates with altered phosphorylation at S62 and T58 and with activated PI3K. In primary samples, altered phosphorylation at S62 and T58 correlates with elevated expression of the PP2A inhibitors SET and CIP2A, which may also promote PI3K pathway activation.

Results

Our previous work has defined a pathway that controls the accumulation of c-Myc protein in non-transformed cells through post-translational modifications that alter c-Myc protein stability (Sears et al, 1999; Sears et al, 2000; Yeh et al, 2004). Since c-Myc levels are often elevated in leukemia (Delgado & Leon, 2010; Nesbit et al, 1999), disruption of this pathway may represent a novel non-genetic mechanism for c-Myc overexpression. Therefore, we hypothesized that increased c-Myc stability through the deregulation of this pathway may contribute to c-Myc overexpression in cancer, specifically in leukemia. To explore this hypothesis, we began by measuring c-Myc protein levels in four leukemia cell lines and two control samples by immunoblot. As shown in Figure 2.1A, we found that c-Myc was highly expressed in two pre-B ALL cell lines (REH, SupB15), one CML cell line (K562), and one AML cell line (HL-60), while c-Myc levels were much lower in both quiescent peripheral blood mononuclear cells (PBMCs) and an EBV-immortalized B cell line (JY). To determine whether high c-Myc levels in these leukemia cell lines were due to amplification of the *MYC* locus, we evaluated *MYC* copy number by fluorescence in situ hybridization (FISH) using both a probe for the *MYC* locus and a probe for the centromeric region of chromosome 8, where *MYC* is located. In three of the four cell lines, we did not find *MYC* gene amplification. In the two pre-B ALL cell lines, we found the normal diploid copy number of both chromosome 8 and the *MYC* locus, and in the K562 cell line, we found one extra *MYC* signal due to trisomy 8 (Figure 2.1B). Consistent with previous reports, we found a large block of *MYC*-signal positive

DNA in the HL-60 cell line, representing *MYC* gene amplification (Figure 2.1B).

This amplification was not located on chromosome 8, as it did not appear

associated with the chromosome 8 centromeric probe. Therefore, out of the four

leukemia cell lines under study, we found amplification of the *MYC* gene only in

the HL-60 cell line.
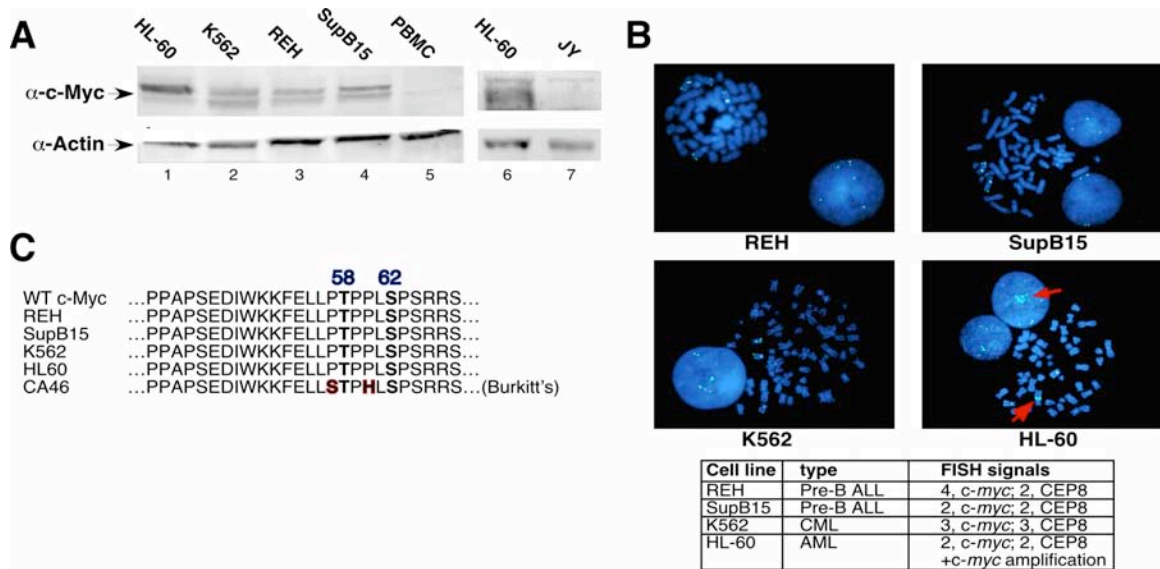
Figure 2.1. c-Myc overexpression occurs in leukemia cell lines that lack *MYC* gene amplification or coding sequence mutations.

A. c-Myc protein levels are elevated in leukemia cell lines. Whole-cell lysates were prepared from HL-60 (AML), K562 (CML), REH (ALL) and SupB15 (ALL) leukemia cell lines, normal PBMCs, and the EBV-immortalized B-lymphocyte cell line JY. Immunoblotting was performed with 25μg protein from each sample. The blots were probed with C33 anti-c-Myc (lanes 1–5) and N262 anti-c-Myc (lanes 6 and 7) along with anti-actin antibodies. **B.** *MYC* gene amplification is seen in HL-60 cells, but not REH, SupB15 or K562 cells. One hundred cells (20 metaphase and 80 interphase) from each cell line were analyzed by FISH using a *MYC* probe (blue) and a CEP8 centromere probe as an identifier of chromosome 8 (green). **C.** No *MYC* coding sequence mutations are present in HL-60, K562, REH and SupB15 cells. Total RNA from each cell line was used for reverse transcription with PCR to amplify the entire *MYC* coding region, which was sequenced. The amino acids for the Box I region of c-Myc, a hot spot for mutations in Burkitt's lymphoma, for each of the four leukemia cell lines is shown along with the CA46 Burkitt's lymphoma cell line with known mutations, for comparison. Data published in (Malempati et al, 2006).

Because mutations affecting c-Myc protein stability have been described in Burkitt's lymphoma (Bahram et al, 2000; Gregory & Hann, 2000), we sequenced the coding region of *MYC* for mutations in these leukemia cell lines. As shown in Figure 2.1C, we found no mutations in *MYC* in these cell lines. As a control, the Burkitt's lymphoma cell line CA46, in which c-Myc half-life is prolonged, is shown with mutations at P57 and P60. Collectively, these results suggest that c-Myc can be overexpressed in leukemia cell lines in the absence of genetic alterations in the *MYC* locus.

Since c-Myc protein levels are tightly controlled in normal cells through the regulation of c-Myc protein stability, we hypothesized that an increase in c-Myc stability could contribute to the high c-Myc expression we observe in these leukemia cell lines. To test this hypothesis, we directly measured c-Myc protein half-life in these cell lines using ^{35}S-methionine/cysteine pulse-chase analyses. As controls, we also performed this pulse-chase analysis on PBMCs and the immortalized B cell line, JY. As shown in Figure 2.2A and 2.2B, the two pre-B ALL cell lines REH and SupB15 showed an extended half-life for c-Myc, up to 3.5 times longer than that measured in control samples. In contrast, both quiescent PBMCs and proliferating JY cells showed rapid turnover of c-Myc (Figure 2.2B), consistent with reports of rapid turnover of c-Myc in both quiescent and proliferating non-transformed cells. Intriguingly, c-Myc turnover in the HL-60 cell line was similar to that of the control cell line JY, suggesting that despite its high expression, c-Myc is not substantially stabilized in HL-60 cells. These results

suggest that high c-Myc levels in leukemia can correlate either with gene amplification, as seen in the HL-60s, or with increased protein stability, as seen in the REH and SupB15 cell lines.

A
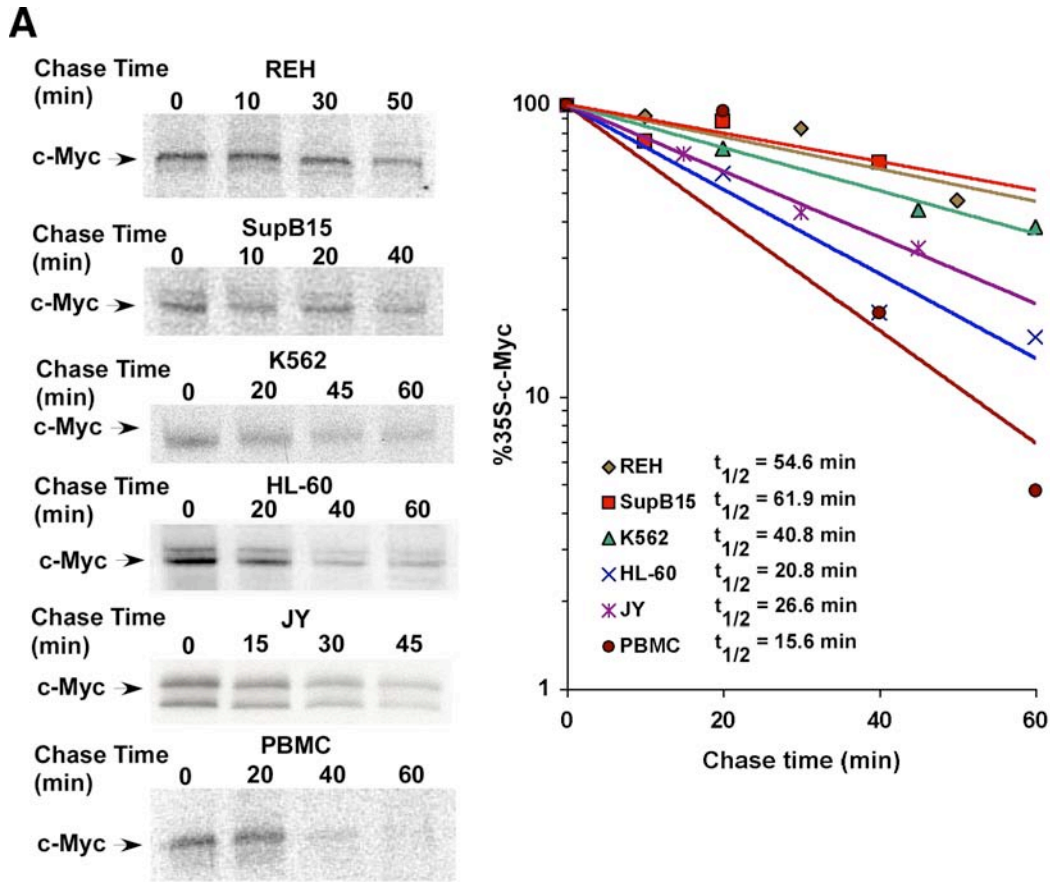
B

Cell line	type	Mean half-life (min) ± SE
REH	Pre-B ALL	62.0 ± 7.4
SupB15	Pre-B ALL	69.7 ± 7.8
K562	CML	41.5 ± 4.1
HL60	AML	20.5 ± 0.3
JY	EBV B cell	20.9 ± 3.3
PBMC	primary	12.1 ± 1.9

Figure 2.2. Leukemia cell lines without *MYC* mutations or gene amplification have stabilized c-Myc protein.

A. The half-life of c-Myc is prolonged in acute lymphoblastic leukemia cell lines. Leukemia cells, JY cells, and PBMCs were pulse-labeled in vivo with ^{35}S-methionine/cysteine and chased in medium with excess unlabeled methionine and cysteine for the indicated times as described in Materials and methods. Endogenous c-Myc was immunoprecipitated from an equal number of cells for each time point and analyzed by gel electrophoresis. ^{35}S-labeled c-Myc from each sample was quantitated by phosphoimager. The rate of degradation of endogenous c-Myc for each leukemia cell line as well as JY and normal PBMCs is represented in the graph by best-fit exponential lines. Half-lives of c-Myc were

calculated from exponential line equations and are shown for each cell type. Pulse-chase results shown here are representative of 2–3 independent experiments for each cell line. **B.** Table showing mean half-life±s.e. for c-Myc in four leukemia cell lines, EBV-immortalized JY cells and PBMCs calculated from 2–3 independent experiments for each cell type. Data published in (Malempati et al, 2006).

As c-Myc protein stability can be controlled by the sequential phosphorylation of the N-terminal residues S62 and T58, we used phosphorylation-specific antibodies to measure c-Myc S62 and T58 phosphorylation in the four leukemia cell lines under study. In addition, by double-labeling with a phospho-specific antibody and a total c-Myc antibody, we were able to quantify both the ratio of pS62 c-Myc to total c-Myc and the ratio of pT58 c-Myc to total c-Myc. As shown in Figure 2.3, we found very little S62 phosphorylation in the HL-60 cells, but T58 phosphorylation was clearly evident (lanes 2 and 9). In contrast, the pre-B ALL cell lines REH and SupB15 have high levels of S62 phosphorylation and relatively less T58 phosphorylation (Figure 3; REH cells, lanes 3 and 6; SupB15 cells, lanes 4 and 7). As a control, we also examined phosphorylation of S62 and T58 in CA46 cells, where c-Myc is stabilized due to a mutation that prevents T58 phosphorylation (P57S). Mutations at P57 or T58 block T58 phosphorylation and increase S62 phosphorylation, which was previously shown in other Burkitt's lymphoma cell lines using phosphopeptide mapping (Hoang et al, 1995; Niklinski et al, 2000). As expected, CA46 cells had no detectable T58 phosphorylation and expressed high levels of S62 phosphorylation (Figure 2.3, lanes 5 and 10), consistent with reports of increased c-Myc stability in this cell line (Bahram et al, 2000; Gregory & Hann, 2000). Together these results suggest that high levels of S62 phosphorylation correlate with increased c-Myc stability. Importantly, the pre-B ALL cell lines have both increased c-Myc stability and elevated levels of pS62, but unlike what has been shown in Burkitt's lymphoma, this is not due to a MYC mutation (Figure 2.1C).
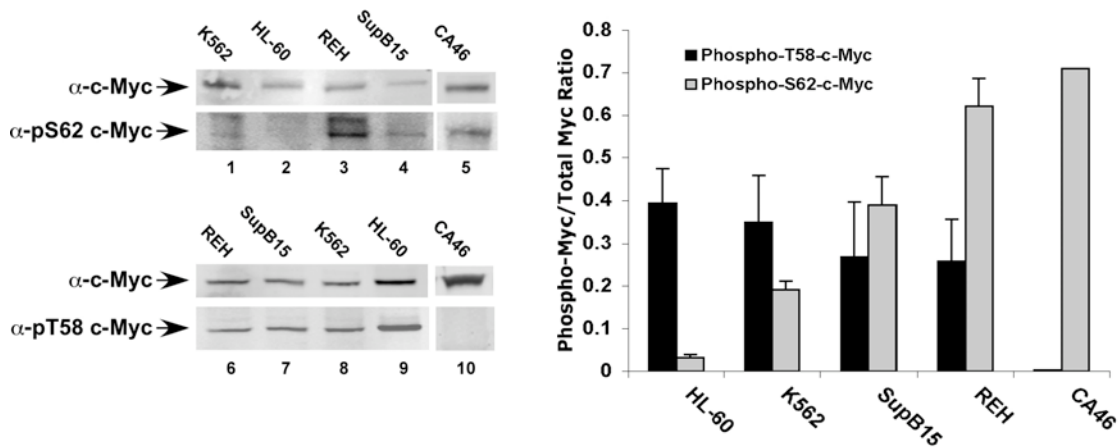
Figure 2.3. Leukemia cell lines with more stable c-Myc show increased levels of serine 62 phosphorylation relative to a cell line with unstable c-Myc.

Whole-cell lysates were prepared from REH, SupB15, K562 and HL-60 leukemia cell lines along with the CA46 Burkitt's lymphoma cell line. Extracts were normalized for total c-Myc as measured from previous analyses. Gel electrophoresis was performed and immunoblots were probed simultaneously with the C33 pan-c-Myc antibody (mouse) and the phospho-S62-c-Myc antibody (rabbit) (lanes 1–4) or the C33 antibody and phospho-T58-c-Myc antibody (rabbit) (lanes 6–9), using different IRDye secondary antibodies for detection (see Materials and methods). The immunoblots shown are representative of three independent experiments. The amount of signal from each antibody was detected and quantitated using an Odyssey Infrared Imager and software from LI-COR Biosciences (see Materials and methods). The bar graph (with s.e.) shows the mean ratio from the three experiments of threonine 58 phospho-specific signal to total c-Myc signal in black and the mean ratio of serine 62 phospho-specific signal to total c-Myc signal in gray for the four leukemia cell lines. Phospho-serine 62 and phospho-threonine 58 signal in the CA46 Burkitt's lymphoma with a known proline to serine mutation at position 57 is also shown (lanes 5 and 10, and graph). Data published in (Malempati et al, 2006).

We have previously shown that T58 phosphorylation is required for the dephosphorylation of S62 and subsequent degradation of c-Myc (Sears et al, 2000; Yeh et al, 2004). Phosphorylation of T58 by the kinase GSK3 is controlled by PI3K signaling, which negatively regulates GSK3 activity (Cross et al, 1995). The phosphorylation pattern in the pre-B ALL cell lines suggests that c-Myc may be stabilized due to signaling through PI3K, which would reduce T58 phosphorylation by suppressing GSK3 activity. In order to determine whether PI3K signaling is contributing to increased c-Myc protein stability in the pre-B ALL cell lines, we used the compound LY294002 to inhibit PI3K activity. In both the REH and SupB15 cell lines, we found that c-Myc protein levels were dramatically reduced upon inhibition of PI3K (Figure 2.4A, left), suggesting that PI3K activity is required for high c-Myc levels in the pre-B ALL cell lines. In contrast, inhibition of PI3K had only a minor effect on c-Myc levels in the HL-60s where c-Myc is unstable (Figure 2.4A, left). To determine whether this decrease in c-Myc protein levels after PI3K inhibition was dependent on proteasomal degradation of c-Myc, we simultaneously treated cells with the PI3K inhibitor LY294002 and the proteasome inhibitor lactacystin. We found that proteasome inhibition partially rescued the decrease in c-Myc protein levels caused by PI3K inhibition (Figure 2.4A, left), suggesting that at least part of the contribution of active PI3K to high c-Myc levels occurs through inhibition of c-Myc proteasomal degradation. We also found that lactacystin treatment alone had a more dramatic effect on c-Myc accumulation in the HL-60 cells, where c-Myc is unstable, than in the REH or SupB15 cells, where c-Myc is more stable (Figure 2.4A, right).

45
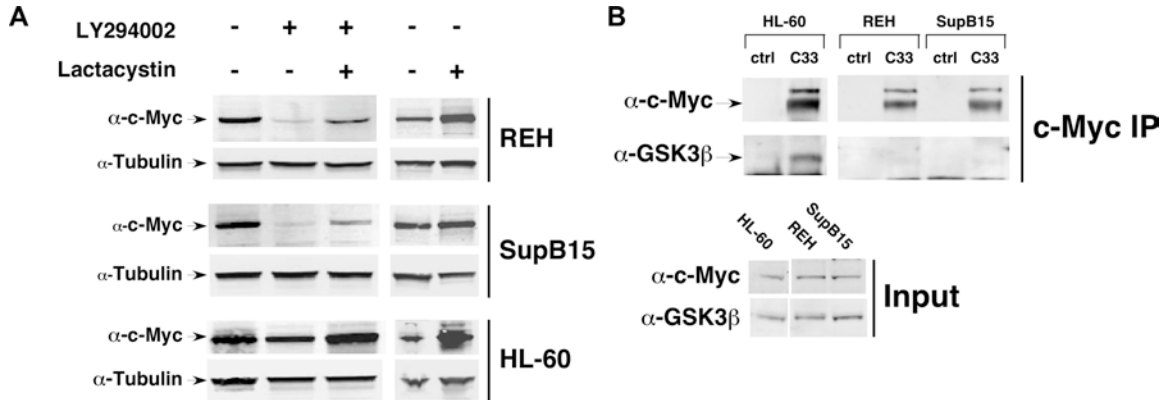
Figure 2.4. PI3K activity and inhibited GSK3β function towards c-Myc correlates with increased c-Myc stability in ALL cell lines.

A. PI3K inhibition decreases c-Myc protein levels in ALL cell lines with stabilized c-Myc; partial recovery by simultaneous proteasome inhibition. Leukemia cell lines were treated for 4 hours with either 20μM LY294002, 10μM lactacystin, or both as indicated. Cells were then harvested, and protein analyzed by gel electrophoresis and immunoblot analysis using anti-c-Myc (N262) and anti-tubulin antibodies. **B.** Co-IP shows decreased association between GSK3β and c-Myc in leukemia cell lines with stabilized c-Myc. Endogenous c-Myc and GSK3β levels in whole-cell lysates from each of the indicated cell lines are shown (Input). Immunoprecipitation (IP) was performed from these lysates using C33 (c-Myc) antibody-conjugated beads or control (ctrl) A+G agarose beads. Input and IP blots were probed with C33 and GSK3β antibodies, as indicated. Data published in (Malempati et al, 2006).

As GSK3 activity is required for T58 phosphorylation (Gregory et al, 2003; Lutterbach & Hann, 1994; Pulverer et al, 1994; Sears et al, 2000), we next investigated whether PI3K signaling inhibits GSK3 activity toward c-Myc. We decided against using serine 9 phosphorylation as a marker of GSK3β inactivation (Ding et al, 2000; McManus et al, 2005) and instead examined the ability of GSK3β to associate with c-Myc through a co-immunoprecipitation experiment. We found that in both of the pre-B ALL cell lines, GSK3β was only weakly associated with c-Myc (Figure 2.4B). In contrast, GSK3β was robustly associated with c-Myc in the HL-60 cells, consistent with the high level of T58 phosphorylation and short c-Myc half-life observed in this cell line. These results suggest that PI3K signaling helps to maintain high c-Myc levels in the pre-B ALL cell lines by inhibiting c-Myc proteasomal degradation, potentially by reducing the association between c-Myc and GSK3.

So far, our results *in vitro* support a role for disrupted c-Myc degradation contributing to the high c-Myc protein levels observed in pre-B ALL. To determine whether these results are relevant for patients with pre-B ALL, we obtained banked bone marrow samples from pediatric patients with pre-B ALL (Table 2.1) and performed both pulse-chase experiments to determine c-Myc half-life and FISH to assess genetic changes at the *MYC* locus. As shown in Figure 2.5, c-Myc half-life was substantially increased in three out of four pre-B ALL samples from pediatric patients. In contrast, c-Myc half-life was 19.6 minutes in normal bone marrow, consistent with that seen in PBMCs and the JY control cell line.

We also examined some of these pre-B ALL samples for *MYC* gene amplification by FISH. Consistent with our results in the pre-B ALL cell lines, the pre-B ALL samples did not contain a *MYC* gene amplification (Table 2.1).

Table 2.1. Clinical features of pediatric ALL cases evaluated for c-Myc protein stabilization.

Patient ID	Age (years)	Gen-der	Diagnosis	Outcome	c-Myc half-life (min)	FISH for MYC
1	6	M	Pre-B ALL	CCR	91.2	IS
2	3	F	Pre-B ALL	BM Relapse→ Death	57.8	2, *MYC*; 2, CEP8
3	2	F	Pre-B ALL	CCR	56.4	2-4, *MYC* 2-4 CEP8[1]
4	16	M	T-cell ALL	N/A	44.6	2, *MYC*; 2, CEP8
5	2	M	Pre-B ALL	CCR	31.4	2, *MYC*; 2, CEP8
6	4	M	T-cell ALL	CCR	17.6	IS
ctrl	N/A	N/A	-	-	19.6	IS

Abbreviations: ALL, acute lymphoblastic leukemia; BM relapse, bone marrow relapse; CCR, complete clinical remission; ctrl, control; F, female; FISH, fluorescent *in situ* hybridization; IS, insufficient sample to perform FISH analysis; M, male; N/A, clinical information not available.

Notes: Age at diagnosis is listed in years. Immunophenotype was determined by flow cytometry at diagnosis for each patient. Measured c-Myc half-life is listed in minutes.

[1]Twenty-nine of the 100 cells had four signals for *MYC* and four for CEP8, indicating tetrasomy 8, 10/100 cells showed trisomy 8 with three signals for *MYC* and three for CEP8, 57/100 showed normal two *MYC*, two CEP8, and 4/100 showed one *MYC* and two CEP8.

FISH was performed on 100 interphase cells for each sample.

Table published in (Malempati et al, 2006).
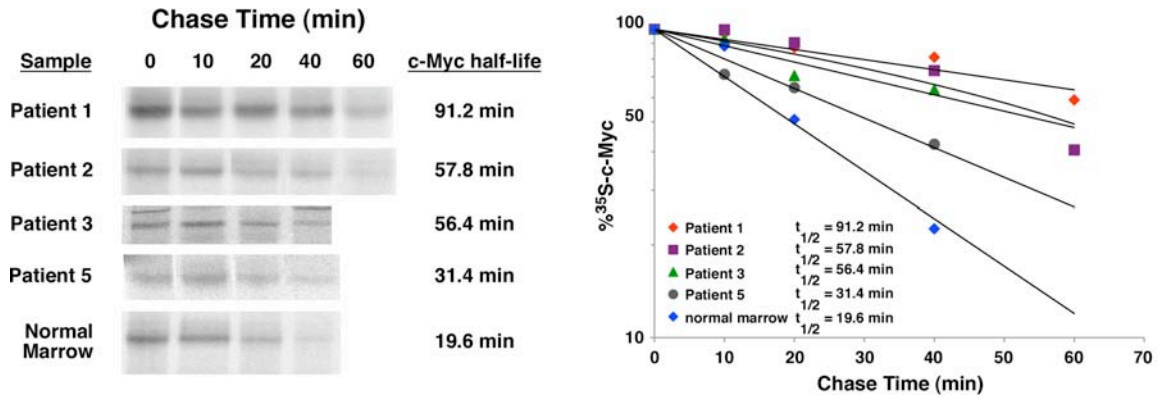
Figure 2.5. c-Myc protein half-life is prolonged in bone marrow samples from pediatric pre-B ALL patients.

A. Stored diagnostic bone marrow samples from pediatric ALL patients were obtained after consent was received from the Oregon Health & Science University Institutional Review Board. Ficolled samples were thawed and maintained in media with 20% FBS for 16–20 h before analysis. Pulse-chase analyses were performed as described for Figure 2.2 and in Materials and methods. This figure shows results from the four pre-B ALL samples in which sufficient c-Myc was detected for quantitation and assessment of half-life. Pulse-chase analyses were also performed on a normal bone marrow sample as a control. c-Myc protein half-life is shown for each sample. The rate of c-Myc degradation over time is depicted in the graph for all four leukemia samples and for the representative normal marrow sample. Data published in (Malempati et al, 2006).

Since our data in pre-B ALL cell lines showed that high c-Myc protein levels are associated with high S62 phosphorylation and low T58 phosphorylation, we were also interested in measuring c-Myc S62 and T58 phosphorylation in samples from B ALL patients. Unfortunately, the samples shown in Table 2.1 were of limited quantity, so we were only able to perform pulse-chase experiments and, in some cases, FISH for *MYC* copy number. In order to extend our study of c-Myc phosphorylation in primary B ALL, we obtained a second set of primary B ALL samples (Table 2.2) and analyzed them for total c-Myc levels and phosphorylation at S62 and T58. As shown in Figure 2.6A, c-Myc levels were variable in the eight B ALL samples. In two cases, high c-Myc levels correlated with increased *MYC* RNA expression (Figure 2.6B, B25 and B68). As a control, we isolated CD19+ B cells from normal peripheral blood. We further analyzed the B ALL samples for levels of S62 and T58 phosphorylation and found that in 5 of 8 of the B ALL samples S62 phosphorylation was elevated relative to the CD19+ cells. T58 phosphorylation was low or undetectable in all of the samples (Figure 2.6A; note the higher molecular weight band is cross-reactive with pS62).

Table 2.2. Clinical features of B ALL cases evaluated for c-Myc S62 and T58 phosphorylation.

Patient ID	Age	Gender	Specimen type	Sample collection[1]	Immunophenotype[2]	pS62 c-Myc[3]	pT58 c-Myc[3]
B25	1	F	bone marrow	relapse	partial CD10, CD19, TDT	+++	+
B40	adult	M	bone marrow	diagnosis	CD10, CD19, TDT	+++	-
B55	1	M	bone marrow	diagnosis	CD10, CD19, CD34, TDT	+	-
B54	23	M	bone marrow	relapse	CD10, CD19, CD34, TDT	++	-
B61	68	F	orbital mass	diagnosis	CD10, CD19, CD20, TDT	+	+
B63	NA	NA	NA	NA	NA	++	-
B66	46	M	blood	diagnosis	CD10, CD19, TDT	+	-
B68	1	F	bone marrow	relapse	CD19, CD34, TDT	++	++

Abbreviations: B ALL, B cell acute lymphoblastic leukemia; F, female; M, male; NA, clinical information not available; TDT, terminal deoxynucleotidyl transferase

[1]Indicates whether sample was collected at the time of initial diagnosis or upon relapse.
[2]Immunophenotype was determined by flow cytometry for each patient.
[3]Relative expression level; - = not detected, + = low, ++ = moderate, +++ = high.

Since S62 phosphorylation is elevated in many of our primary B ALL samples, we hypothesized that this elevation may be due to reduced PP2A activity. PP2A activity could be inhibited through several potential mechanisms, including downregulation of specific PP2A B regulatory subunits or upregulation of endogenous inhibitors of PP2A, like SET or CIP2A. Since the PP2A B regulatory subunit B56α is required for the dephosphorylation of S62 by PP2A, we measured the expression level of B56α (*PPP2R5A*) in this panel of B ALL samples by quantitative real time PCR (qPCR). As shown in Figure 2.6C, we found that two B ALL samples expressed slightly less *PPP2R5A* mRNA than the other B ALL samples analyzed. We next measured the expression level of both SET and CIP2A, two proteins that inhibit PP2A activity, in B ALL samples and in CD19+ B cells as a control. While we did not find a substantial increase in *SET* expression in these B ALL samples (Figure 2.6D), we did find a modest increase in *CIP2A* expression in 6 of 8 B ALL samples (Figure 2.6E). In many cases this increase in *CIP2A* expression correlated with high S62 phosphorylation and low T58 phosphorylation. While not conclusive, these data suggest that PP2A activity may be inhibited in B ALL, which could contribute to the high S62/low T58 phosphorylation pattern seen in many of these samples.
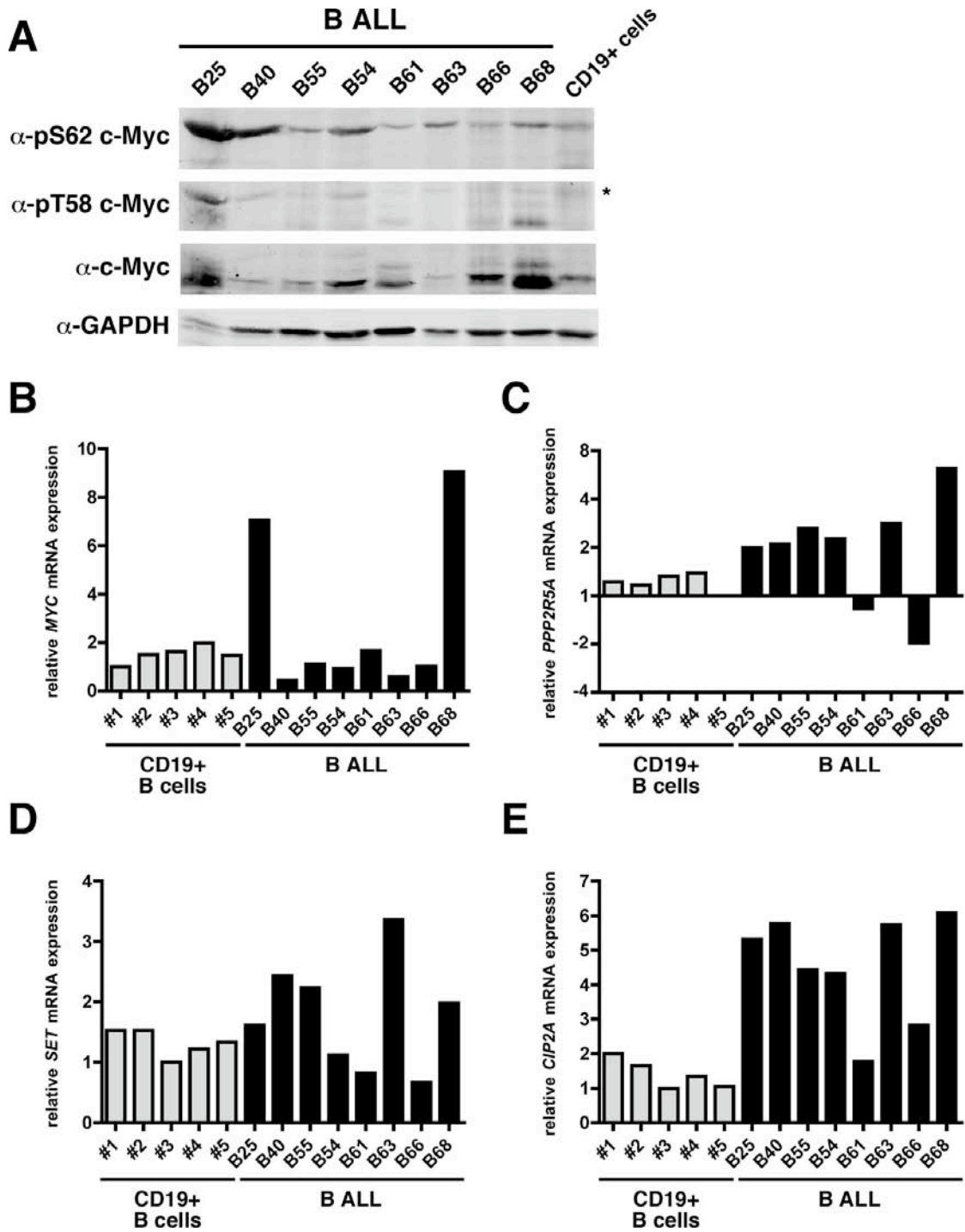
Figure 2.6 c-Myc serine 62 phosphorylation correlates with elevated expression of the PP2A inhibitor *CIP2A* in primary B ALL samples.

A. pS62, pT58, and total c-Myc levels in primary B ALL samples. Stored bone marrow samples from B ALL patients were obtained after consent was received from the Oregon Health & Science University Institutional Review Board. Ficolled samples were thawed and maintained in media with 20% FBS for 4 h before analysis. Cells were lysed in hot 1.5X sample buffer and 4 million cells were loaded in each lane. Protein was separated by SDS-PAGE and immunoblotted using antibodies to pS62, pT58, and total c-Myc (Y69+C19) as described in Materials and methods. Asterisk indicates a non-specific band. **B.** *MYC* mRNA expression in primary B ALL samples. B ALL samples were recovered as in (A) and lysed in Trizol reagent. RNA was purified as described in Materials and methods, reverse transcribed, and cDNA was used for qPCR to detect *MYC* transcript levels. Expression was normalized to expression of *18S* and graphed relative to CD19+ B cells. **C.** B56α (*PPP2R5A*) mRNA expression in primary B ALL samples. qPCR was performed as in (B), using primers specific for *PPP2R5A*. **D.** *SET* mRNA expression in primary B ALL samples. qPCR was performed as in (B), using primers specific for *SET*. **E.** *CIP2A* mRNA expression in primary B ALL samples. qPCR was performed as in (B), using primers specific for *CIP2A*.

While our studies thus far have focused on altered c-Myc protein stability and phosphorylation in B ALL, c-Myc has also been implicated in the development of T cell ALL. In addition to T ALL translocations that juxtapose MYC and T cell receptor loci (Boxer & Dang, 2001), c-Myc has been implicated in the pathogenesis of T ALL as a transcriptional target of Notch (Weng et al, 2006), which is frequently activated in T ALL (Weng et al, 2004). However, whether c-Myc is stabilized in T ALL has not been explored. To determine whether c-Myc stability is increased in T ALL, we measured c-Myc half-life in a panel of 6 T ALL cell lines by ^{35}S-methionine/cysteine pulse-chase analysis. We found that c-Myc half-life was increased in all cases (Figure 2.7A and 2.7B). As before, the control B cell line JY had a short c-Myc half-life (Figure 2.7B). Interestingly, both c-Myc and Notch are targeted for proteasomal degradation by the same E3 ligase, Fbw7, which is mutated in a small percentage of T ALL cases (O'Neil et al, 2007; Thompson et al, 2007). However, c-Myc stability was increased in these T ALL cell lines regardless of their Fbw7 mutational status, which suggests that mechanisms other than Fbw7 mutation may be responsible for increased c-Myc stability in T ALL.
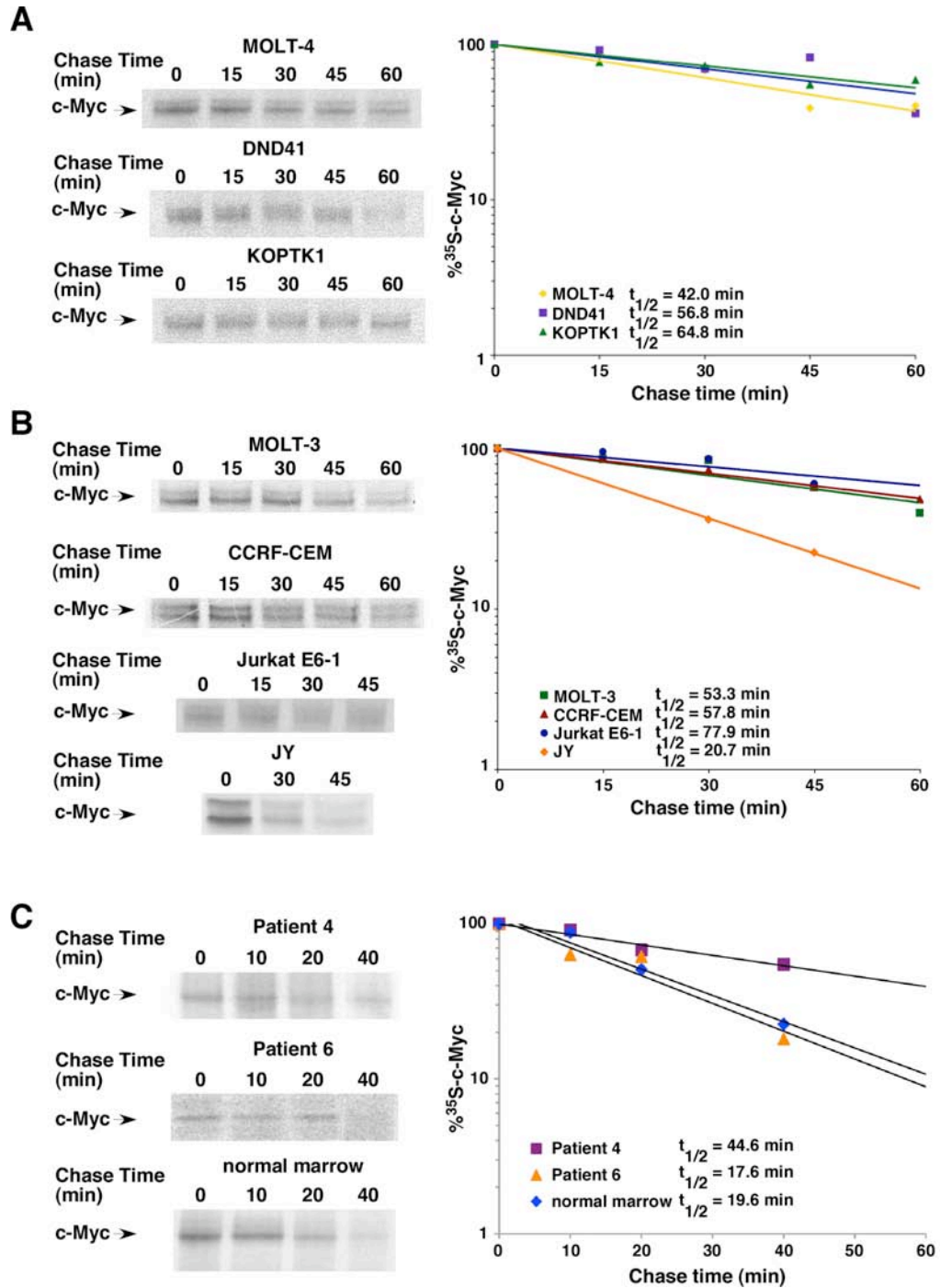
Figure 2.7. c-Myc is stabilized in T ALL cell lines and some T ALL patient samples.

A. The half-life of c-Myc is prolonged in T cell acute lymphoblastic leukemia cell lines with wildtype Fbw7. Pulse-chase analysis of T ALL cell lines was performed and graphed as in Figure 2.2. **B.** The half-life of c-Myc is prolonged in T ALL cell

57

lines with mutant Fbw7. Pulse-chase analysis of T ALL cell lines was performed and graphed as in Figure 2.2. **C.** The half-life of c-Myc is prolonged in one of two bone marrow samples from T ALL patients. Pulse-chase analysis of primary T ALL samples was performed and graphed as in Figure 2.5. Data in (A) and (B) published in (O'Neil et al, 2007); data in (C) published in (Malempati et al, 2006).

To determine whether c-Myc protein stability is increased in primary samples from T ALL patients, we also measured c-Myc protein stability in two pediatric T ALL samples (Table 2.1). We found that c-Myc was modestly stabilized in one of the samples, while the other sample had a short c-Myc half-life similar to that of normal bone marrow (Figure 2.7C). To determine whether the sample with modest c-Myc stabilization carried a *MYC* gene amplification, we assessed *MYC* copy number by FISH and did not find evidence of a *MYC* gene amplification (Table 2.1).

As described above, due to limited quantity, we were not able to study these T ALL samples further. We therefore obtained an additional five T ALL samples (Table 2.3) in order to study c-Myc protein levels and c-Myc S62 and T58 phosphorylation. In these five samples, c-Myc was readily detectable (Figure 2.8A), and in only one case did this correlate with high *MYC* mRNA (Figure 2.8B, T21). We therefore hypothesized that the high levels of c-Myc seen in these samples may be due to changes in c-Myc phosphorylation. As shown in Figure 8A, we detected higher levels of S62 phosphorylation and virtually no T58 phosphorylation in three out of five T ALL samples relative to a representative CD3+ T cell sample, suggesting that the high c-Myc levels are at least partially due to phosphorylation at S62. To determine what might account for this higher S62 phosphorylation, we again hypothesized that PP2A activity may be inhibited. While we found no downregulation of B56α in any of the T ALL samples (Figure 2.8C), we did find a striking upregulation of *SET* in two samples and *CIP2A* in an

additional sample (Figure 2.8D and 2.8E). These results suggest that PP2A

inhibition may be a mechanism of high S62 phosphorylation in T ALL.

Table 2.3. Clinical features of T ALL cases evaluated for c-Myc S62 and T58 phosphorylation.

Patient ID	Age	Gen-der	Specimen type	Sample collection[1]	Immunophenotype[2]	pS62 c-Myc[3]	pT58 c-Myc[3]
T23	18	M	blood	diagnosis	CD3, CD8, TDT	+++	-
T21	14	F	blood	relapse	CD3, CD4, TDT	+	+
T20	29	M	bone marrow	diagnosis	CD2, CD3, CD4, CD7, CD8, CD10, TDT	++	-
T34	3	F	bone marrow	diagnosis	CD1, CD2, CD3, CD7, CD10, TDT	+++	-
T35	4	F	blood	relapse	CD3, CD5, CD7, CD8, CD10	++	-

Abbreviations: F, female; M, male; T ALL, T cell acute lymphoblastic leukemia; TDT, terminal deoxynucleotidyl transferase.

[1]Indicates whether sample was collected at the time of initial diagnosis or upon relapse.
[2]Immunophenotype was determined by flow cytometry for each patient.
[3]Relative expression level; - = not detected, + = low, ++ = moderate, +++ = high.
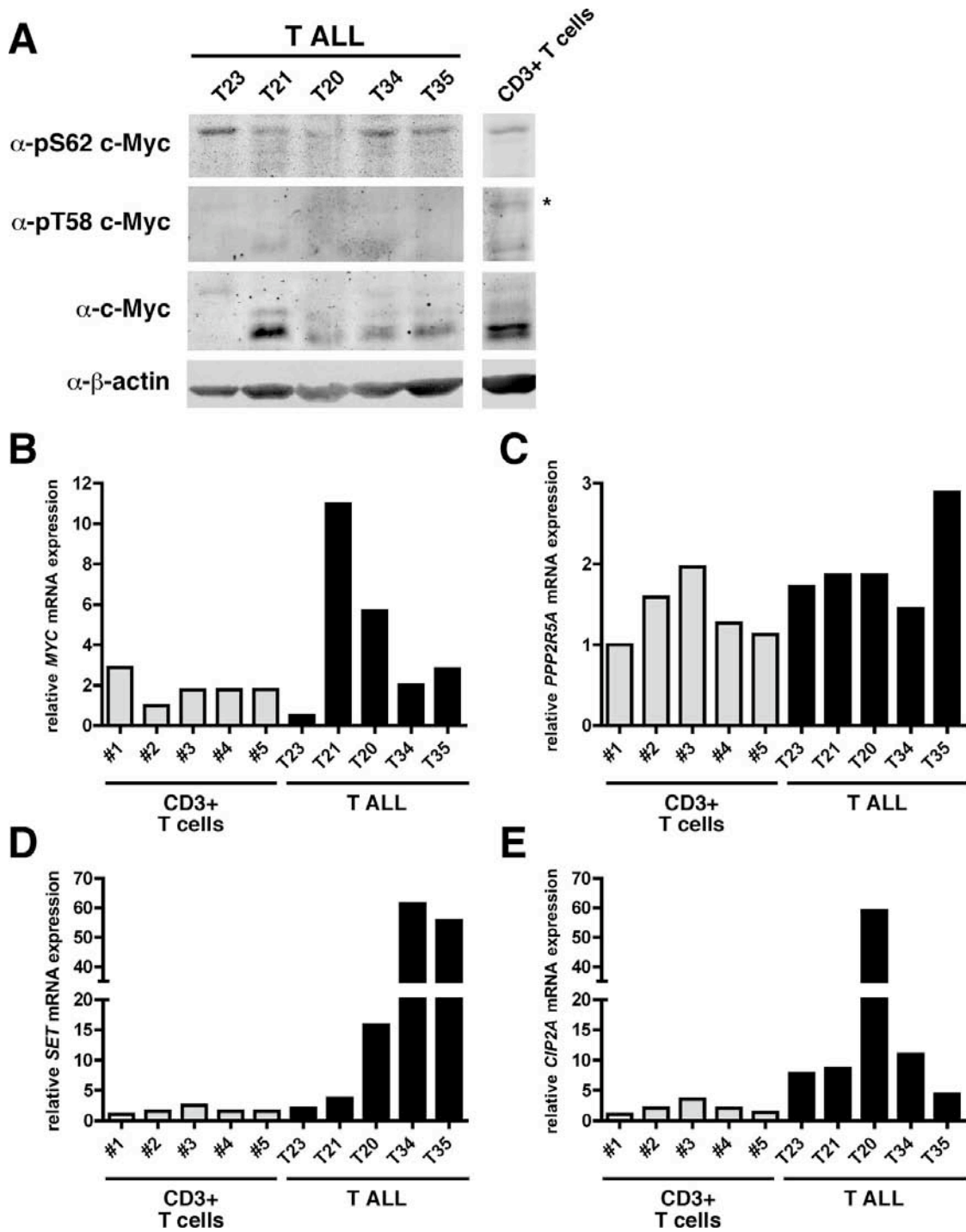
Figure 2.8 c-Myc serine 62 phosphorylation correlates with elevated expression of the PP2A inhibitors *SET* and *CIP2A* in primary T ALL samples.

A. pS62, pT58, and total c-Myc levels in primary T ALL samples. Stored bone marrow samples from T ALL patients were obtained after consent was received from the Oregon Health & Science University Institutional Review Board. Ficolled samples were thawed and maintained in media with 20% FBS for 4 h before

analysis. Cells were lysed in hot 1.5X sample buffer and 5 million cells were loaded in each lane (4 million for CD3+ T cells). Protein was separated by SDS-PAGE and immunoblotted using antibodies to pS62, pT58, and total c-Myc (Y69+C19) as described in Materials and methods. Asterisk indicates a non-specific band. **B.** *MYC* mRNA expression in primary T ALL samples. T ALL samples were recovered as in (A) and lysed in Trizol reagent. RNA was purified as described in Materials and methods, reverse transcribed, and cDNA was used for qPCR to detect *MYC* transcript levels. Expression was normalized to expression of *18S* and graphed relative to CD3+ T cells. **C.** B56α (*PPP2R5A*) mRNA expression in primary T ALL samples. qPCR was performed as in (B), using primers specific for *PPP2R5A*. **D.** *SET* mRNA expression in primary T ALL samples. qPCR was performed as in (B), using primers specific for *SET*. **E.** *CIP2A* mRNA expression in primary T ALL samples. qPCR was performed as in (B), using primers specific for *CIP2A*.

Discussion

In this study we have found that c-Myc protein is stabilized in the absence of *MYC* mutations in acute lymphoblastic leukemia. Specifically, we have shown that c-Myc is stabilized in both pre-B ALL cell lines and samples from pre-B ALL patients. Additionally, in pre-B ALL cell lines c-Myc stabilization correlates with high levels of S62 phosphorylation, which have been shown to increase c-Myc protein stability in fibroblasts (Sears et al, 2000). Also, our studies with LY294002 suggest that in pre-B ALL cell lines increased c-Myc stability depends, at least partially, on signaling through PI3K to inhibit c-Myc proteasomal degradation.

Previously, c-Myc protein stability has been investigated primarily in the context of Burkitt's lymphoma, in which *MYC* is both constitutively expressed due to translocation and also commonly mutated. These studies have shown that when c-Myc is mutated at T58 or P57, c-Myc protein stability is increased (Gregory & Hann, 2000; Niklinski et al, 2000). In contrast, our results show that in two pre-B ALL cell lines c-Myc protein stability is increased in the absence of *MYC* mutations (Figure 2.1, Figure 2.2), suggesting that coding sequence mutations are able, but are not required, to increase c-Myc stability. Our results support the work of others showing that c-Myc stability is also increased in some Burkitt's lymphoma cell lines that do not carry *MYC* mutations (Gregory & Hann, 2000). Collectively, the results suggest that when *MYC* is not mutated, other mechanisms can promote increased c-Myc stability in leukemia.

Our results support the idea that increased c-Myc stability is a common feature of lymphoblastic leukemia. We have shown that c-Myc stability is increased both in pre-B ALL cell lines (Figure 2.2) and in diagnostic bone marrow samples from pre-B ALL patients (Figure 2.5). We have also shown that c-Myc stability is increased in T ALL cell lines and occasionally in samples from T ALL patients (Figure 2.7). However, increased c-Myc stability may not be restricted to only lymphoblastic leukemias. Indeed, our preliminary investigation in cell lines suggests that c-Myc can be stabilized in acute myeloid leukemia as well (Figure 2.9). These results are consistent with the idea that while oncogenes like Ras are commonly deregulated by activating mutations, c-Myc is commonly deregulated through mechanisms that increase its expression (Meyer & Penn, 2008).
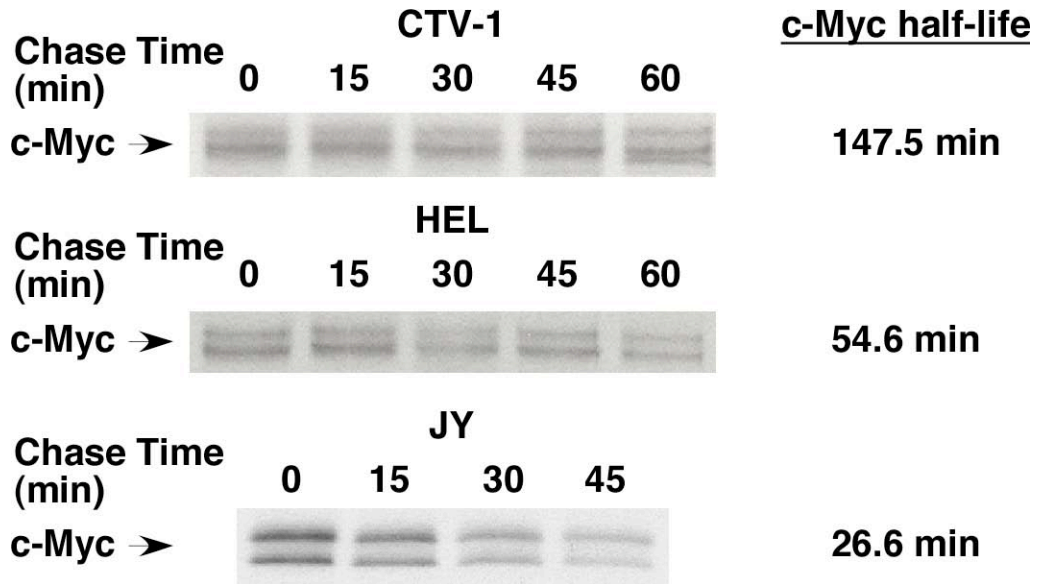
Figure 2.9. The half-life of c-Myc is prolonged in acute myeloid leukemia cell lines.

Pulse-chase analysis of AML cell lines and the immortalized B cell line JY was performed as in Figure 2.2.

We have also shown that c-Myc is commonly phosphorylated at S62 in both ALL cell lines (Figure 2.3) and samples from ALL patients (Figure 2.6, Figure 2.8). Through studies using the c-Myc mutant T58A, we know that S62 phosphorylation not only confers increased c-Myc stability (Salghetti et al, 1999; Sears et al, 2000) but also affects c-Myc function. Expression of T58A causes increased colony formation (Pulverer et al, 1994; Yeh et al, 2004) and accelerates lymphoma development in mice by blocking c-Myc-induced apoptosis (Hemann et al, 2005). Importantly, recent studies have shown that chromatin-bound c-Myc can be phosphorylated at S62 ((Benassi et al, 2006; Hydbring et al, 2010), A. Farrell and R. Sears, unpublished data), suggesting that S62 phosphorylation not only increases c-Myc protein levels and stability but may also potentiate c-Myc transcriptional activity at specific target genes.

What is the mechanism of increased c-Myc stability and increased S62 phosphorylation? As c-Myc is phosphorylated at S62 by both ERK and CDKs in response to proliferative signals and by JNK in response to stress signals (Hann, 2006), diverse mechanisms may contribute to the c-Myc stabilization phenotype in these leukemia cells. However, our results suggest that PI3K activity may play a role in this process. The PI3K pathway has been shown to control the activity of GSK3 (Cross et al, 1995), which phosphorylates c-Myc at T58 and promotes c-Myc degradation (Gregory et al, 2003; Lutterbach & Hann, 1994; Pulverer et al, 1994; Sears et al, 2000). Our results show that blocking PI3K in pre-B ALL cell lines reduces c-Myc protein levels, and this is at least partially dependent on

proteasomal degradation of c-Myc. We also find elevated S62 phosphorylation in primary B and T ALL patient samples. While we did not directly assess PI3K pathway activation in these samples, we did find increased expression of SET and CIP2A, which may contribute to PI3K pathway activation. SET and CIP2A are endogenous inhibitors of PP2A (Junttila et al, 2007; Li et al, 1996), a phosphatase that has been shown to attenuate signaling through the PI3K pathway by dephosphorylating Akt (Andjelkovic et al, 1996; Padmanabhan et al, 2009; Rodgers et al, 2011). Importantly, reactivation of PP2A in leukemia cell lines has been shown to downregulate signaling through the PI3K pathway (Cristobal et al, 2011; Matsuoka et al, 2003; Roberts et al, 2010). However, whether inhibition of PP2A, through elevated expression of SET and CIP2A or other mechanisms, contributes to PI3K pathway activation in ALL remains to be rigorously tested.

In conclusion, our results show that c-Myc stabilization and S62 phosphorylation are common in lymphoblastic leukemia and in fact may constitute a major mechanism of high c-Myc expression in lymphoblastic leukemia. Our results also underscore the importance of defining the mechanisms contributing to increased c-Myc stability and increased S62 phosphorylation in lymphoblastic leukemia. Importantly, the pathways responsible for maintaining high c-Myc expression are likely to be druggable, and therefore may constitute a means of reducing c-Myc protein levels in these leukemias. Indeed, PI3K inhibitors and compounds to activate PP2A are already under development or in clinical trials (Aktas et al,

2010; Ciraolo et al, 2011; Neviani et al, 2007; Switzer et al, 2011). Further study

of the mechanisms by which c-Myc can be stabilized in lymphoblastic leukemia

will clarify relevant pathways for the development of additional targeted

therapies.

Chapter 3: Prevalence of c-Myc serine 62 phosphorylation in myeloid progenitors and acute myeloid leukemia

Abstract

c-Myc is an important regulator of both hematopoiesis and the development of leukemia, but whether phosphorylation of c-Myc is involved in these processes is unknown. Here we describe the prevalence of c-Myc serine 62 (S62) phosphorylation in both human myeloid progenitor cells and acute myeloid leukemia. We find that c-Myc S62 phosphorylation is high in progranulocytes and decreases when these cells are differentiated *in vitro*. We also find that c-Myc is phosphorylated at S62 both in acute myeloid leukemia (AML) patient samples and in cell lines and that this correlates with activating mutations in several receptor tyrosine kinases and Ras. Finally, we find that c-Myc protein levels and DNA binding activity are maintained by activating mutations in Ras and FLT3 in AML cell lines. We propose that phosphorylation of c-Myc at S62 is a regulated event during the expansion of myeloid progenitor cells and may be a downstream mediator of common oncogenic mutations found in AML.

Introduction

c-Myc is a short-lived transcription factor that both activates and represses transcription in order to control many cellular functions, including cellular proliferation, growth, and terminal differentiation (Meyer & Penn, 2008). In the hematopoietic system, c-Myc plays important roles in hematopoiesis, bone marrow homeostasis, and the development of leukemia (Delgado & Leon, 2010). During embryonic development, deletion of *Myc* is lethal due to defects in primary hematopoiesis (Davis et al, 1993; Dubois et al, 2008; He et al, 2008), while deletion of *Myc* in the adult bone marrow causes stem cell depletion and bone marrow failure (Laurenti et al, 2008; Wilson et al, 2004). Thus, proper c-Myc expression is critical for both the development and maintenance of the hematopoietic system. In human leukemia, c-Myc expression is often elevated, and modeling this elevated expression in mice results in malignant transformation and leukemia in many hematopoietic lineages (Delgado & Leon, 2010). Therefore, it is critical to understand how c-Myc expression and activity are regulated in both normal and malignant contexts.

c-Myc protein stability is a major determinant of the expression level of c-Myc in cells, and abundant evidence suggests that c-Myc stability and activity are both regulated by phosphorylation. c-Myc stability is controlled in part by the hierarchical phosphorylation of two conserved residues, serine 62 (S62) and threonine 58 (T58), where phosphorylation of S62 by ERK or CDKs stabilizes c-Myc, and subsequent phosphorylation of T58 by GSK3 triggers proteasomal

degradation of c-Myc (Gregory et al, 2003; Gregory & Hann, 2000; Sears et al, 1999; Sears et al, 2000). Importantly, mutation at T58 increases both c-Myc stability and c-Myc S62 phosphorylation (Lutterbach & Hann, 1994; Sears et al, 2000). Functionally, changes in Myc stability can drive the conversion of hematopoietic stem cells to multipotent progenitor cells, dependent on T58 phosphorylation (Reavie et al, 2010). Phosphorylation can also control c-Myc transcriptional activity, as phosphorylation of S62 is required for c-Myc to associate with at least some of its target genes (Benassi et al, 2006; Hydbring et al, 2010).

In myeloid cells, the functional impact of high S62 phosphorylation has been well studied through the use of v-Myc, which frequently harbors a T58 mutation and, consequently, has high S62 phosphorylation (Lutterbach & Hann, 1994). In primary myeloid cells, expression of v-Myc drives transformation, growth factor independence, and increased colony formation (Lee & Reddy, 1999; Symonds et al, 1989). Importantly, v-Myc promotes these effects to a greater extent than c-Myc (Lee & Reddy, 1999; Symonds et al, 1989), and reversion of the T58 mutation abrogates these effects (Patschinsky et al, 1986; Symonds et al, 1989). These results help explain not only the prevalence of T58 mutations found in v-Myc and Burkitt's lymphoma (Bahram et al, 2000) but also the prevalence of S62 phosphorylation found in some lymphoblastic leukemias (chapter 2 and (Malempati et al, 2006)).

Though S62 phosphorylation has important implications for c-Myc function, little is known about the dynamics of endogenous c-Myc S62 phosphorylation in primary myeloid cells or in myeloid leukemia. In this study we examine endogenous c-Myc S62 and T58 phosphorylation levels both in human bone marrow populations and in an *in vitro* culture system of directed myeloid differentiation and report that c-Myc S62 phosphorylation is high in myeloid progenitor cells and decreases with differentiation. We also find, through the study of both primary acute myeloid leukemia (AML) samples and cell lines, that c-Myc is robustly phosphorylated at S62 and that this correlates with common mutations in AML that activate pathways responsible for c-Myc phosphorylation.

Results

Characterization of phospho-specific serine 62 and threonine 58 c-Myc antibodies

When we began our investigation of endogenous c-Myc S62 and T58 phosphorylation in primary myeloid cells, we consistently observed a complex banding pattern for c-Myc by immunoblot. Therefore, we first performed a careful characterization of the bands detected by both pan-c-Myc antibodies and S62 and T58 phospho-specific antibodies (Figure 3.1). The predominant form of S62-phosphorylated c-Myc that we observed migrated as a high molecular weight band, approximately 68 kDa, and was recognized by two different phospho-S62 (pS62) antibodies (arrowhead, Figure 3.1A, 3.1B, and 3.1C) and three total Myc antibodies (N262, C33, and C19; arrowhead, Figure 3.1A and 3.1B). We also observed less abundant forms of pS62 c-Myc that were present in some cell types and under certain conditions, and these bands migrated between 60-64 kDa (bracket, Figure 3.1A, 3.1B, and 3.1D). These less abundant forms of pS62 c-Myc are also recognized by total Myc antibodies (N262 and C19; bracket, Figure 3.1A and 3.1B).

The predominant form of pT58 c-Myc that we observed migrated at approximately 60kDa, and its presence, along with other T58-phosphorylated bands between 60-64kDa, was dependent upon wildtype T58 and functional GSK3 (bracket, Figure 3.1A) as evidenced by their absence with LiCl treatment to inhibit GSK3 and in the CA46 Burkitt's lymphoma cell line that carries a

mutation in *MYC* preventing T58 phosphorylation. These T58-phosphorylated bands were recognized by the total c-Myc antibodies N262, Y69, and C19, while the c-Myc antibody C33 reacted only weakly with these bands. The total c-Myc antibody N262 also recognizes similar molecular weight bands that were not phosphorylated at T58 (Figure 3.1A, lanes 3 and 4), suggesting that these bands represent c-Myc that is both T58 phosphorylated (all three bands, Figure 3.1A, lane 1) and non-T58/S62 phosphorylated (lower two bands of triplet, Figure 3.1A, lanes 3 and 4 vs lane 1). The pT58 antibody also recognizes a band at 68kDa, but since this band is present in the CA46 cell line (asterisk, Figure 3.1A) where T58 cannot be phosphorylated due to a mutation (Hoang et al, 1995; Malempati et al, 2006), we believe this is a cross-reacting band that does not represent T58 phosphorylation.

To further characterize these bands, we treated cells with the proteasome inhibitor MG132 to block c-Myc degradation. As shown in Figure 3.1D, 4 hours of proteasome inhibition results in accumulation of the lower molecular weight forms of phosphorylated and total c-Myc (brackets, Figure 3.1D), while the high molecular weight pS62 c-Myc does not seem affected by this short MG132 exposure (arrowhead, Figure 3.1D). Importantly, upon serum withdrawal, levels of T58-phosphorylated c-Myc increase and levels of S62-phosphorylated c-Myc decrease (bracket and arrowhead, respectively; Figure 3.1E).

In summary, we have observed that in both cell lines and primary hematopoietic cells multiple species of c-Myc are phosphorylated at S62 and T58. In addition, the predominant S62-phosphorylated species and the predominant T58-phosphorylated species migrate to different positions (68 vs 60 kDa) when analyzed by SDS-PAGE.
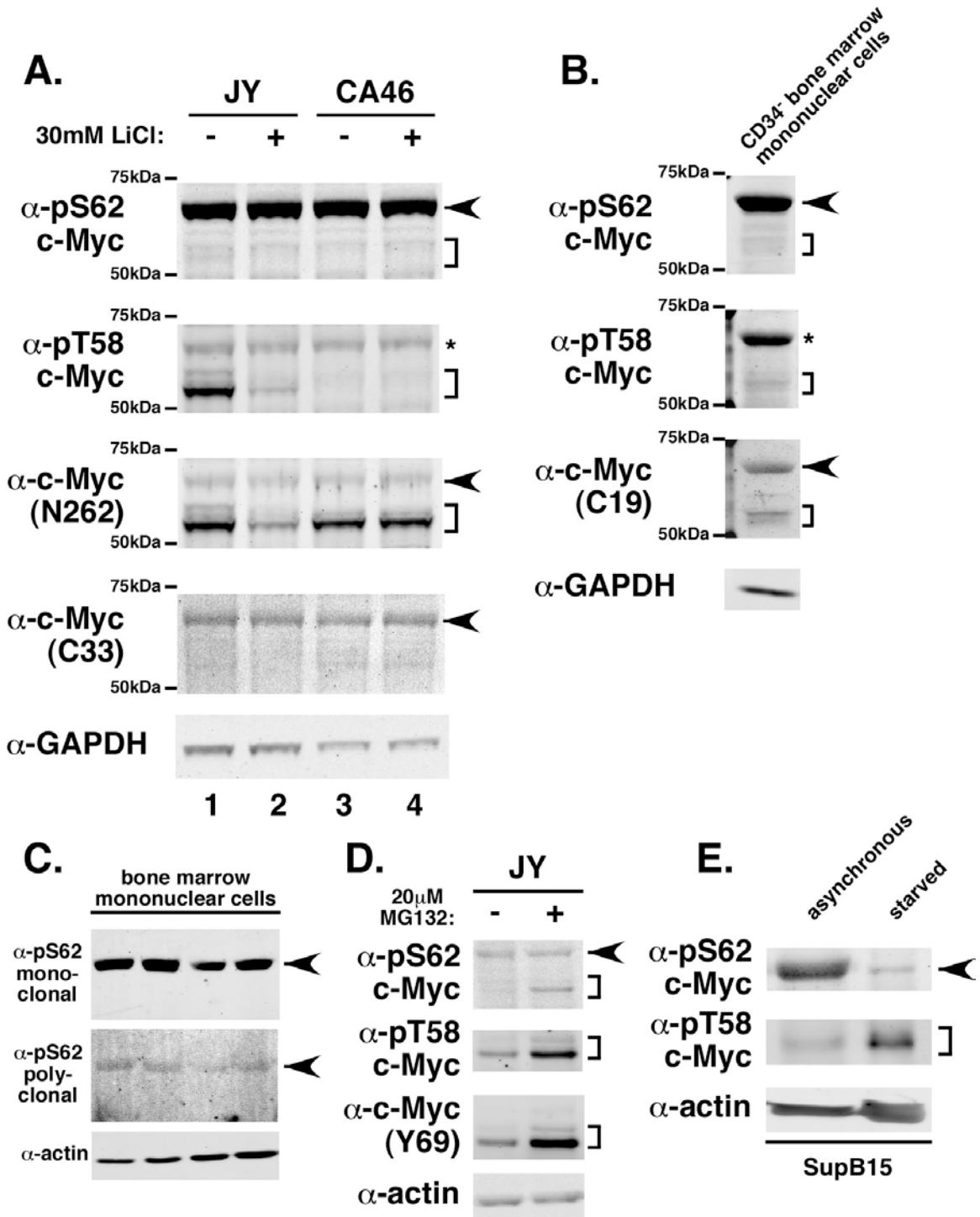
Figure 3.1. Characterization of pan-c-Myc and phospho-specific S62 and T58 c-Myc antibodies.

A. Characterization of pS62 (33A12), pT58, and total c-Myc (N262 and C33) antibodies by inhibiting T58 phosphorylation in cell lines. Proliferating B cell lines JY (c-Myc wt) and CA46 (c-Myc P57S) were treated with 30mM LiCl for 3 hours

and analyzed by immunoblot for expression of pS62, pT58, and total c-Myc. 2.5e5 cells were loaded per lane. **B.** Characterization of pS62 (33A12), pT58, and total c-Myc (Y69 and C19) antibodies in cells from bone marrow. Fresh CD34⁻ bone marrow mononuclear cells were analyzed by immunoblot for expression of pS62, pT58, and total c-Myc. 4e6 cells were loaded. **C.** New monoclonal pS62 antibody and previously characterized polyclonal pS62 antibody recognize the same band. Frozen bone marrow mononuclear cells were recovered and analyzed by immunoblot for expression of pS62 c-Myc using both a monoclonal (33A12) and a polyclonal pS62 antibody. **D.** Phosphorylated c-Myc accumulates when proteasomes are inhibited. Proliferating JY cells were treated with DMSO or 20μM MG132 for 4 hours and analyzed by immunoblot for levels of pS62 (33A12), pT58, and total c-Myc (Y69). **E.** Serum starvation reduces S62 phosphorylation and increases T58 phosphorylation. Proliferating SupB15 cells were cultured in media containing 10% FBS (asynchronous) or 0.2% FBS (starved) for 48 hours and analyzed by immunoblot for levels of pS62 (33A12) and pT58 c-Myc. 2.5e5 cells were loaded per lane. Arrowhead indicates high molecular weight form of c-Myc. Bracket indicates lower molecular weight forms of c-Myc. Asterisk indicates a non-specific band.

c-Myc serine 62 phosphorylation is high in progenitors and decreases during myeloid differentiation

After characterizing our phospho-specific and pan-c-Myc antibodies, we examined c-Myc S62 and T58 phosphorylation in bone marrow cells. To do this, we performed the fractionation scheme shown in Figure 3.2A and described in the Methods. We first depleted whole bone marrow of red blood cells (RBCs) and examined the remaining cells for c-Myc levels and phosphorylation. In this cell population, we detected only the lower molecular weight c-Myc band(s), and they were phosphorylated at both S62 and T58 (Figure 3.2B, lane 1). However, when we fractionated RBC-depleted bone marrow by density sedimentation and removed CD34^{+} cells, we discovered that CD34-depleted low density bone marrow cells displayed a striking enrichment in the high molecular weight isoform of pS62 c-Myc, while maintaining the lower molecular weight species of c-Myc that are pT58, pS62, and non-pT58/pS62 (brackets, Figure 3.2B, lane 2). In contrast, when we examined high density neutrophils from the same fractionation, we detected only the lower species of c-Myc, which was phosphorylated at both S62 and T58 (Figure 3.2B, lane 3).

Since c-Myc stability is increased in hematopoietic multipotent progenitor cells (Reavie et al, 2010), and several different CD34^{-} progenitor populations exist in the low density bone marrow fraction (CFU-G, CFU-M, erythroid precursors, and pro-B cells; (Novershtern et al, 2011)), we hypothesized that the high molecular weight pS62 isoform of c-Myc that is more stable is coming from a progenitor

population. Since isolating these progenitor populations from human bone

marrow for examination by immunoblot would require a prohibitively high number

of cells, we instead tested whether progenitor cells predominantly express the

high molecular weight pS62 c-Myc by employing an *in vitro* culture system where

we could direct granulocytic differentiation from CD34$^+$ bone marrow cells. In this

system, the culture progresses through morphologically identifiable stages from

rapidly dividing progranulocytes to post-mitotic, terminally differentiated

neutrophils (based on (Gowda et al, 1986)). Culturing CD34$^+$ bone marrow cells

under these conditions for 2 days resulted in the majority of cells resembling

progranulocytes (Figure 3.2C, panel 4), a restricted granulocyte progenitor that

transiently expresses high levels of *MYC* mRNA (Gowda et al, 1986), while cells

cultured for 6 or 12 days were skewed heavily toward post-mitotic band forms

and polymorphonuclear (PMN) cells, respectively (Figure 3.2C, panels 5 and 6).

Consistent with our hypothesis, the progranulocytes expressed higher levels of c-

Myc protein (Figure 3.2D, lane 4) but also exhibited robust levels of the high

molecular weight pS62 c-Myc, while later timepoints showed a dramatic

decrease in both this isoform of c-Myc and in total c-Myc levels. Importantly,

these high levels of S62 phosphorylation are not simply a byproduct of *in vitro*

culture, as culturing high density neutrophils (Figure 3.2C, panel 3) did not result

in such a robust level of S62 phosphorylation (Figure 3.2E) as compared to the

low density bone marrow cells (lane 3 vs lane 1). This demonstrates that there is

an enrichment of a high molecular weight pS62 c-Myc during the rapid expansion

of progranulocytes *in vitro*, likely indicating an initial stabilization of c-Myc that is lost as the cells differentiate.

Since T58 phosphorylation has been shown to trigger S62 dephosphorylation and subsequent proteasomal degradation of c-Myc (Gregory et al, 2003; Sears et al, 2000; Yeh et al, 2004), we next asked whether the reduction in S62 phosphorylation and c-Myc protein levels during differentiation is dependent on T58 phosphorylation by GSK3. Indeed, we found that pre-treating progranulocytes with the GSK3 inhibitor LiCl for 4 days prior to harvesting at day 6 increased the level of S62 phosphorylation (Figure 3.2F), suggesting that a GSK3-dependent pathway contributes to the reduction of S62 phosphorylation seen at day 6 (population 5).
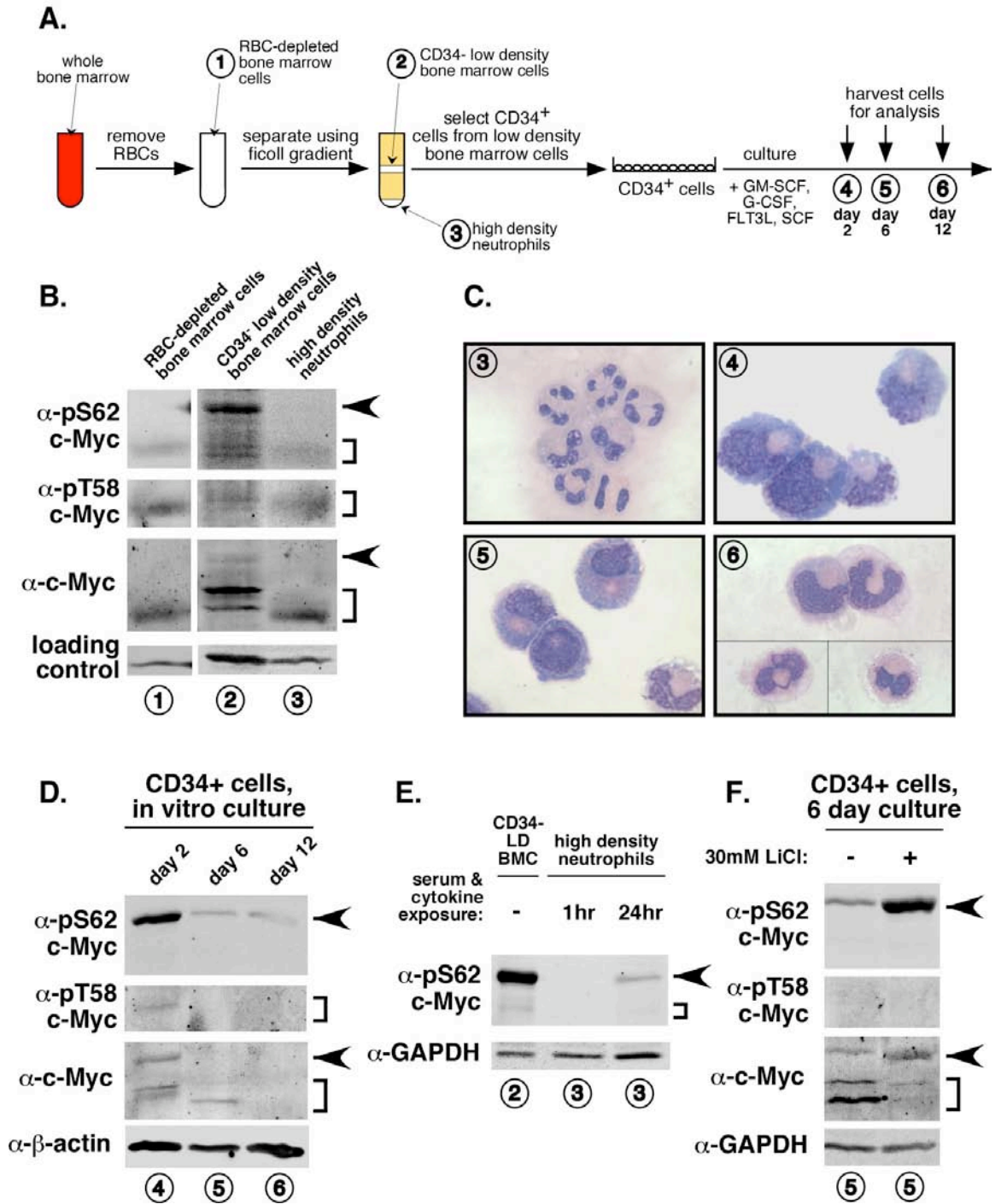
Figure 3.2. c-Myc is phosphorylated at S62 during myeloid differentiation.

A. Schematic of human bone marrow fractionation and *in vitro* myeloid differentiation. See *Methods* for full description. **B.** c-Myc is differentially phosphorylated at S62 and T58 between low density bone marrow cells and high density neutrophils. Fresh red blood cell-depleted bone marrow cells, CD34⁻ low density bone marrow cells (LD BMC), and high density neutrophils were analyzed by immunoblot for expression of pS62, pT58, and total c-Myc

(Y69+C19). 4e6 cells were loaded per lane. Loading control, left – β-actin, right – GAPDH. **C.** Representative images of Giemsa-stained cell populations during *in vitro* myeloid differentiation. Cells were spun onto glass slides, stained with Giemsa stain, and photographed at 1000X magnification. **D.** S62 phosphorylation is reduced during *in vitro* myeloid differentiation. CD34$^+$ cells were cultured (see *Methods*), harvested at the indicated timepoints, and analyzed by immunoblot for expression of pS62, pT58, and total c-Myc (Y69+C19). 2e5 cells were loaded per lane. **E.** Serum and cytokine exposure do not induce robust S62 phosphorylation in high density neutrophils. Fresh high density neutrophils were cultured (see *Methods*) for the indicated times. Neutrophils and uncultured CD34$^-$ LD BMCs (CD34- LD BMC) were analyzed by immunoblot for expression of pS62 c-Myc. 7.5e5 cells were loaded per lane. **F.** Inhibition of GSK3 increases S62 phosphorylation during *in vitro* myeloid differentiation. CD34$^+$ cells were cultured for 48 hours (see *Methods*) then treated with the GSK3 inhibitor lithium chloride (30mM) and cultured for an additional 4 days. Cells were harvested after 6 days of culture and analyzed by immunoblot for expression of pS62, pT58, and total c-Myc (Y69+C19). Arrowhead indicates high molecular weight pS62 band. Bracket indicates lower molecular weight forms of c-Myc. Circled numbers in each panel indicate a population from the schematic in (A).

c-Myc S62 phosphorylation in AML correlates with the activation of upstream signaling pathways

c-Myc has well-established roles both in driving proliferation and in blocking the terminal differentiation of myeloid cells (Delgado & Leon, 2010). Acute myeloid leukemia is a disease characterized by the accumulation of immature myeloid cells, a consequence of deregulated proliferation and an inability to differentiate (Lowenberg et al, 1999). Since our data has established S62 phosphorylation as a feature of proliferating myeloid progenitors, we asked whether high S62 phosphorylation was a feature of AML. In a panel of 15 apheresis samples from patients with AML (Table 3.1), we found much higher levels of pS62 c-Myc in all 15 samples (arrowhead, Figure 3A) relative to normal monocytes (sample N3) and normal polymorphonuclear (PMN) cells (sample N1, N2), which were even lower than normal monocytes (N3, lane 3). In contrast, levels of pT58 c-Myc (bracket, Figure 3.3A) were variable across the AML samples; half of the samples had reduced levels of pT58, and half of the samples had increased pT58, relative to normal monocytes and PMN cells.

Since *MYC* can be transcriptionally upregulated in AML by both transcription factor fusion products and activated tyrosine kinases like FLT3 (Kim et al, 2005; Muller-Tidow et al, 2004; Rice et al, 2009), we also examined *MYC* mRNA expression in these AML samples. As controls, we examined *MYC* mRNA expression in normal bone marrow, monocytes, and polymorphonuclear cells. While the differentiated cells (CD14+ monocytes and polymorphonuclear cells)

had lower *MYC* mRNA expression than normal bone marrow, consistent with the

downregulation of *MYC* during differentiation, the expression level of *MYC* in

most AML samples was within the range of *MYC* expression found in normal

bone marrow (Figure 3.3B). This suggests that c-Myc is not only highly S62

phosphorylated in AML, similar to normal progranulocytes, but in many cases

MYC mRNA is also highly expressed.
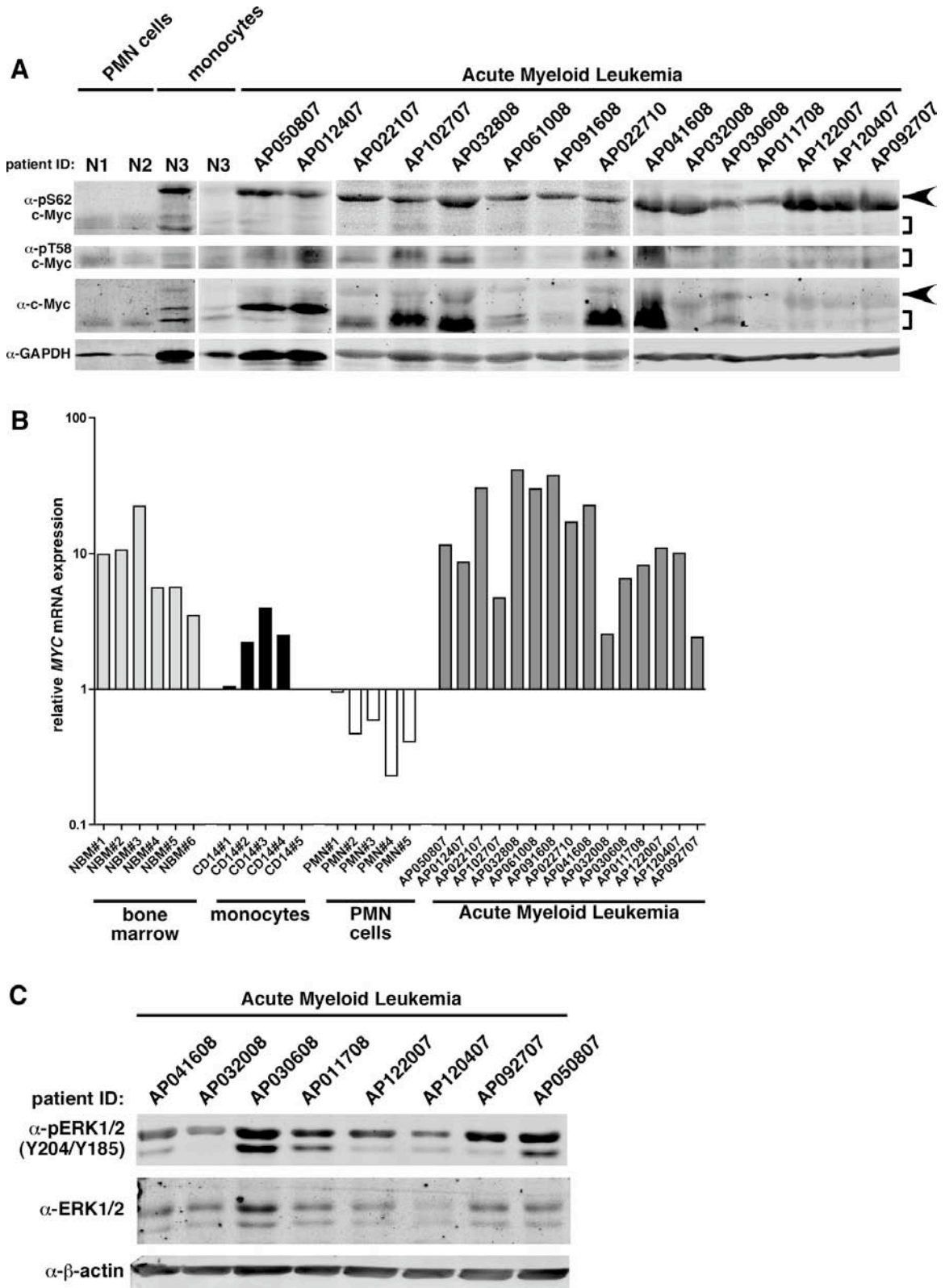
Figure 3.3. c-Myc S62 phosphorylation correlates with ERK activation in primary acute myeloid leukemia samples.

A. Levels of pS62 and pT58 c-Myc in primary acute myeloid leukemia (AML) samples and in differentiated myeloid cells from healthy volunteers. Frozen apheresis samples from 15 AML patients were recovered (except AP022710, which was fresh) or differentiated myeloid cells (monocytes or polymorphonuclear cells) were isolated from 3 fresh peripheral blood samples, and cells were analyzed by immunoblot for levels of pS62, pT58, and total c-Myc (Y69+C19). 4e6 cells were loaded per lane. Arrowhead indicates high molecular weight pS62 band. Bracket indicates lower molecular weight forms of c-Myc. **B.** *MYC* mRNA expression in normal bone marrow (NBM), CD14$^+$ monocytes (CD14$^+$), polymorphonuclear cells (PMN), and primary AML samples. Samples were recovered or isolated as in (A) and lysed in Trizol reagent. RNA was purified as described in Materials and methods, reverse transcribed, and cDNA was used for qPCR to detect *MYC* transcript levels. Expression was normalized to expression of *18S* and graphed relative to CD14+#5. **C.** Expression of pERK1/2 in primary AML samples. A subset of samples from (A) was analyzed by immunoblot for expression of pERK1/2 (Y204/Y185) and total ERK1/2. 5e5 cells were loaded per lane.

Activating mutations in tyrosine kinases like FLT3 or signaling molecules like Ras are frequently found in AML (Renneville et al, 2008) and may play a role in maintaining c-Myc S62 phosphorylation. We sequenced our 15 AML samples by Sequenom MassARRAY for mutations in *FLT3*, *RAS*, and other common cancer-associated mutations. As shown in Table 3.1, we found that 8 of 15 samples carry an activating mutation in *N-* or *K-RAS*, *MET*, *c-KIT*, or *FLT3* (either a point mutation or internal tandem duplication (ITD)). All of these molecules have been previously shown to signal through the MAPK and PI3K pathways (Derksen et al, 2003; Renneville et al, 2008), which are also responsible for modulating c-Myc S62 and T58 phosphorylation (Sears et al, 1999; Sears et al, 2000). Importantly, all of these mutations correlate with robust S62 phosphorylation in our AML samples.

Because activated ERK can enhance c-Myc protein stability by directly phosphorylating c-Myc at S62 (Lutterbach & Hann, 1994; Sears et al, 1999; Sears et al, 2000), we analyzed pERK levels by immunoblot in a subset of our AML samples. As shown in Figure 3.3C, ERK phosphorylation was readily detected in all of the AML samples analyzed, including those with mutations in *FLT3* or *RAS* (patients AP032008, AP030608, AP011708, AP120407, AP050807).

Table 3.1. Clinical characteristics, mutations, karyotype, and c-Myc S62 and T58 phosphorylation status of acute myeloid leukemia patients.

Patient ID	Age	Gen-der	WBC count[1]	AML sub-type	Mutations[2]	Karyotype	NPMc+	FLT3 -ITD	pS62 c-Myc[3]	pT58 c-Myc[3]
AP050807	40	F	12.5	M3	K-Ras Q61P	t(15;17)	ND	ND	++	++
AP012407	22	M	NA	M2	Met E168D	normal	NA	Pos	++	+++
AP022107	75	F	277	M1	NPM1[4]	normal	ND	Neg	++	++
AP102707	9	M	113.8	M2	wildtype	normal	ND	Neg	++	+++
AP032808	20	M	359.4	M4eo	wildtype	inv(16)	ND	Neg	+++	+++
AP061008	55	M	34.4	M2	Met N375S[5,6]	inv(16); trisomy22; trisomy8	Neg	Neg	++	+
AP091608	81	F	85.5	M0	wildtype	normal	Neg	Neg	++	+
AP022710	69	M	NA	M4	Met N375S[5]	trisomy8	NA	Pos	++	+++
AP041608	41	F	56.6	M5	wildtype	t(9;11); trisomy8; addtl copy der 9	Neg	Neg	+++	+++
AP032008	76	M	214	M5	FLT3 S451F NPM1[4]	normal	Pos	Neg	+++	+
AP030608	37	M	109	M5	IDH1 R132H N-Ras Q61H NPM1[7]	normal	Pos	Neg	++	+
AP011708	72	M	174.4	M5	K-Ras G12V	monosomy7	Neg	Neg	++	+
AP122007	38	M	82.8	M2	IDH1 R132H NPM1[4]	normal	Pos	Neg	+++	+
AP120407	52	M	60.5	M2	NPM1[4]	normal	Pos	Pos	+++	+
AP092707	79	M	96	M5	NPM1[4]	normal	Pos	ND	+++	+

Abbreviations: F, female; FLT3, fms-related tyrosine kinase 3; FLT3-ITD, FLT3 with internal tandem duplication; IDH1, isocitrate dehydrogenase 1; M, male; NA, not available; ND, not determined; neg, negative; NPM1, nucleophosmin 1; NPMc+, cytoplasmic localization of nucleophosmin 1; pos, positive; pt, patient; WBC, white blood cell.

[1] Value of WBC count is in thousands of cells per microliter.
[2] Mutations determined by Sequenom MassARRAY.
[3] relative expression level; + = low, ++ = moderate, +++ = high.
[4] NPM1 W288 frameshift mutation, insertion of TCTG.
[5] Met N375S was scored as a single nucleotide polymorphism.
[6] Pt. 4 was also positive for c-KIT exon 8 insertion/deletion.
[7] NPM1 W288 frameshift mutation, insertion of CCTG.

The activation of upstream signaling pathways in AML maintains c-Myc levels and activity

To test whether these activating mutations are responsible for maintaining c-Myc S62 phosphorylation, we turned to AML cell lines bearing the same activating mutations as some of our primary AML samples (Figure 3.4A). As shown in Figure 3.4B, proliferating Kasumi-1, MOLM-14, MOLM-13, and MV4-11 AML cells all have high levels of high molecular weight pS62 c-Myc. We hypothesized that inhibiting MAPK activity downstream of these activating mutations would reduce S62 phosphorylation. However, treating these cell lines with the MEK inhibitor U0126 reduces the level of both pERK and one of the total c-Myc bands (lower band, bracket; Figure 3.4C) but not the high molecular weight pS62 c-Myc band (arrowhead; Figure 3.4C).

FLT3-ITD is a common mutation in AML and is known to confer constitutive activation to the FLT3 receptor (Gilliland & Griffin, 2002; Kiyoi et al, 1998). To test whether FLT3 activity contributes to c-Myc S62 phosphorylation in cell lines with FLT3-ITD, we treated MOLM-13, MOLM-14, and MV4-11 cells with AC220, an inhibitor that is highly specific for FLT3-ITD (Zarrinkar et al, 2009). In the MOLM-13 and MOLM-14 cell lines, but not the MV4-11 cells, FLT3 inhibition reduced levels of pERK, suggesting that FLT3 activity signals through the MAPK pathway. In addition, this result suggests the *RAS* mutation present in the MV4-11 cells is maintaining ERK phosphorylation regardless of FLT3 inhibition (Figure 3.4D). FLT3 inhibition also reduced the lower total c-Myc band in the MOLM-13

and MOLM-14 cell lines but not the MV4-11 cell line (lower band, bracket; Figure

3.4D). This suggests that FLT3 activity contributes to the maintenance c-Myc

levels in the MOLM-13 and MOLM-14 cell lines. However, inhibition of FLT3 did

not reduce the high molecular weight pS62 c-Myc (arrowhead; Figure 3.4D). This

suggests that these cells contain two different pools of c-Myc: one that is

sensitive to short-term inhibition of FLT3 and MAPK signaling and one that is

resistant. However, we do find that longer treatment (24hrs) with these inhibitors

can deplete this prevalent form of pS62 c-Myc found in AML (Figure 3.4E and

3.4F).

Even though short-term inhibition of FLT3 and MAPK activity did not reduce the

level of high molecular weight pS62 c-Myc, these pathways may still control c-

Myc DNA binding activity. To determine whether signaling through FLT3 and

MAPK affects c-Myc promoter binding, we performed chromatin

immunoprecipitation in the MOLM-14 cells after treatment with AC220 or U0126.

Blocking FLT3 or MAPK activity with these inhibitors dramatically reduced the

association of c-Myc with its target gene nucleolin (Figure 3.5). Taken together,

these data suggest that constitutively active FLT3 or Ras maintain c-Myc protein

levels and promotes c-Myc chromatin association, potentially by signaling

through ERK kinase.
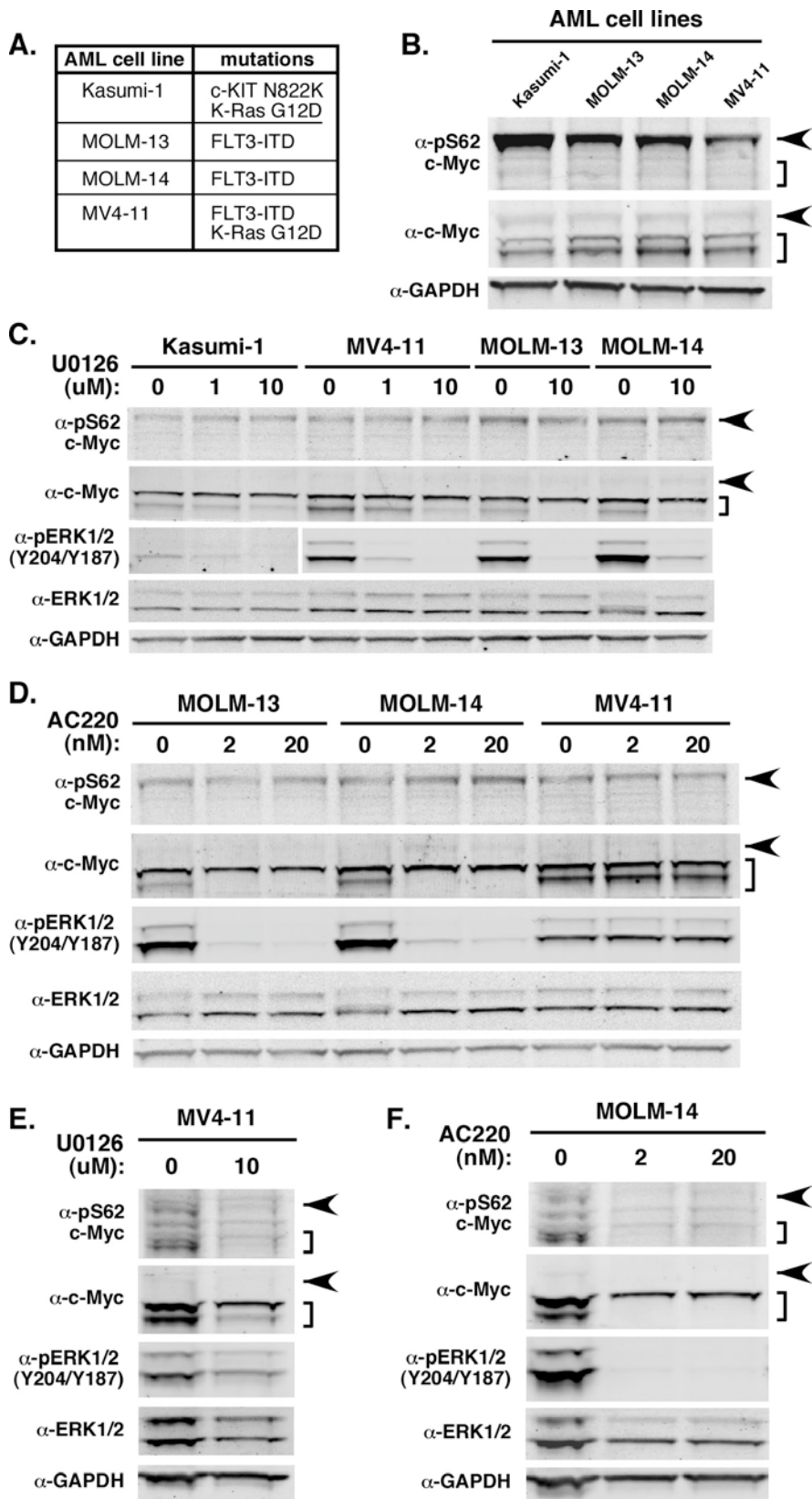
Figure 3.4. Activated FLT3 and Ras control c-Myc levels and serine 62 phosphorylation in AML cell lines.

A. Table showing mutations present in the indicated AML cell lines. **B.** AML cell lines express high molecular weight pS62 c-Myc. Proliferating Kasumi-1, MOLM-14, MOLM-13, and MV4-11 cells were harvested and analyzed by immunoblot for expression of pS62 and total c-Myc (C19). 2e5 (left) or 2.25e5 (right) cells were loaded per lane. **C.** Inhibition of MEK in AML cell lines with FLT3 or Ras mutations reduces c-Myc protein levels. Kasumi-1, MV4-11, MOLM-13, and MOLM-14 cells were starved in media containing 1% FBS for 24 hours, then treated with DMSO or the MEK inhibitor U0126 (1 or 10μM) for 4 hours. Cells were harvested and analyzed by immunoblot for expression of pS62 c-Myc, total c-Myc (C19), pERK1/2, and total ERK1/2. 2.25e5 cells were loaded per lane. **D.** Inhibition of FLT3 in AML cell lines with FLT3-ITD, but not FLT3-ITD and mutant K-Ras, reduces ERK phosphorylation and c-Myc protein levels. MOLM-13, MOLM-14, and MV4-11 cells were starved in media containing 1% FBS for 24 hours, then treated with DMSO or the FLT3 inhibitor AC220 (2 or 20nM) for 8 hours. Cells were harvested and analyzed by immunoblot for expression of pS62 c-Myc, total c-Myc (C19), pERK1/2, and total ERK1/2. 2.25e5 cells were loaded per lane. **E.** Prolonged inhibition of MEK in MV4-11 cells reduces c-Myc levels and the level of high and low molecular weight pS62 c-Myc. MV4-11 cells were starved in media containing 1% FBS for 24 hours, then treated with DMSO or the MEK inhibitor U0126 (10μM) in 1% FBS for an additional 24 hours. Cells were harvested and analyzed by immunoblot for expression of pS62 c-Myc, total c-Myc (C19), pERK1/2, and total ERK1/2. 4.5e5 cells were loaded per lane. **F.** Prolonged inhibition of FLT3 in MOLM-14 cells reduces ERK phosphorylation, c-Myc levels, and the level of high and low molecular weight pS62 c-Myc. MOLM-14 cells were starved in media containing 1% FBS for 24 hours, then treated with DMSO or the FLT3 inhibitor AC220 (2 or 20nM) in 1% FBS for an additional 24 hours. Cells were harvested and analyzed by immunoblot for expression of pS62 c-Myc, total c-Myc (C19), pERK1/2, and total ERK1/2. 4.5e5 cells were loaded per lane.
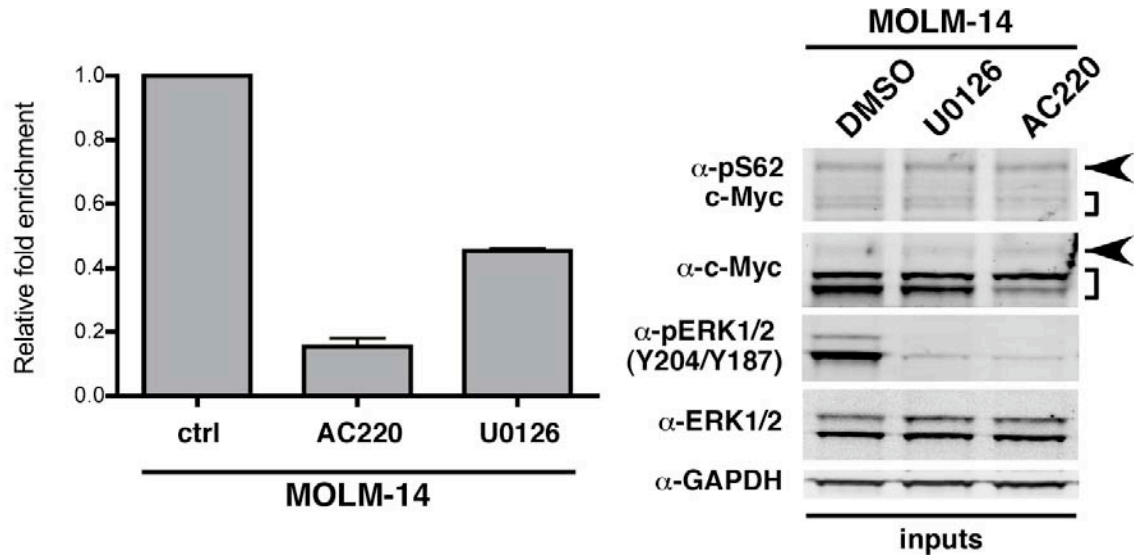
Figure 3.5. Activated FLT3 and Ras control c-Myc DNA binding activity in an AML cell line.

MOLM-14 cells were starved in media containing 1% FBS for 48 hours, treated with DMSO, the FLT3 inhibitor AC220 (20nM), or the MEK inhibitor U0126 (10μM) for 30 min, and then stimulated with 20% FBS. Cells were harvested after 1 hr of serum stimulation and subjected to chromatin immunoprecipitation using a total c-Myc antibody (N262) or rabbit IgG to control for background binding. Immunoprecipitated DNA was amplified by qPCR using primers for nucleolin, and enrichment is calculated as a percentage of the input DNA and is relative to the amount of amplification in the IgG pull-down. Enrichment is then graphed relative to the enrichment in DMSO-treated cells. Arrowhead indicates high molecular weight pS62 band. Bracket indicates lower molecular weight forms of c-Myc.

Discussion

In this study we examined endogenous c-Myc S62 and T58 phosphorylation levels in both primary human bone marrow and acute myeloid leukemia. We found that c-Myc is phosphorylated at S62 in myeloid progenitor cells and that this decreases during myeloid differentiation. We also found that c-Myc is robustly phosphorylated at S62 in AML and that this correlates with common mutations in AML that activate pathways responsible for c-Myc phosphorylation. In our experiments, we observed that progranulocytes, a type of myeloid progenitor cell, express a high molecular weight form of pS62 c-Myc, but that in terminally differentiated neutrophils this expression is lost, while expression of pT58 is gained. This is supported by our observation that CD34⁻ low density bone marrow cells, a fraction containing progranulocytes and other progenitor cells, were enriched for this high molecular weight form of pS62 c-Myc. We also observed that this high molecular weight form of pS62 c-Myc was expressed by all of the primary AML samples and cell lines that we examined. Finally, we demonstrated that c-Myc levels and activity in AML cell lines were at least partially dependent on constitutively active signaling pathways downstream of mutations in FLT3 or Ras.

Our results showing S62 phosphorylation in progranulocytes extend our previous findings in fibroblasts that c-Myc protein stability and S62 and T58 phosphorylation are regulated as cells emerge from quiescence and enter the cell cycle. One biological context where this occurs is during the transition of self-

renewing LT-HSCs (long-term hematopoietic stem cells) to multipotent progenitor cells. LT-HSCs (defined as Lin$^-$ Sca$^+$ Kit$^+$ CD150$^+$ CD148$^-$ in mice) are a quiescent hematopoietic stem cell population (Wilson et al, 2008) that expresses *Myc* mRNA (Laurenti et al, 2008) but has low levels of c-Myc protein (Reavie et al, 2010). As these cells differentiate into progenitor populations with lower self-renewal capacity, *Myc* mRNA levels remain constant (Laurenti et al, 2008), but c-Myc protein levels increase due to the stabilization of c-Myc protein (Reavie et al, 2010). Importantly, c-Myc stability in LT-HSCs, as well as in more differentiated populations like multipotent progenitors and myeloerythroid progenitors, is controlled by the pT58-dependent E3 ligase Fbw7 (Reavie et al, 2010), suggesting that a pT58-dependent degradation pathway controls c-Myc protein levels in these populations. Since T58 phosphorylation requires prior S62 phosphorylation (Sears et al, 2000), c-Myc protein stability in these populations is likely modulated by the interplay of S62 and T58 phosphorylation. As stabilized c-Myc both depletes LT-HSCs and impairs their self-renewal capacity (Reavie et al, 2010), we speculate that LT-HSCs, as they exit the bone marrow niche, may receive signals that culminate in the phosphorylation of S62, which transiently stabilizes c-Myc and drives the expansion of progenitor cells. These signals may maintain S62 phosphorylation, and thus c-Myc stabilization, in multipotent progenitors and committed progenitors like progranulocytes (Figure 3.2). Following this, c-Myc is downregulated both at the protein level (Figure 3.2) and the mRNA level (Gowda et al, 1986) for the completion of terminal differentiation. This is supported by the dramatically lower level of *MYC* mRNA and protein in

polymorphonuclear cells compared to bone marrow mononuclear cells (Figure 3.2B and 3.3B) and many studies showing that high c-Myc expression is incompatible with terminal differentiation both *in vitro* and *in vivo* (Amanullah et al, 2000; Coppola & Cole, 1986; Jayapal et al, 2010; Larsson et al, 1988; Takayama et al, 2010; Wall et al, 2008).

The finding that AMLs with diverse mutations and FAB classifications all share expression of high molecular weight pS62 c-Myc is intriguing in light of the natural occurrence of high S62 phosphorylation in myeloid progenitor cells. If S62 phosphorylation is a feature of proliferating progenitor cells, then it is reasonable that leukemic cells, which are also undifferentiated and rapidly dividing, likewise express high levels of S62 phosphorylation. However, an important distinction is that proliferating progenitor cells likely stabilize c-Myc in response to the regulated stimulation of signaling pathways, while leukemic cells may stabilize c-Myc in response to persistent stimulation of these pathways, such as that provided by activating mutations. Mutations in Ras and in receptor tyrosine kinases like FLT3 and c-KIT are common in AML and confer constitutive activation to these molecules. Our results suggest that these activating mutations maintain high c-Myc protein levels in AML and may do so through the activation of ERK (Figure 3.4). However, mutations in FLT3-ITD and K-Ras may not be functionally redundant. This is supported by our result in the AML cell line MV4-11 that both pERK and total c-Myc were reduced upon inhibition of MEK but not inhibition of FLT3 (Figure 3.4C and 3.4D). This is likely due to the presence of an

activating K-Ras mutation, which can maintain high c-Myc levels even though FLT3-ITD is inhibited.

Our original hypothesis was that FLT3-ITD and Ras mutations signal through ERK to maintain pS62, and we have previously shown that ERK can phosphorylate S62 in response to serum stimulation (Sears et al, 2000). However, we did not find a change in the total level of the high molecular weight pS62 c-Myc after short-term inhibition of FLT3 or MEK, though pERK and total c-Myc levels were decreased (Figure 3.4C and 3.4D). We have also observed that the lower molecular weight forms of c-Myc that are S62-phosphorylated do respond to short-term inhibition of FLT3 or MEK (data not shown). These data lead us to speculate that the lower molecular weight forms of c-Myc are responsible for the changes in c-Myc DNA binding activity with FLT3 or MEK inhibition (Figure 3.5), and that the high molecular weight pS62 form of c-Myc is bound in an insoluble pool that is not degraded quickly like the lower molecular weight form (Figure 3.1D). This is supported by our results that 48 hours of starvation are required to fully deplete the high molecular weight form of pS62 c-Myc from cells (Figure 3.1E).

While here we focused on whether FLT3 and Ras mutations maintain S62 phosphorylation in AML, other common mutations found in AML may also play a role in stabilizing c-Myc. Several of our primary AML samples carried an insertional mutation in Nucleophosmin1 (NPM1) that causes its cytoplasmic

localization (NPMc+; (Falini et al, 2005)). NPMc+ mutations are the most common mutation in karyotypically normal AML and are hypothesized to be an initiating mutation in this AML subtype (Falini et al, 2011; Falini et al, 2005; Martelli et al, 2010). NPM1 has been reported to bind directly to c-Myc and to enhance both c-Myc transcriptional activity and c-Myc transforming activity (Li et al, 2008). In addition, the mutant form of NPM1, NPMc+, has been directly implicated in stabilizing c-Myc through the aberrant degradation of Fbw7γ (Bonetti et al, 2008), which could be an additional mechanism of c-Myc stabilization in AML.

We were surprised to find such a complex c-Myc banding pattern in different populations of myeloid cells, both normal and leukemic. However, we believe that these bands represent bona fide c-Myc for two reasons. First, the three major bands (Figure 3.1, arrowhead and bracket) are detected by as many as seven c-Myc antibodies. The majority of these antibodies differ in the epitopes they were raised against and the species in which they were produced. Second, these bands change in response to proteasome inhibition (Figure 3.1D), serum starvation (Figure 3.1E), and/or GSK3 inhibition (Figure 3.2F), all of which are established techniques for modulating c-Myc protein stability. Because of these factors, we find it unlikely that these bands are non-specific or a technical artifact.

Why then are there such differences in the migration and banding patterns of c-Myc across these samples? The reason for the differential migration of the c-Myc

isoforms we have described and why they change with the differentiation status of the cells is unknown. c-Myc is predicted to run at 49kDa, but has long been reported to run at 64 and 68kDa in human cells (Hann & Eisenman, 1984). Higher molecular weight forms of c-Myc have been attributed to both the use of an alternate translation start site (Myc1 vs Myc2) and post-translational modifications. However, we do not think that the high molecular weight pS62 band represents Myc1. In our hands, this high molecular weight pS62 band is most abundant in proliferating cell lines at low cell density and is downregulated upon serum withdrawal (Figure 3.1). In contrast, expression of Myc1 is induced both by growth arrest from extremely high cell densities and during nutrient deprivation (Hann et al, 1992). The possibility that this high molecular weight pS62 band may be due to a post-translational modification is more likely. However, we do not think this band represents a monoubiquitinated form of c-Myc, as we were not able to detect a ubiquitin moiety following immunoprecipitation with our monoclonal pS62 antibody (data not shown). An intriguing possibility is that this band represents a form of c-Myc isomerized by Pin1 to a cis conformation, creating a bend in the protein that impedes its migration. Pin1 promotes both the *trans-cis* and *cis-trans* isomerization of c-Myc proline 63 – *trans-cis* isomerization occurs following phosphorylation of S62 by the trans-specific kinase ERK, and *cis-trans* isomerization occurs following T58 phosphorylation and before dephosphorylation of S62 by the trans-specific phosphatase PP2A ((Yeh et al, 2004); A. Farrell and R. Sears, unpublished data). This possibility is supported by our data that the high molecular weight

pS62 band does not appear to be T58-phosphorylated, and the lower molecular weight c-Myc band(s) can be phosphorylated at both S62 and T58. In addition, prolines are known to affect the conformation of proteins (Hung et al, 2002; Proft et al, 1995; Williamson, 1994) and other groups have suggested that changes in protein migration on an SDS-PAGE gel could derive from proline *cis-trans* conformational changes (Kirkland et al, 1998), though this has not been formally demonstrated.

Despite our uncertainty of the mechanism behind the slower migrating pS62 c-Myc band, our finding that this form of pS62 c-Myc is present in AMLs with constitutively active mutations in FLT3 and Ras has important implications. While our panel of primary samples is small and is derived from patients who underwent apheresis due to high white cell counts, the universal expression of pS62 c-Myc that we observed suggests that a strategy to promote c-Myc degradation may be a beneficial therapy for AML, regardless of subtype. Currently, patients diagnosed with AML are stratified into risk groups using their mutation and karyotype information, but the majority of AML diagnoses receive the same induction therapy regardless of underlying genetic abnormalities (with the exception of acute promyelocytic leukemia) (Tallman et al, 2005). Therefore, if S62 phosphorylation is a common integration point downstream of diverse tumor-associated mutations, then instead of searching for targeted therapies for AML that are based on specific mutations, perhaps promoting c-Myc degradation could serve as a "unified" targeted therapy for AML. In addition, we observed S62

phosphorylation in samples where specific activating mutations were not found, suggesting that promoting c-Myc degradation may be relevant even without identifying the specific signaling pathway(s) responsible for inhibiting it.

Though c-Myc has been considered "undruggable" both because it is a transcription factor and because it is important for the homeostasis of the hematopoietic system and other tissues, a proof of principle study has already demonstrated the feasibility of therapeutically targeting c-Myc. By reversibly inhibiting c-Myc transcriptional activity, Soucek et al. showed that inhibiting c-Myc was not catastrophic for normal tissues, contrary to what one might have expected, and inhibiting c-Myc could also regress lung tumors driven by K-Ras (Soucek et al, 2008). While this approach did not promote c-Myc degradation, it suggests that there is merit in the idea of inhibiting c-Myc activity as a therapy for cancer. Therapies that are currently available to promote c-Myc degradation are compounds that are specific not for c-Myc itself but for kinases and phosphatases that regulate c-Myc phosphorylation. Besides inhibiting S62 phosphorylation with kinase inhibitors like AC220, which we tested here, another approach is to reactivate PP2A, a serine/threonine phosphatase required for c-Myc degradation because it removes S62 phosphorylation (Arnold & Sears, 2006; Yeh et al, 2004).

Mechanisms of PP2A inactivation have only recently been identified in AML. These mechanisms include downregulation of PP2A B regulatory subunits (B56β

and B56γ; (Roberts et al, 2010)) and upregulation of the endogenous PP2A inhibitors CIP2A, SET, and SETBP1 (Cristobal et al, 2011). Indeed, we also find upregulation of SET (Figure 3.6A), and to a lesser extent CIP2A (Figure 3.6B), at the mRNA level in our small panel of AML samples. In addition, compounds that activate PP2A, like FTY720, forskolin, or OP449 (an inhibitor of SET; (Christensen et al, 2011)), have already been developed, and FTY720 is well tolerated in humans (Aktas et al, 2010). FTY720 has also been shown to reactivate PP2A in chronic myelogenous leukemia (Neviani et al, 2007), which can be inactivated by the upregulation of SET. Importantly, reactivating PP2A in this context downregulated c-Myc levels (Neviani et al, 2005). Further, recent studies done by a collaborator also support that SET levels are elevated in primary AML samples (Anupriya Agarwal, unpublished data). In her studies, treating some AML patient samples and cell lines (including Kasumi-1, which were used in Figure 3.4) with the SET inhibitor OP449 reduces proliferation and increases apoptosis (Anupriya Agarwal, unpublished data). These data suggest that reactivation of PP2A through the inhibition of SET may be useful for the treatment of AML.

In summary, these results suggest that c-Myc S62 phosphorylation and stabilization may be a common downstream effect of constitutively activated signaling pathways in AML and that promoting c-Myc degradation could be a therapeutic approach for the treatment of AML and other cancers that express pS62 c-Myc.
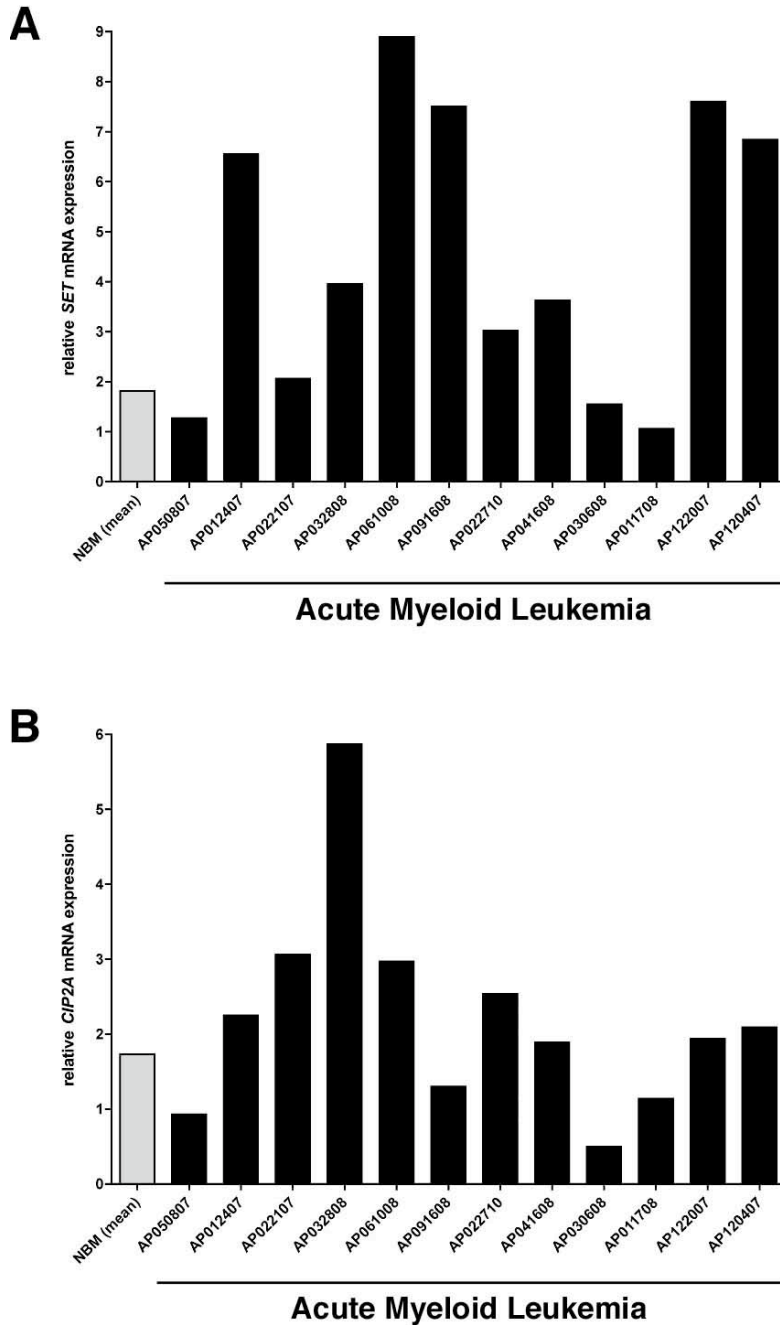
Figure 3.6. *SET* and *CIP2A* **mRNA levels are elevated in some primary AML samples.**

A. *SET* mRNA expression in primary AML samples. AML samples were thawed and maintained in media with 20% FBS for 4 h before analysis. Cells were lysed in Trizol reagent, RNA was purified and reverse transcribed, and cDNA was used for qPCR to detect *SET* transcript levels. Expression was normalized to expression of *18S* and graphed relative to normal bone marrow. **B.** *CIP2A* mRNA expression in primary AML samples. qPCR was performed as in (A), using primers specific for *CIP2A*.

Chapter 4: Axin1 is deregulated in some leukemias and opposes the development of c-Myc-driven T cell lymphoma in mice

Abstract

AXIN1 is a scaffolding protein and tumor suppressor that is deregulated in many types of solid tumors. Based on both our recent description of AXIN1 as a scaffold for assembling a c-Myc degradation complex and our results showing that Myc degradation and complex formation can be disrupted in leukemia, we asked 2 questions: 1) Is c-Myc degradation disrupted in leukemia through the deregulation of AXIN1? and 2) Can AXIN1 suppress c-Myc-driven tumorigenesis *in vivo*? To address the first question, we examined both leukemia cell lines and patient samples with previously characterized defects in c-Myc degradation and found both reduced AXIN1 levels and a novel *AXIN1* mutation in B cell leukemia. This mutant form of AXIN1 was defective for forming a c-Myc degradation complex and failed to suppress c-Myc transcriptional activity. To address the second question, we established a mouse model of c-Myc-driven lymphoma in which we also expressed ectopic AXIN1 and found that ectopic AXIN1 appeared to be incompatible with lymphoma development in this model. Together these results suggest that *AXIN1* functions as a tumor suppressor in B cell leukemia and demonstrate that AXIN1's tumor suppressive function *in vivo* extends beyond the Wnt signaling pathway.

Introduction

AXIN1 is a multidomain scaffolding protein that regulates multiple signaling pathways. Originally characterized as a negative regulator of Wnt signaling during development, AXIN1 has also been shown to regulate TGFβ signaling, SAPK/JNK signaling, and p53-mediated cell fate decisions (Salahshor & Woodgett, 2005). In the Wnt pathway, AXIN1 facilitates degradation of the transcription factor β-catenin by forming a complex with β-catenin, APC, and GSK3β. Within this complex, β-catenin is phosphorylated by GSK3β, which targets it for degradation (Ikeda et al, 1998).

In addition to promoting the degradation of β-catenin, AXIN1 also promotes the degradation of c-Myc. Our lab has shown that AXIN1 promotes c-Myc degradation by providing a platform for c-Myc T58 phosphorylation and S62 dephosphorylation (Arnold et al, 2009). These changes in c-Myc phosphorylation are catalyzed by the kinase GSK3β and the phosphatase PP2A-B56α, respectively, which both bind directly to AXIN1.

Though AXIN1 regulates many different signaling pathways, and in some cases performs seemingly contradictory roles within a single pathway (Guo et al, 2008; Ikeda et al, 1998; Liu et al, 2006; Mao et al, 2001), the net effect of AXIN1 function is anti-proliferative and pro-apoptotic. These effects imply that AXIN1 should function as a tumor suppressor, and, consistent with this idea, *AXIN1* mutations and reduced expression of *AXIN1* mRNA or protein have been

reported in solid tumors (Nakajima et al, 2003; Salahshor & Woodgett, 2005; Xu et al, 2006). However, *in vivo* evidence of AXIN1's tumor suppressive function is sparse, as few studies have examined AXIN1 in the context of tumor development (Li et al, 2009).

While *AXIN1* mutations have been reported in many solid tumors, functional characterization of many of these mutations is lacking. In addition, studies examining the downstream effects of these mutations have primarily focused on β-catenin. However, most of these studies were conducted prior to the discovery of AXIN1 as a negative regulator of c-Myc protein stability. Therefore, whether changes in *AXIN1* expression or sequence that occur in cancer have an effect on c-Myc degradation has not been investigated. Additionally, whether *AXIN1* mutations occur exclusively in solid tumors is not known, as AXIN1 deregulation has not been studied in leukemia.

Since our previous work has shown that AXIN1 promotes c-Myc degradation and that c-Myc degradation is disrupted in human leukemia, we asked whether deregulation of *AXIN1* by mutation or altered expression leads to disrupted c-Myc degradation in leukemia. As an extension of this, we also asked whether AXIN1 could suppress c-Myc-driven tumorigenesis *in vivo*. To answer these questions, we used leukemia cell lines and patient samples in which c-Myc degradation is disrupted to screen for mutations in *AXIN1* and changes in AXIN1 expression. We also used a mouse model of c-Myc-driven lymphoma to determine whether

overexpressing Axin could delay the development of these tumors. We found that while *AXIN1* mutations in leukemia are rare, reduced AXIN1 expression is more common. Additionally, we found that increasing AXIN1 expression during c-Myc-driven lymphoma development results in the functional inactivation of ectopic AXIN1 rather than a delay in tumor onset, while a further increase in AXIN1 dosage does delay tumor onset.

Results

AXIN1 is a scaffolding protein that interacts with components of multiple signaling pathways to influence cell fate decisions and to promote degradation of certain target proteins. Despite AXIN1's involvement in multiple signaling pathways, AXIN1 is generally regarded as a tumor suppressor, as AXIN1 mutations have been reported in a variety of solid tumors (Salahshor & Woodgett, 2005). Supporting AXIN1's role as a tumor suppressor, our lab has characterized AXIN1 as a mediator of c-Myc degradation. AXIN1 promotes c-Myc degradation through the assembly of a multi-protein nuclear complex, and disruption of this complex is sufficient to stabilize c-Myc (Arnold et al, 2009). Since we have previously shown that c-Myc is both stabilized and has a reduced association with GSK3β in pre-B ALL cell lines (Malempati et al, 2006), we hypothesized that mutations in *AXIN1* could potentially stabilize c-Myc in lymphoblastic leukemias.

To determine whether lymphoblastic leukemia cell lines with stabilized c-Myc carry a mutation in *AXIN1*, we cloned and sequenced *AXIN1* mRNA from three leukemia cell lines, HL-60, REH, and SupB15. Unexpectedly, the form of *AXIN1* that was recovered in all three cell lines was consistently missing exon 9. This form of *AXIN1* is a naturally occurring splice variant, AXIN1 variant 2 (*AXIN1V2*), which lacks a portion of the PP2A binding domain (Figure 4.1A). Besides discovering preferential expression of *AXIN1V2*, we also discovered an interesting mutation in the SupB15 cell line. This cell line carries an in-frame deletion of nucleotides 1117-1254 of the *AXIN1* cDNA (nucleotides 1506-1643 in

the full-length mRNA, encompassing all of exon 5), which removes residues 373-418 within the region where GSK3 binds to AXIN1 (Figure 4.1A). Further, this is a heterozygous deletion, as we recovered both wildtype and mutant PCR products while cloning this mutant form of *AXIN1*. We mapped c-Myc binding to exon 7 (data not shown).

To determine if this AXIN1 deletion mutant (AXIN1^{SupB15}) was defective in assembling a degradation complex for c-Myc, we performed a co-immunoprecipitation (co-IP) experiment in 293 cells to assess the association of c-Myc and GSK3β with AXIN1. As controls, we also assessed the ability of c-Myc and GSK3β to co-IP with full-length AXIN1 (AXIN1v1), the natural splice variant of AXIN1 (AXIN1v2), and an engineered deletion mutant of AXIN1 lacking the entire GSK3β binding domain (ΔEx4-5, Figure 4.1A). As shown in Figure 4.1B, c-Myc did not bind as robustly to AXIN1^{SupB15} or AXIN1$^{\Delta Ex4-5}$ as it did to full-length AXIN1v1 (lane 4 and 5 vs lane 2). Importantly, GSK3β did not co-IP with either of these forms of AXIN1, consistent with these deletions removing the GSK3β binding domain of AXIN1. We also found that c-Myc and GSK3β did not co-IP as robustly with AXIN1v2 (lane 3 vs lane 2), in which a portion of the PP2A binding domain is spliced out, consistent with the idea that this c-Myc degradation complex assembles in a cooperative manner (Arnold et al, 2009).
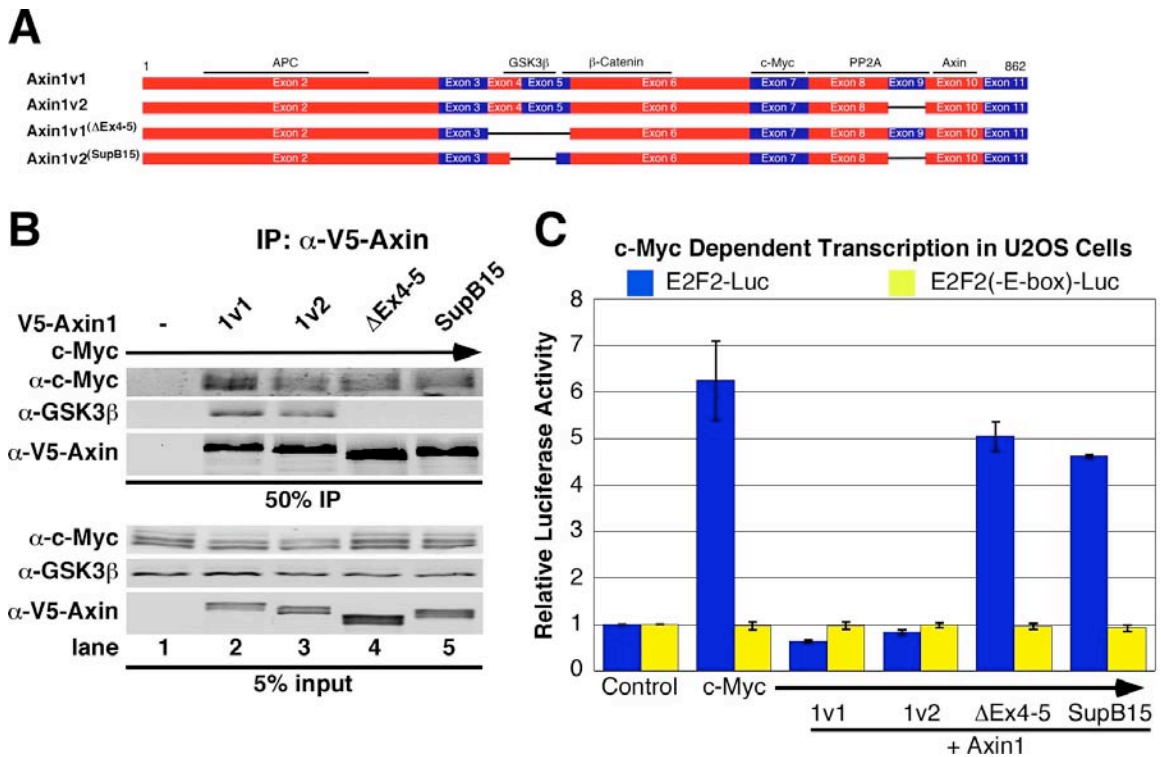
Figure 4.1. A mutant form of AXIN1 found in leukemia is defective in forming a c-Myc degradation complex and fails to suppress c-Myc-dependent transcription.

A. Schematic of full-length and mutant AXIN1 proteins. Exons are numbered. Relevant interacting proteins and the regions they bind are shown above. **B.** A leukemia-derived AXIN1 mutant is defective in forming a c-Myc degradation complex. The indicated V5-tagged AXIN1 constructs and c-Myc were co-transfected into 293 cells, and AXIN1 constructs were immunoprecipitated with anti-V5 antibody. Input and bound proteins were detected by immunoblot with the indicated antibodies. **C**. A leukemia-derived AXIN1 mutant fails to suppress c-Myc-dependent transcription. 293 cells were co-transfected with β-gal, c-Myc, the indicated AXIN1 constructs, and either E2F2-Luc or E2F2(-E-box)-Luc, as indicated. Luciferase activity was measured and adjusted for β-gal and the averages ± s.d. of three separate experiments were graphed. Data published in (Arnold et al, 2009).

Since AXIN1v1 promotes c-Myc degradation and suppresses c-Myc-dependent transcription (Arnold et al, 2009), we next asked whether the AXIN1^{SupB15} mutant could also suppress c-Myc dependent transcription. To test this, we performed a luciferase assay using the E2F2 promoter, which is a known c-Myc target gene (Sears et al, 1997), and expressed both full-length AXIN1v1 and the deletion constructs used in Figure 4.1B. We found that expression of both AXIN1v1 and AXIN1v2 suppressed c-Myc-dependent luciferase activity, while expression of AXIN1^{SupB15} and AXIN1$^{\Delta Ex4-5}$ did not substantially reduce c-Myc-dependent luciferase activity (Figure 4.1C). This suggests that recruitment of GSK3β to c-Myc is important for AXIN1's ability to suppress c-Myc-dependent transcription. Additionally, the deletion of the GSK3β binding domain in the AXIN1^{SupB15} mutant provides a potential mechanism for the increase in c-Myc protein stability and the reduced association of GSK3β with c-Myc that we observed in the SupB15 cell line ((Malempati et al, 2006) and Figure 2.2, 2.4).

Since the AXIN1^{SupB15} mutant is the first description of an *AXIN1* mutation in leukemia, we were interested in determining whether *AXIN1* mutations were a common occurrence in leukemia. To do this, we isolated genomic DNA from 26 primary leukemia samples (8 B ALL, 9 T ALL, and 9 AML) and amplified all 11 exons of *AXIN1*, including portions of each flanking intron, using 16 overlapping pairs of primers. The resulting PCR products were then directly sequenced. As shown in Table 4.1, we found many sequence variants in this panel of leukemia samples, including some variants that were present in as many as 19 samples.

However, none of these variants are predicted to change the amino acid sequence of AXIN1, and many of them were present in the NCBI single nucleotide polymorphism database (dbSNP). These results suggest that mutations in *AXIN1* in leukemia are rare. Consequently, determining the frequency of *AXIN1* mutations in leukemia may require a much larger panel of samples.

Table 4.1. Sequence variants in *AXIN1*.

Exon	Position (bp)[1]	DNA sequence[2]	Position (amino acid)[1]	Amino acid substi-tution[2]	Reported as SNP?[3]	Sample	Type of leukemia
2	-19	C>C/A			rs758033	B68	B ALL
						T22	T ALL
						AP092707	AML
						AP122007	AML
						AP011708	AML
						AP032008	AML
2	762	T>C/C	254	D>D	rs1805105	B25	B ALL
						B40	B ALL
						T23	T ALL
						AP092707	AML
						AP011708	AML
2	762	T>T/C	254	D>D	rs1805105	B54	B ALL
						B61	B ALL
						B63	B ALL
						B68	B ALL
						T21	T ALL
						T22	T ALL
						T24	T ALL
						T34	T ALL
						T35	T ALL
						AP102707	AML
						AP120407	AML
						AP122007	AML
						AP032008	AML
3	1019i+75	G>G/A			no	T20	T ALL
						T34	T ALL
						AP122007	AML
4	1116i+20	T>T/C			rs2301522	B61	B ALL
						B63	B ALL
						B68	B ALL
						T21	T ALL
						T22	T ALL
						T23	T ALL
						T24	T ALL
						T34	T ALL
						T35	T ALL
						AP120407	AML
						AP122007	AML
						AP032008	AML
4	1116i+20	T>C/C			rs2301522	B25	B ALL
						B40	B ALL
						B54	B ALL
						AP092707	AML
						AP102707	AML
						AP011708	AML

5	1254i+17	G>G/A			rs62032881	T22	T ALL
						AP092707	AML
						AP122007	AML
						AP011708	AML
5	1254i+73	ins_C			no	B40	B ALL
						T20	T ALL
						T34	T ALL
6	1284	G>G/A	428	S>S	rs214250	B25	B ALL
						B68	B ALL
						T20	T ALL
						T21	T ALL
						T24	T ALL
						AP092707	AML
						AP011708	AML
						AP032008	AML
6	1284	G>A	428	S>S	rs214250	B40	B ALL
6	1677	G>A	559	Q>Q	no	B54	B ALL
7	1827	T>T/C	609	A>A	rs214252	B25	B ALL
						B68	B ALL
						T20	T ALL
						T21	T ALL
						T24	T ALL
						AP092707	AML
						AP011708	AML
						AP032008	AML
7	1827	T>C	609	A>A	rs214252	B40	B ALL
9	2187i-65	A>A/G			rs412243	B40	B ALL
						T20	T ALL
						AP122007	AML
						AP011708	AML
9	2187i-65	A>G			rs412243	T22	T ALL
						AP092707	AML
						AP032008	AML
10	2462i+25	C>C/A			rs387467	B25	B ALL
						T20	T ALL
						T21	T ALL
						AP092707	AML
						AP011708	AML
						AP032008	AML
10	2462i+25	C>A			rs387467	B40	B ALL

Abbreviations: AML, acute myeloid leukemia; B ALL, B cell acute lymphoblastic leukemia; SNP, single nucleotide polymorphism; T ALL, T cell acute lymphoblastic leukemia

[1]The DNA sequence position is derived from GenBank accession number NM_003502.3, in which the A at position 390 is the beginning of the coding sequence (ATG). This A is termed position 1 for the DNA sequence above, and the corresponding methionine is numbered as amino acid 1. The numbering for intronic variants is determined from the nearest coding nucleotide. For example, position 1019i+75 is 75bp 3' to coding nucleotide 1019, which is the last base in exon 3.

[2]DNA sequence is represented as the reference base (from NM_003502.3) > reported base. Heterozygous changes are represented as N/N. Amino acid residue and substitution are listed for variants located in the coding region.

[3]If the SNP has been previously reported, its reference ID in the NCBI SNP database, dbSNP, is listed.

Characterization of high c-Myc protein levels and aberrant c-Myc phosphorylation in this panel of leukemia patient samples suggests that c-Myc degradation may be disrupted in many of these samples (chapters 2 and 3). Since we did not find any mutations in *AXIN1* in these samples, we hypothesized that reduced expression of *AXIN1* could contribute to both the high level of c-Myc protein and the absence of T58 phosphorylation in many of these samples (Figure 2.6, 2.8, 3.3). To examine this, we used quantitative real time PCR (qPCR) to measure *AXIN1* expression in these leukemia samples. As shown in Figure 4.2, *AXIN1* mRNA levels were not reduced in any B ALL (Figure 4.2A), T ALL (Figure 4.2B), or AML samples (Figure 4.2C) when compared to CD19+ B cells, CD3+ T cells, or normal bone marrow, respectively. Instead, in most cases *AXIN1* mRNA levels were higher than in these control samples.
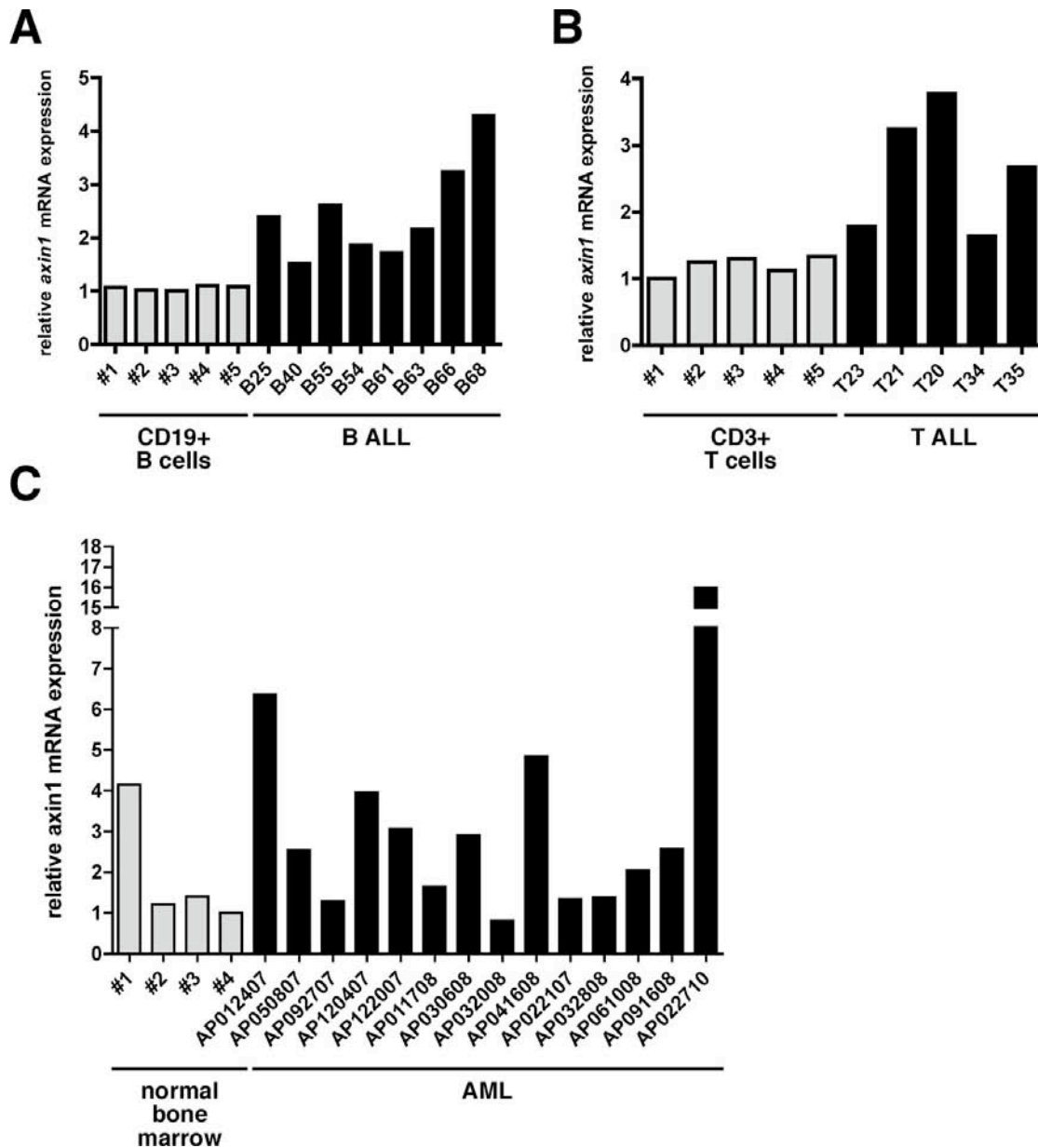
Figure 4.2. *AXIN1* **mRNA expression is not reduced in a panel of leukemia samples.**

A. *AXIN1* expression is not reduced in B ALL samples. mRNA expression of *AXIN1* in B ALL samples and CD19+ B cells from peripheral blood was measured by qPCR, normalized to *18S* expression, and graphed relative to expression in CD19+ B cells. **B.** *AXIN1* expression is not reduced in T ALL samples. mRNA expression of *AXIN1* in T ALL samples and CD3+ T cells from peripheral blood was measured by qPCR, normalized to *18S* expression, and graphed relative to expression in CD3+ T cells. **C.** *AXIN1* expression is not reduced in AML samples. mRNA expression of *AXIN1* in AML samples and

normal bone marrow was measured by qPCR, normalized to *18S* expression, and graphed relative to expression in normal bone marrow.

As mentioned above, the *AXIN1* gene encodes two splice variants, *AXIN1V1* and *AXIN1V2* (Figure 4.3A). Since we found that *AXIN1V2* is the predominant form of *AXIN1* expressed in the REH and SupB15 leukemia cell lines, and this form of AXIN1 binds less robustly to c-Myc and GSK3β, we hypothesized that B ALL samples may express more *AXIN1V2* than *AXIN1V1*. To determine whether *AXIN1V2* expression is enriched in B ALL, we measured the expression level of both splice variants by qPCR. In contrast to the B ALL cell lines, we found that the ratio of *AXIN1V2* to *AXIN1V1* expression was lower in seven out of eight B ALL samples (Figure 4.3B), suggesting that expression of *AXIN1V2* is not commonly enriched in B ALL. We did find one B ALL sample that expressed a higher ratio of *AXIN1V2* to *AXIN1V1* (B40, Figure 4.3B); however, the degree of enrichment was quite modest.
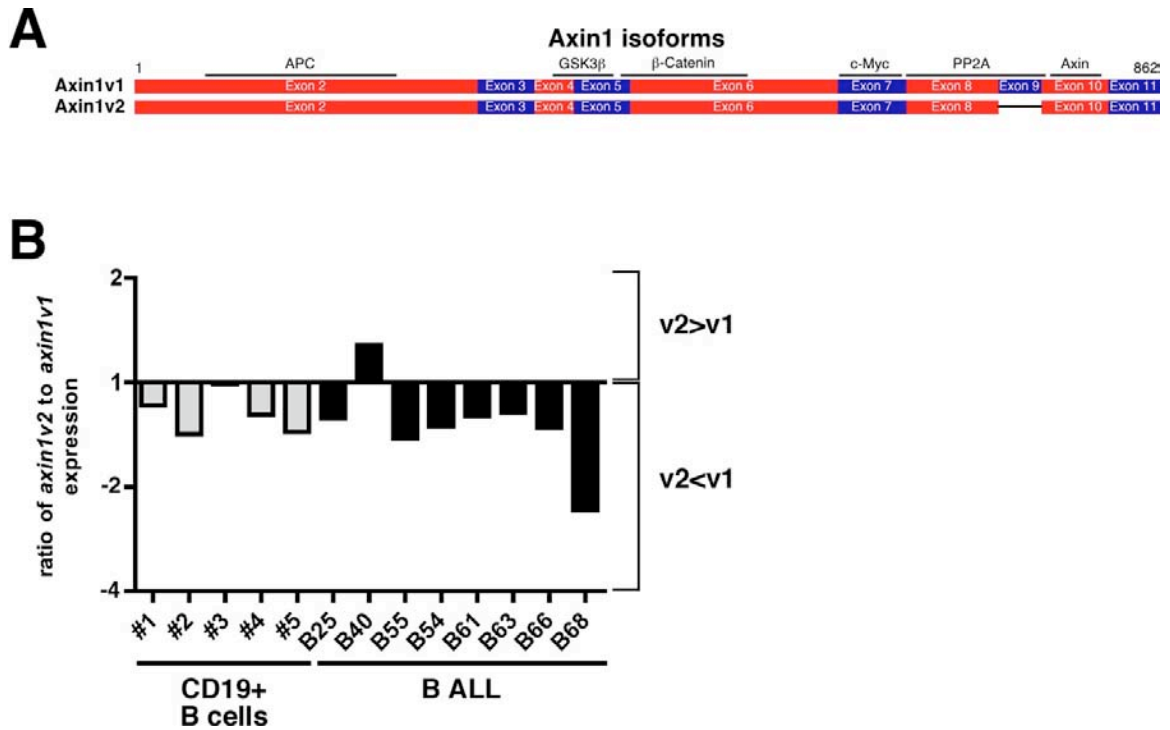
Figure 4.3. *AXIN1V2* **is not enriched in primary B ALL samples.**

A. Schematic of AXIN1 splice variants, AXIN1v1 and AXIN1v2. **B.** Ratio of expression of *AXIN1V2* to *AXIN1V1* in primary B ALL samples. mRNA expression of *AXIN1V1* and *AXIN1V2* were measured by qPCR and normalized to *18S* expression. Ratio of *AXIN1V2* to *AXIN1V1* was graphed relative to the ratio from sample #3, CD19+ B cells.

AXIN1 is the rate-limiting component of β-catenin degradation because its expression level is several orders of magnitude lower than other components of the degradation complex (Lee et al, 2003). Since the β-catenin and c-Myc degradation complexes share several components, AXIN1 is likely to be the rate-limiting component of the c-Myc degradation complex as well. We therefore hypothesized that reduced AXIN1 protein levels may contribute to the increased c-Myc protein levels and reduced T58 phosphorylation observed in our panel of B ALL samples (Figure 2.6). To test this hypothesis, we evaluated AXIN1 levels in these samples by immunoblot. We found a reproducible, significant reduction in AXIN1 protein levels in three out of eight B ALL samples (B25, B40, B63; Figure 4.4) that correlated with high S62 phosphorylation and low or absent T58 phosphorylation (Figure 2.6). These three samples do not exhibit reduced *AXIN1* mRNA expression (Figure 4.2A), which suggests that the reduced AXIN1 protein levels may be due to changes in AXIN1 expression at the post-transcriptional level.
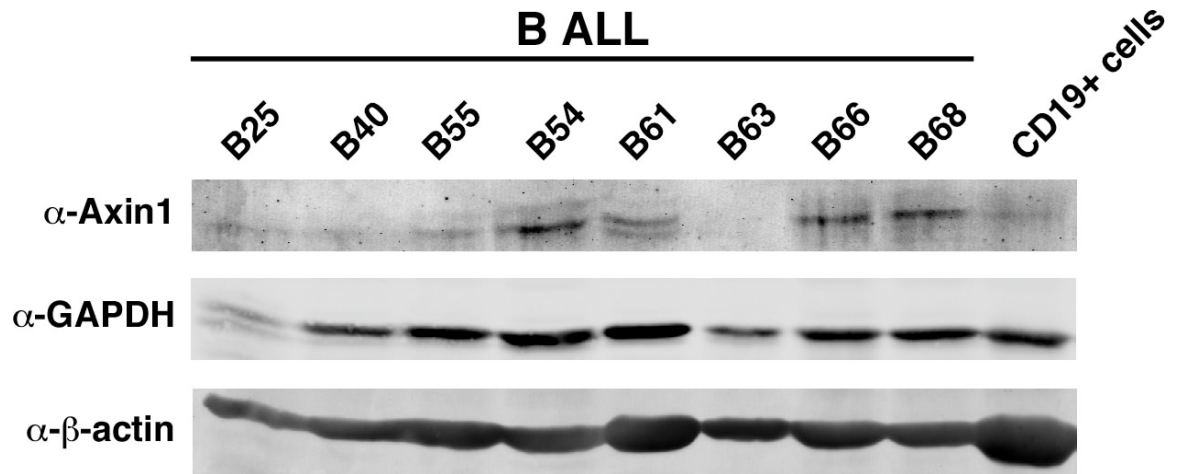
Figure 4.4. AXIN1 protein is reduced in some primary B ALL samples.

4 million cells from each B ALL sample and from CD19+ B cells were separated by SDS-PAGE and analyzed for expression of AXIN1 (C76H11) by immunoblot.

If AXIN1 is the rate limiting component for both β-catenin and c-Myc degradation, one would expect that increasing the level of AXIN1 would accelerate the degradation of these proteins. Indeed, this has been demonstrated for β-catenin, where a modest increase in AXIN1 levels dramatically reduces the half-life of β-catenin (Lee et al, 2003). Since c-Myc is stabilized in many of the leukemia cell lines we have examined (Figure 2.2, 2.7, 2.9), we hypothesized that increasing the level of AXIN1 protein in these cells may promote c-Myc degradation, reducing c-Myc protein levels. To test this, we treated these cell lines with IWR-1, a small molecule that blocks AXIN1 degradation (Chen et al, 2009; Huang et al, 2009) and thereby increases AXIN1 levels. In both ALL and AML cell lines with stabilized c-Myc, IWR-1 treatment increased AXIN1 protein levels (Figure 4.5). In some cases, IWR-1 treatment also resulted in a modest decrease in c-Myc protein levels (HEL cell line; Figure 4.5C). In other cases, c-Myc levels either did not change (REH and SupB15, Figure 4.5A) or increased (DND41, Figure 4.5B; CTV-1, Figure 4.5C). These results suggest that increasing AXIN1 protein levels can decrease c-Myc levels, depending on cell context.
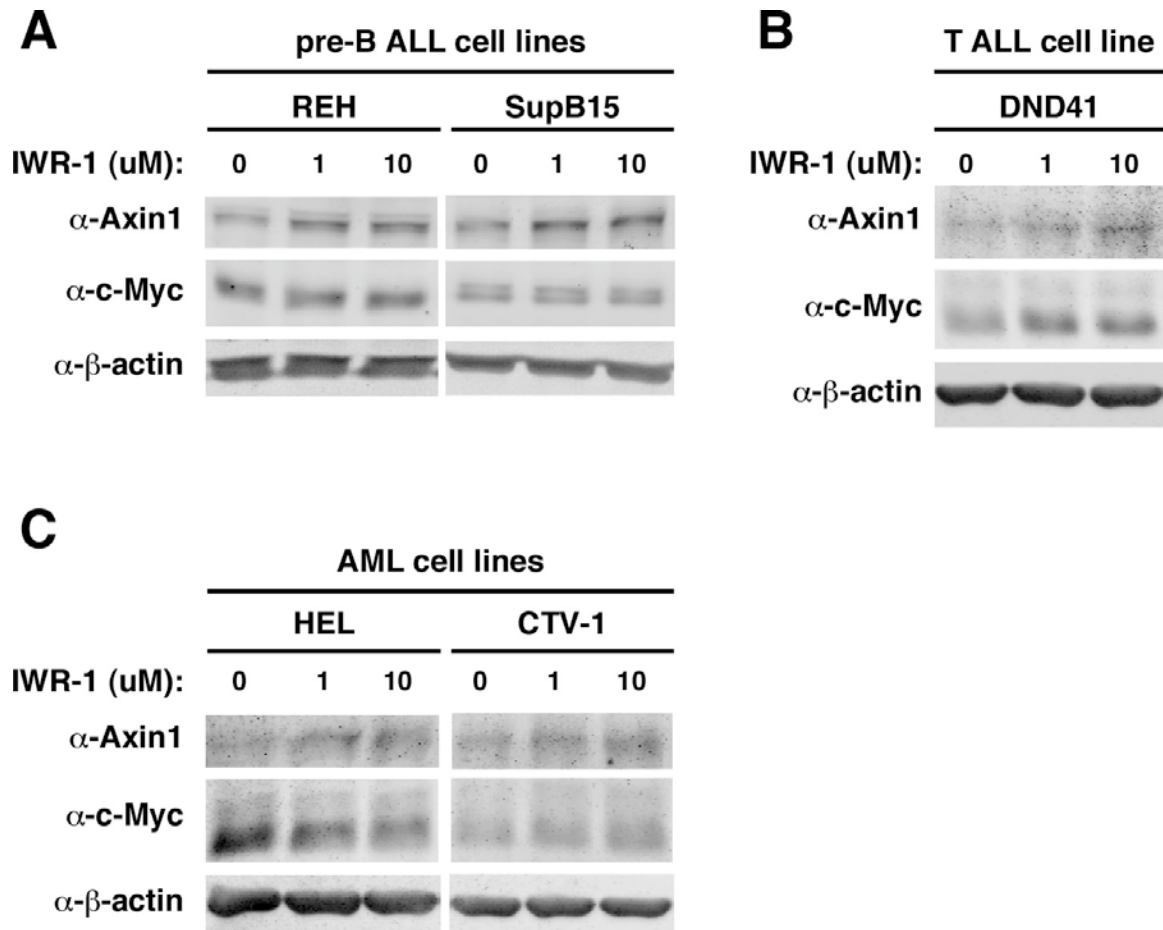
Figure 4.5. Increasing AXIN1 protein levels in leukemia cell lines has variable effects on c-Myc protein levels.

A. c-Myc levels do not decrease in response to increased AXIN1 levels in pre-B ALL cell lines. Pre-B ALL cell lines, REH and SupB15, were treated with increasing doses of the AXIN1-stablizing compound IWR-1 for 24 hours. Equal cell numbers were separated by SDS-PAGE and analyzed for levels of AXIN1 (A0481) and c-Myc (N262) by immunoblot. **B.** c-Myc levels do not decrease in response to increased AXIN1 levels in a T ALL cell line. The T ALL cell line DND41 was treated with IWR-1 and analyzed for AXIN1 (A0481) and c-Myc (Y69) levels as in (A). **C.** c-Myc levels decrease in response to increased AXIN1 levels in some AML cell lines. The AML cell lines HEL and CTV-1 were treated with IWR-1 and analyzed for AXIN1 (A0481) and c-Myc (Y69) levels as in (A).

Our data thus far support the idea that c-Myc stabilization is a common feature of both myeloid and lymphoid leukemias, which implies that in these leukemias c-Myc degradation is disrupted. Our data have also shown that in some of these leukemia samples, AXIN1 is deregulated, whether by mutation or reduced expression. Since we have shown that *in vitro* AXIN1 regulates both c-Myc stability and c-Myc transcriptional activity (Arnold et al, 2009), we next asked whether AXIN1 could suppress c-Myc-driven tumorigenesis *in vivo*. For this study, we chose a well-established model of *MYC*-driven T cell lymphoma, the *EµSR-tTa/tet-o-MYC* mouse (hereafter abbreviated *EµtTa/tetoMYC*) (Felsher & Bishop, 1999). In this model, the human *MYC* gene is expressed under the control of a doxycycline-regulated promoter (*tet-o-MYC*, Figure 4.6A) that is "on" when the TET-transactivator is expressed and doxycycline is absent (TET-OFF system). Expression of the TET-transactivator is driven by an immunoglobulin enhancer combined with a viral promoter (*EµSR-tTa*, Figure 4.6A). This promoter is active in T cells and other hematopoietic cells and, when combined with the tet-o-MYC gene, drives the development of lymphoma with 100% penetrance (Felsher & Bishop, 1999). When we analyzed the *EµtTa/tetoMYC* mice by immunoblot for c-Myc expression, we found that c-Myc levels were low in thymocytes and higher in some lymphomas (Figure 4.6B). This suggested to us that, even though *MYC* was constitutively expressed at the transcriptional level, in some cases lymphomagenesis may be associated with c-Myc protein stabilization.
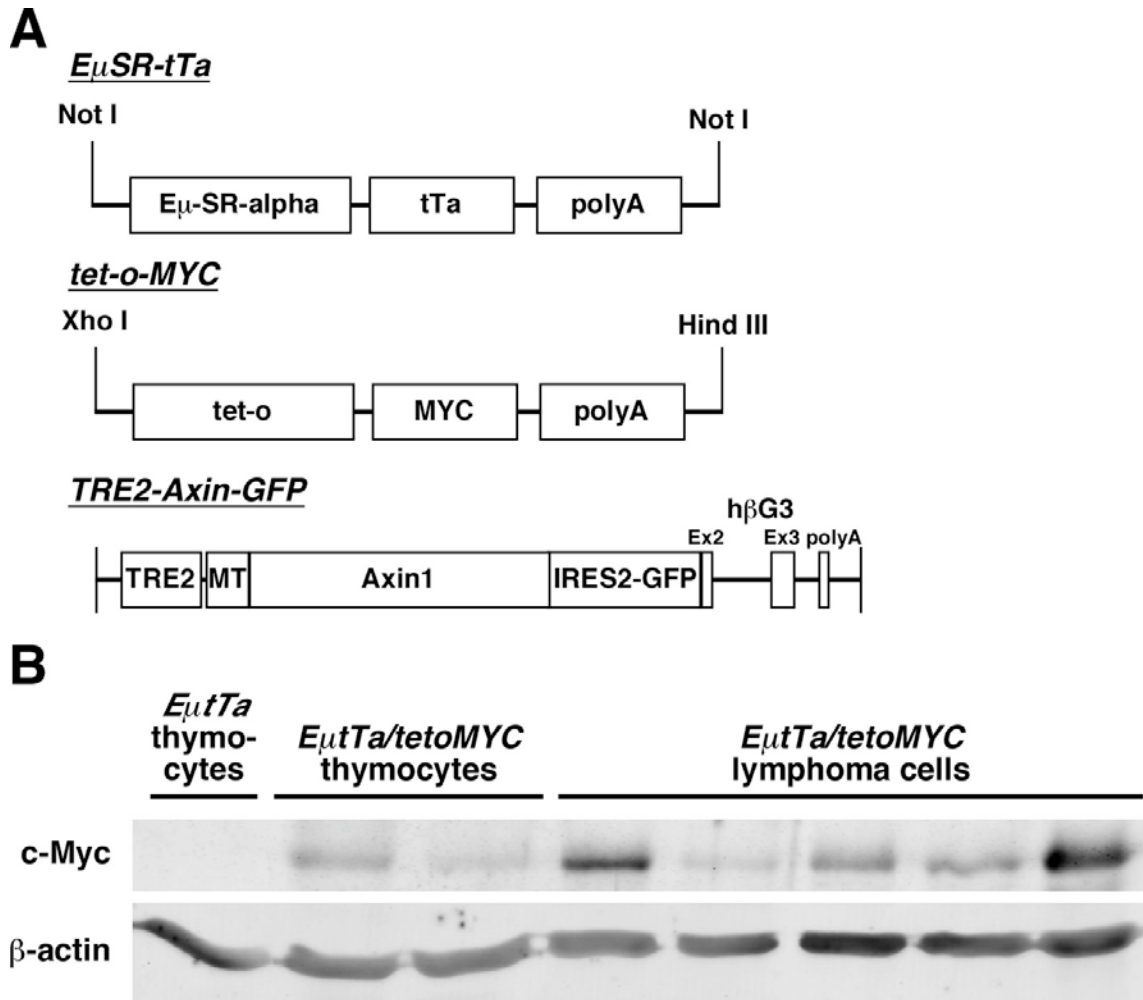
Figure 4.6. c-Myc expression increases during lymphoma development in *EµtTa/tetoMYC* transgenic mice.

A. Schematic of transgene constructs. The *EµSR-tTa* construct encodes a TET-transactivator. The *tet-o-MYC* construct encodes human *MYC*. The *TRE2-Axin-GFP* construct encodes murine *Axin1* with an N-terminal Myc-tag followed by an IRES sequence and GFP. *tet-o* and *TRE2* are TET-responsive promoters. *EµSR-tTa* and *tet-o-MYC* constructs are from (Felsher & Bishop, 1999) and *TRE2-Axin-GFP* is from (Hsu et al, 2001). MT, Myc-tag. **B.** c-Myc expression increases with lymphoma development in *EµtTa/tetoMYC* mice. Thymocytes from 5-week-old *EµtTa* and *EµtTa/tetoMYC* mice and lymphoma cells from moribund *EµtTa/tetoMYC* mice were analyzed for c-Myc (N262) expression by immunoblot. Cells were lysed in Ab lysis buffer, and 25µg of protein were loaded in each lane.

Since c-Myc stability may increase during lymphoma development in this model, we used this model to test the hypothesis that promoting c-Myc degradation can delay the development of lymphoma. To test this hypothesis, we chose to establish a model where both c-Myc and AXIN1 were driven by the same TET-transactivator and therefore were expressed together in the same cell. To do this, we obtained *TRE2-Axin-GFP* mice (hereafter abbreviated as *TREAxin*), a line of transgenic mice that express AXIN1 in a TET-regulated manner (Figure 4.6A) (Hsu et al, 2001). When bred into the *EμtTa/tetoMYC* background, offspring carrying all three transgenes (*EμtTa/tetoMYC/TREAxin*) express both c-Myc and AXIN1 under the control of the same TET-transactivator, allowing us to determine whether increasing the dosage of AXIN1 can delay the development of *MYC*-driven lymphoma in this model.

We established cohorts of mice ectopically expressing *MYC* (*EμtTa/tetoMYC*), *Axin1* (*EμtTa/TREAxin*), or both *MYC* and *Axin1* (*EμtTa/tetoMYC/TREAxin)* and maintained them in the absence of doxycycline to ensure constitutive expression of both genes. As a negative control, we also maintained a cohort of all three genotypes on doxycycline (administered in the drinking water) to suppress transgene expression. To verify that these transgenes were expressed, we isolated RNA from the thymus of these mice and performed RT-PCR for expression of ectopic *MYC* and ectopic *Axin1*. As shown in Figure 4.7A, both ectopic *MYC* and *Axin1* mRNA were expressed in the thymus as expected based on the genotype of each animal. Additionally, we were able to detect low levels of

ectopic AXIN1 protein in the thymus by immunoblotting (Figure 4.7B). We also performed immunofluorescence (IF) for ectopic AXIN1 on sections of thymus tissue from young mice. Surprisingly, the frequency of cells expressing ectopic AXIN1 was very low (Figure 4.7C), corroborating the weak ectopic AXIN1 expression observed in our immunoblots. Histological examination of these thymuses revealed no obvious morphological changes in thymic architecture (data not shown), in contrast to the phenotype reported when AXIN1 is driven by the MMTV promoter, in which cortical thymocytes undergo massive apoptosis and the thymus loses its architecture (Hsu et al, 2001). We subsequently performed IF for c-Myc as well and discovered that c-Myc was also expressed in very few cells (data not shown), which also corroborated our previous observation of low c-Myc expression by immunoblot (Figure 4.6B).
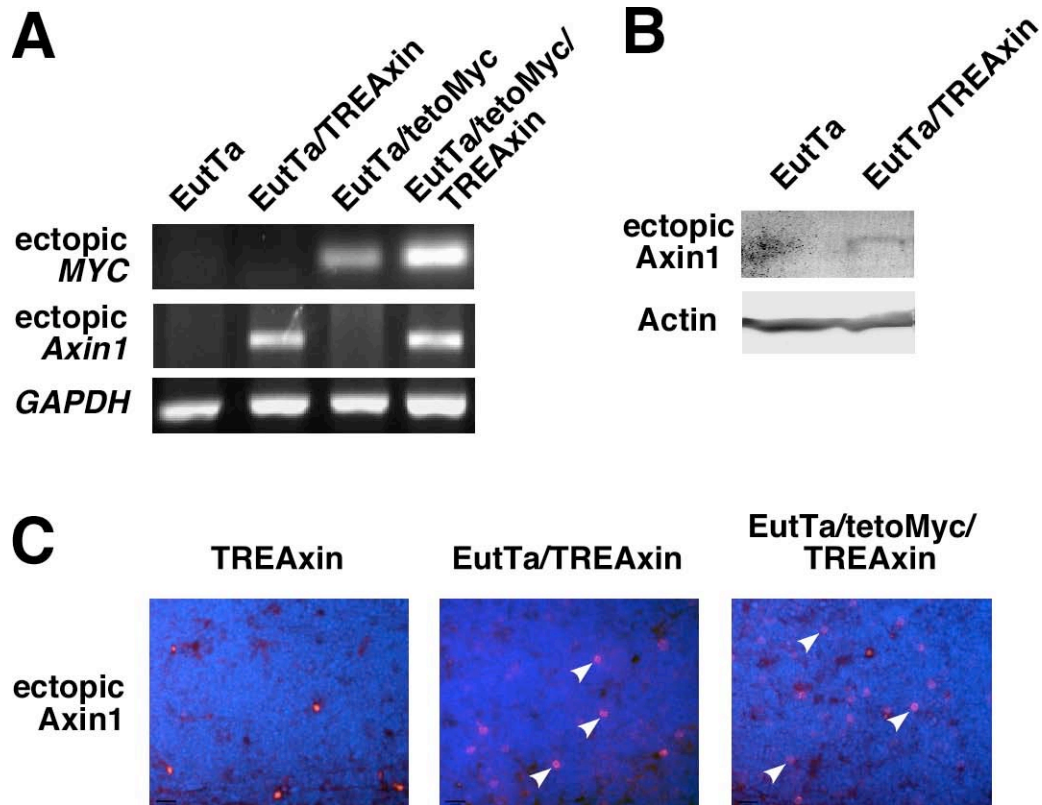
Figure 4.7. Expression of ectopic MYC and AXIN1 in transgenic mice.

A. Expression of ectopic *MYC* and *Axin1* in the thymus of transgenic mice. RNA was isolated from the thymus of 6-week-old mice of the genotypes shown. RT-PCR was performed using primers against human *MYC* and the GFP portion of the *Axin-GFP* transcript. **B&C.** Expression of ectopic AXIN1 in the thymus of *EμTa/TREAxin* mice. Thymocytes from young mice were analyzed for expression of ectopic AXIN1 by immunoblot (B) or immunofluorescence (C) using an anti-Myc tag antibody (71D10) that does not react with full-length Myc. In (B), cells were lysed in Ab lysis buffer, and 25μg of protein were loaded in each lane. In (C), arrowheads indicate positive cells; brightly fluorescent cells in the *TREAxin* panel (C, left) are red blood cells that stain non-specifically.

Regardless of the low number of thymocytes expressing MYC and AXIN1, these mice still succumbed to lymphoma. We followed these cohorts of mice for lymphoma incidence, as shown in Figure 4.8. Surprisingly, the *EµtTa/tetoMYC* cohort and the *EµtTa/tetoMYC/TREAxin* cohort developed lymphoma at the same rate. Additionally, there was no difference in the presentation or gross pathology of the moribund animals between these two genotypes (data not shown); animals of both genotypes faithfully recapitulated the phenotype described in (Felsher & Bishop, 1999). As expected, mice expressing AXIN1 (*EµtTa/TREAxin*) and mice of all genotypes maintained on doxycycline remained tumor-free for the duration of the study (>430 days).
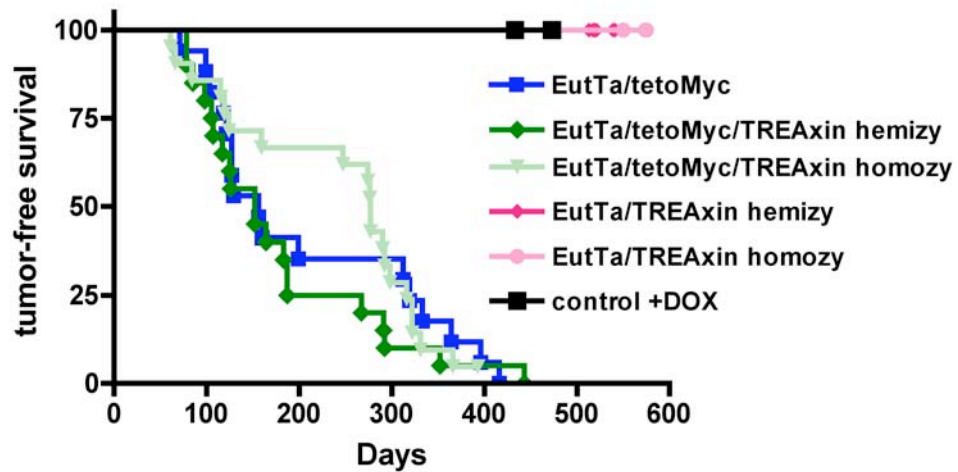
Figure 4.8. Lymphoma onset in cohorts of mice expressing TET-responsive *MYC* and *Axin1* transgenes.

Kaplan-meier survival curve of mice of the indicated genotypes. Number of mice in each cohort were as follows: *EµtTa/tetoMYC*, N=17; *EµtTa/tetoMYC/TREAxin* hemizygous, N=20; *EµtTa/tetoMYC/TREAxin* homozygous, N=21; *EµtTa/TREAxin* hemizygous, N=13; *EµtTa/TREAxin* homozygous, N=5; mice of any tumor-prone genotype maintained on Doxycycline ("control +DOX"), N=20.

Since the *EμtTa/tetoMYC/TREAxin* mice developed lymphoma at the same rate and with the same presentation as the *EμtTa/tetoMYC* mice, we examined tumors from the *EμtTa/tetoMYC/TREAxin* mice to determine whether they still expressed ectopic c-Myc and AXIN1. In order to evaluate the expression of c-Myc, we isolated thymic tumors from both *EμtTa/tetoMYC* and *EμtTa/tetoMYC/TREAxin* mice and examined c-Myc expression by immunoblot. As shown in Figure 4.9A, c-Myc was robustly expressed in lymphomas from *EμtTa/tetoMYC* mice. Likewise, c-Myc was robustly expressed in lymphomas from *EμtTa/tetoMYC/TREAxin* mice (Figure 4.9B). We also found high c-Myc levels when tumors of each genotype were analyzed for c-Myc expression by immunofluorescence (Figure 4.9C). While c-Myc levels were generally high in all tumors, we did note variability in c-Myc levels both between individual tumors (Figure 4.9A, 4.9B) and between individual cells within a tumor (Figure 4.9C). However, there did not appear to be a difference in the variability of c-Myc expression in the *EμtTa/tetoMYC* tumors versus the *EμtTa/tetoMYC/TREAxin* tumors.
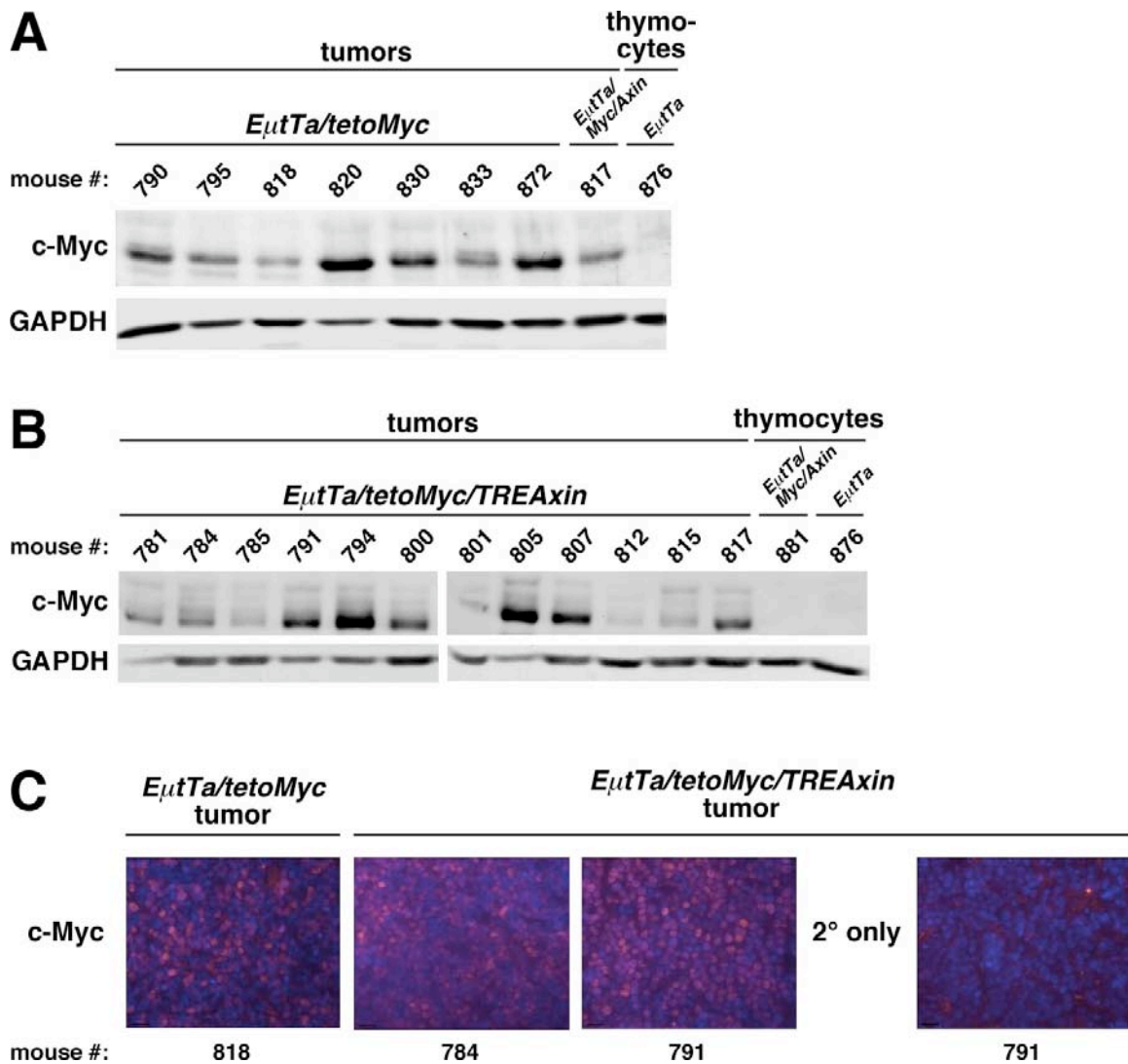
Figure 4.9. c-Myc expression in lymphomas from transgenic mice.

A. c-Myc expression in lymphoma cells from *EμTa/tetoMYC* mice. Lymphoma cells from *EμTa/tetoMyc* mice were lysed in Ab lysis buffer, and 25μg of protein were loaded in each lane. Protein was separated by SDS-PAGE and analyzed for c-Myc expression by immunoblot using the pan-MYC antibody N262, which recognizes both mouse and human MYC. **B.** c-Myc expression in lymphoma cells from *EμTa/tetoMYC/TREAxin* mice. Lymphoma cells from *EμTa/tetoMYC/TREAxin* mice were analyzed for c-Myc expression by immunoblot as in (A), using the pan-MYC antibody Y69 that recognizes both mouse and human MYC. **C.** c-Myc expression in thymic lymphomas from *EμTa/tetoMYC* and *EμTa/tetoMYC/TREAxin* mice. Thymic tumors from mice of the indicated genotypes were analyzed for expression of c-Myc by immunofluorescence using an antibody against the N terminus of full-length c-Myc (Y69).

We next examined the expression of ectopic AXIN1 in tumors from the

EμTa/tetoMYC/TREAxin mice. As shown in Figure 4.10A, ectopic AXIN1 protein

was undetectable in more than half of these tumors. This was supported by

qPCR data showing a dramatic reduction in the expression of ectopic *Axin1*

mRNA from the same tumors (Figure 4.10B). However, examination of genomic

DNA from these tumors revealed that all of the tumors still carried the *TRE2-*

Axin-GFP transgene (Figure 4.10C). These data suggest that the tumors lacking

ectopic *Axin1* expression had transcriptionally silenced the *TRE2-Axin-GFP*

transgene.

The lack of *Axin1* expression in the majority of tumors from

EμTa/tetoMYC/TREAxin mice suggests that expression of ectopic AXIN1 may

not be compatible with the development of c-Myc-driven lymphoma. For this to

be the case, the tumors from *EμTa/tetoMYC/TREAxin* mice that still express

ectopic AXIN1 would need to have functionally inactivated ectopic AXIN1, which

would make the tumors phenotypically the same as the ones that lack ectopic

AXIN1 expression. To explore this hypothesis, we examined ectopic AXIN1

localization by immunofluorescence in the *EμTa/tetoMYC/TREAxin* tumors.

Validating our previous results, tumors that lack ectopic AXIN1 expression at the

mRNA and protein level are also negative by immunofluorescence (784, Figure

4.10D), and tumors that express ectopic AXIN1 protein are positive for ectopic

AXIN1 expression by immunofluorescence (791). However, examination of

ectopic AXIN1 localization in tumor 791 revealed a predominantly punctate and

cytoplasmic distribution (Figure 4.10E). When we compared the localization of ectopic AXIN1 in tumors to ectopic AXIN1 in the thymus of young *EμtTa/tetoMYC/TREAxin* mice, we found that AXIN1 appeared primarily membrane-associated in the thymus of young mice and lacked the punctate staining pattern that was prominent in the tumor cells. These data, while preliminary, suggest that ectopic AXIN1 can be functionally inactivated during c-Myc-driven tumorigenesis by more than one mechanism – transcriptional silencing and, possibly, altered subcellular localization.

A tumors / thymocytes

B relative *TREAxin* expression — EµTa/tetoMyc/TREAxin tumors

C EµTa/tetoMyc/TREAxin tumor DNA — tail DNA

D EµTa/tetoMyc/TREAxin tumor / EµTa/tetoMyc tumor / EµTa/tetoMyc/TREAxin tumor

E EµTa/tetoMyc/TREAxin — thymus / tumor
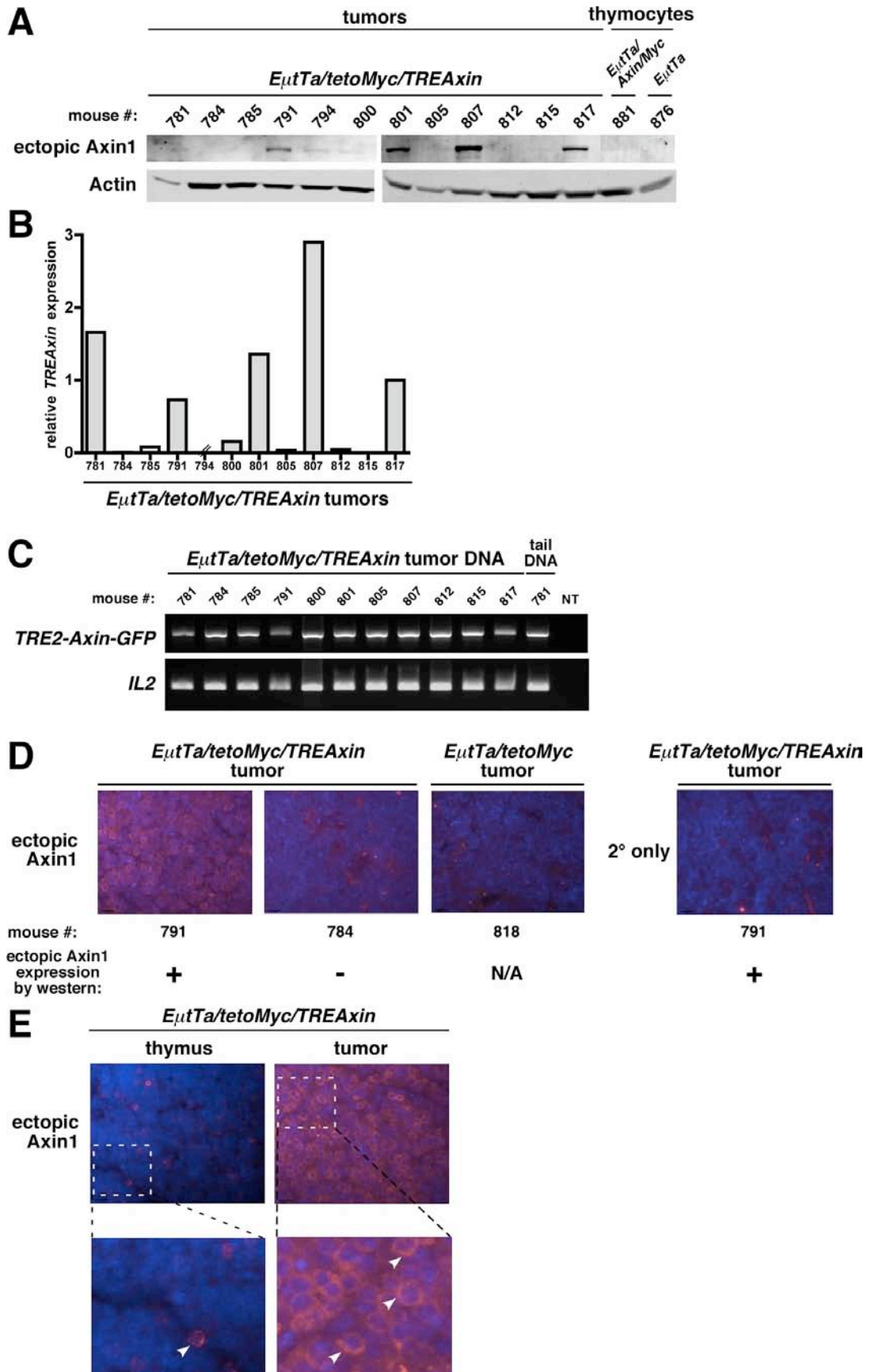
Figure 4.10. Ectopic AXIN1 is functionally inactivated during lymphoma development in *EμtTa/tetoMYC/TREAxin* mice.

A&B. Ectopic AXIN1 is downregulated in *EμtTa/tetoMYC/TREAxin* tumors. Lymphoma cells from *EμtTa/tetoMYC/TREAxin* mice were analyzed for ectopic AXIN1 expression by immunoblot using an anti-Myc tag antibody (71D10) (A) or by qPCR using primers against the GFP portion of the *Axin-GFP* transcript (B). In (A), Lymphoma cells from *EμtTa/tetoMYC* mice were lysed in Ab lysis buffer, and 25μg of protein were loaded in each lane. Protein was separated by SDS-PAGE and analyzed for AXIN1 (A0481) expression by immunoblot. **C.** *TRE2-Axin-GFP* transgene is present in the genomic DNA of tumors from *EμtTa/tetoMYC/TREAxin* mice. Genomic DNA was isolated from lymphoma cells from *EμtTa/tetoMYC/TREAxin* mice and the *TRE2-Axin-GFP* transgene was detected by PCR using primers against the GFP portion of the transgene. Tail DNA was used as a positive control and adding no template (NT) served as a negative control. **D&E.** Ectopic AXIN1 is differentially localized in an *EμtTa/tetoMYC/TREAxin* tumor. A thymus or thymic tumor from mice of the indicated genotypes was analyzed for expression of ectopic AXIN1 by immunofluorescence using an anti-Myc tag antibody (71D10) that does not react with full-length Myc.

137

While these results point to a role for AXIN1 in negatively regulating c-Myc-driven lymphoma development, they are not conclusive, since ectopic expression of AXIN1 did not delay the onset of lymphoma. We next asked whether increasing the dosage of AXIN1 could delay the onset of lymphoma. In order to answer this question, we established additional cohorts of mice that carried two copies of the *TRE2-Axin-GFP* transgene (hereafter abbreviated *TREAxin$^{+/+}$*), *EμtTa/tetoMYC/TREAxin$^{+/+}$* and a control group, *EμtTa/TREAxin$^{+/+}$*, and monitored them for tumor development. As shown in Figure 4.8, we found that in the *EμtTa/tetoMYC/TREAxin$^{+/+}$* mice tumor onset increased from a median of 152 days to a median of 277 days. These data suggest that AXIN1 may function as a tumor suppressor in this model of c-Myc-driven T cell lymphoma.

Discussion

In this study, we found that deregulation of *AXIN1* by mutation likely disrupted c-Myc degradation in a B cell leukemia cell line and that in some B ALL patient samples, reduced AXIN1 protein expression correlates with high c-Myc levels and high S62 phosphorylation. In our *in vivo* study of AXIN1's tumor suppressor function, we found that expressing ectopic AXIN1 during c-Myc-driven lymphoma development results in the functional inactivation of ectopic AXIN1 but does not delay tumor onset, while a further increase in AXIN1 dosage does delay tumor onset.

While *AXIN1* mutations and expression changes have been widely reported in solid tumors (Salahshor & Woodgett, 2005), neither have been reported for *AXIN1* in leukemia. Our discovery of an in-frame deletion in *AXIN1* represents the first report of an *AXIN1* mutation in leukemia (Figure 4.1, published in (Arnold et al, 2009)). In addition, we also found that AXIN1 protein expression was reduced in 3 out of 8 B ALL patient samples (Figure 4.4), again the first such report of altered AXIN1 expression in leukemia. Whether mutations and altered expression of *AXIN1* occur in other types of leukemia or are limited to B ALL is not known. In addition to the B ALL samples, we also sequenced *AXIN1* in T ALL and AML samples; however, our panel was relatively small, so the discovery of rare mutations was unlikely. We also examined AXIN1 protein expression in our primary T ALL and AML samples, but these studies were inconclusive, leaving open the question of whether AXIN1 protein expression is reduced in these types

of leukemia. In addition, other potential mechanisms of AXIN1 deregulation, such as altered phosphorylation or subcellular localization may exist, but these have also not been examined.

The discovery of both a mutation and altered expression of AXIN1 in B ALL led us to look for correlations between these alterations and disrupted c-Myc degradation. We found that in two out of three B ALL patient samples, reduced AXIN1 protein expression correlated with both high c-Myc protein levels and high c-Myc S62 phosphorylation (B25, B40; Figure 2.6 and 4.4). While we did not determine whether reduced AXIN1 levels are responsible for high c-Myc levels and S62 phosphorylation in these samples, our result is consistent with the effect of AXIN1 knockdown on c-Myc levels and S62 phosphorylation in 293 cells (Arnold et al, 2009). In addition, the AXIN1^{SupB15} mutation also correlates with high c-Myc levels and high S62 phosphorylation in the SupB15 leukemia cell line. Functional characterization of the AXIN1^{SupB15} mutant in 293 cells revealed that this form of AXIN1 does not bind to GSK3β and has a reduced association with c-Myc (Figure 4.1B). These results complement and potentially explain the reduced association between c-Myc and GSK3β that we previously found in the SupB15 cell line (Figure 2.4).

Our results showing a correlation between *AXIN1* mutation or reduced AXIN1 expression and elevated c-Myc levels and S62 phosphorylation suggest that future studies examining AXIN1 expression in cancer should also look for

correlations with c-Myc levels and S62 phosphorylation. Previous studies of

AXIN1 mutations or expression in cancer have focused on whether these

changes correlate with β-catenin accumulation; however, these studies have not

always found such a correlation. For example, one study of anaplastic thyroid

cancer found *AXIN1* mutations in 82% of the samples analyzed, which was

followed up by looking at β-catenin accumulation as a marker of Wnt pathway

activation and c-Myc levels as a marker of β-catenin transcriptional activity

(Kurihara et al, 2004). Interestingly, high c-Myc levels were present in 59% of

their samples but did not correlate with β-catenin accumulation (found in 41% of

samples). The authors concluded that high c-Myc levels were independent of

aberrant Wnt signaling in these samples (Kurihara et al, 2004), but in light of our

results, *AXIN1* mutations in these thyroid cancer samples may be contributing to

high c-Myc levels by disrupting c-Myc degradation. Such studies support the idea

that c-Myc levels and phosphorylation status should be analyzed when *AXIN1*

mutations are found in cancer.

Our characterization of the AXIN1[SupB15] mutant revealed that in addition to its

altered binding capacity, the AXIN1[SupB15] mutant also did not suppress c-Myc

dependent transcription. This result, combined with our results showing that

AXIN1 associates with E-box binding sites in c-Myc target genes ((Arnold et al,

2009) and A. Farrell, unpublished data) suggests that c-Myc degradation restricts

c-Myc transcriptional activity. If this is the case, then the phenotype of the

AXIN1[SupB15] mutant suggests that c-Myc stabilization promotes its transcriptional

activity. In support of this, unpublished data from our lab suggests that in a breast cancer cell line where c-Myc is stabilized and unable to associate with AXIN1, c-Myc can participate in multiple cycles of promoter binding and release. Further study of this hypothesis is currently underway.

During our investigation of *AXIN1* mutations in leukemia cell lines, we found that *AXIN1V2* was the predominant form of *AXIN1* expressed in these cell lines. The significance of *AXIN1V2* expression is unclear. While AXIN1v2 binds less robustly to c-Myc and GSK3β, it can still suppress c-Myc-dependent transcriptional activity, at least in 293 cells (Figure 4.1). It also still binds weakly to PP2Ac even though it lacks a portion of the PP2A binding domain (Arnold et al, 2009). It is possible that expression of *AXIN1V2* may be enriched in some cancers, which is supported by our finding that expression of *AXIN1V2* is enriched in primary breast cancer samples versus matched normal breast tissue (Zhang et al, 2011). This enrichment in *AXIN1V2* may be due to a shift in splice site usage specifically on *AXIN1* transcripts or due to a global change in splicing, which has been reported in cancer (David & Manley, 2010). However, the results from our primary B cell leukemia samples do not support an enrichment of *AXIN1V2* in leukemia, as the majority of our B ALL samples expressed a higher ratio of *AXIN1V1* to *AXIN1V2* relative to CD19+ B cells. In the one B ALL sample that did express a higher ratio of *AXIN1V2* to *AXIN1V1* (B40, Figure 4.3), the degree of enrichment is modest compared to the enrichment we found in our breast cancer samples, in which the ratio of *AXIN1V2* to *AXIN1V1* expression

was often 10-fold higher in primary breast tumors compared to their matched

normal samples (Zhang et al, 2011).

If AXIN1 is the rate-limiting component for both β-catenin and c-Myc degradation,

one would expect that increasing the level of AXIN1 would accelerate the

degradation of these proteins. Indeed, this has been demonstrated for β-catenin,

where a modest increase in AXIN1 levels dramatically reduced the half-life of β-

catenin (Lee et al, 2003). Likewise, we have previously shown that modest

AXIN1 overexpression can promote c-Myc ubiquitination and degradation (Arnold

et al, 2009). In contrast, gross overexpression of AXIN1 results in dominant

negative effects, including the stabilization of both β-catenin and c-Myc due to

the formation of incomplete degradation complexes (Arnold et al, 2009; Lee et al,

2003). Our attempt to promote c-Myc degradation in leukemia cell lines through

the use of a small molecule that increases AXIN1 protein levels (IWR-1; (Chen et

al, 2009)) was not successful. However, results from these experiments were

variable, and AXIN1 protein levels were not consistently increased. A second

compound that blocks AXIN1 degradation was recently described (XAV939), and

this compound has the same mechanism of action as IWR-1 but is 10-fold more

potent (Huang et al, 2009). It is possible that repeating these experiments with

XAV939 might yield different results.

In contrast to the results from leukemia cell lines, our results from increasing

AXIN1 expression in a c-Myc-driven lymphoma model suggest that in the face of

excess AXIN1 expression, AXIN1 must be inactivated in this model for tumorigenesis to proceed. We unexpectedly found that ectopic *Axin1* was transcriptionally downregulated in seven out of twelve *EμtTa/tetoMYC/TREAxin* tumors analyzed, and examination of a tumor without AXIN1 downregulation revealed an intriguing potential change in AXIN1 localization from membrane-associated to punctate cytoplasmic localization. While more tumors need to be analyzed for changes in AXIN1 subcellular localization, these results suggest that ectopic AXIN1 can be inactivated by multiple mechanisms in order for tumorigenesis to proceed in this model. In addition, the highly similar presentation and onset of tumors in both the *EμtTa/tetoMYC* and *EμtTa/tetoMYC/TREAxin* mice also suggest that ectopic AXIN1 may be functionally inactivated.

Further increasing AXIN1 expression in this tumor model did appear to delay the onset of tumorigenesis. However, this interpretation is complicated by changes in the background strain of the mice. The *TRE2-Axin-GFP* transgene and the *EμtTa/tetoMYC* transgenes were carried on different background strains (129/BL6 vs FVB/N), and we did not backcross the mice prior to setting up our cohorts of experimental animals. For our initial experiment comparing tumor onset in the *EμtTa/tetoMYC* and *EμtTa/tetoMYC/TREAxin* mice, the cohorts were established from an F1 generation (*EμtTa/tetoMYC* x *TRE2-Axin-GFP*). However, establishing the *EμtTa/tetoMYC/TREAxin*^{+/+} cohort required a breeding scheme that reduced the contribution of the FVB/N strain from 50% to ~10%. The

contribution of the background strain to tumor latency is well illustrated by comparing the onset of lymphoma in the mixed-background F1 generation described above to that of the parental strain, inbred FVB/N (Figure 4.11). Therefore, because of the change in background strain composition between the *EμtTa/tetoMYC/TREAxin* and *EμtTa/tetoMYC/TREAxin*^{+/+} cohorts, we cannot say conclusively that the increase in AXIN1 dosage is responsible for the increase in latency in the *EμtTa/tetoMYC/TREAxin*^{+/+} cohort. However, the *EμtTa/tetoMYC/TREAxin*^{+/+} mice that lived longer than ~200 days did not die of lymphoma, but instead appeared to die of an intestinal neoplasia (data not shown). Future experiments will examine Axin1 expression in lymphomas from *EμtTa/tetoMYC/TREAxin*^{+/+} mice to determine whether this increase in AXIN1 dosage was circumvented during tumor development, as we found in many of the *EμtTa/tetoMYC/TREAxin*^{+/-} mice (Figure 4.10).

In summary, we have shown that *AXIN1* can be deregulated in B cell leukemia either through mutation or altered expression, and that this can directly affect both c-Myc degradation and c-Myc transcriptional activity. In addition, we have examined AXIN1's tumor suppressor role in a model of MYC-driven lymphoma and found that ectopic AXIN1 appears to be incompatible with the development of lymphoma in this model. Together these results suggest that AXIN1 functions as a tumor suppressor in B cell leukemia and demonstrate that AXIN1's tumor suppressive function *in vivo* extends beyond the Wnt signaling pathway.
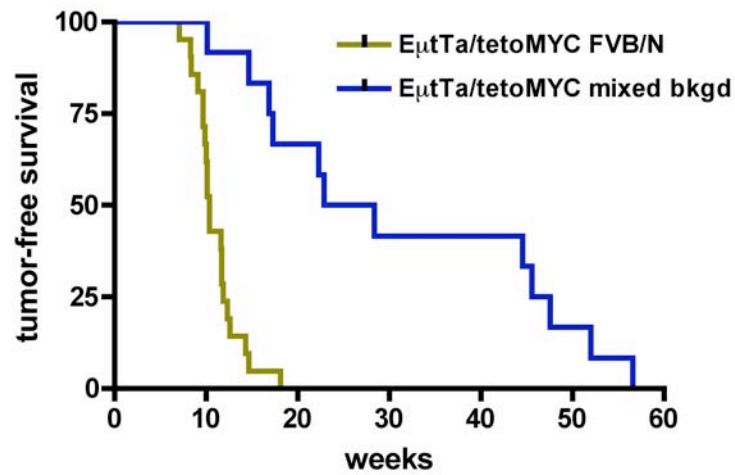
Figure 4.11. Median survival depends on the background strain of the mice.

Kaplan-meier survival curve for *EμTa/tetoMYC* mice of different backgrounds that were followed for development of lymphoma. Mixed background = F1 cross between pure FVB/N and mixed 129/BL6. FVB/N cohort, N=21; mixed background cohort, N=12.

Chapter 5. Summary and discussion

c-Myc is commonly stabilized in acute lymphoblastic leukemia

The central question addressed by this dissertation was whether increased c-Myc protein stability is a mechanism of c-Myc overexpression in leukemia. The work presented here demonstrates that indeed c-Myc protein stability is commonly increased in acute lymphoblastic leukemia and that this increased protein stability is coupled to changes in phosphorylation at the conserved N-terminal residues serine 62 and threonine 58. Previous work by our lab established that in normal cells c-Myc protein stability is regulated by these two residues during cell cycle entry, and that sequential phosphorylation of these sites was critical for the controlled accumulation of c-Myc in early G1 (Sears et al, 1999; Sears et al, 2000). At the time, the idea that this phosphorylation-dependent accumulation of c-Myc could be hijacked during cancer development had not been formally tested, but there was some evidence in the literature to support the possibility. One example came from a study of Burkitt's lymphoma cell lines, in which the *MYC* locus is translocated and is often mutated. This study examined the effect of these mutations on c-Myc protein stability, and while they found that c-Myc was stabilized when mutated at T58 or P57, in some cell lines c-Myc was stabilized in the absence of these mutations (Gregory & Hann, 2000). This suggested that c-Myc could be stabilized by a mechanism other than mutation. However, whether this was a common but unstudied phenomenon or simply limited to Burkitt's lymphoma was unknown.

In chapter 2, I showed that c-Myc stabilization is commonly found in acute lymphoblastic leukemia cell lines and patient samples and that this is coupled to increased S62 phosphorylation. This is consistent with mutational data showing that c-Myc with high pS62 (due to mutation at T58) has increased stability (Lutterbach & Hann, 1994; Sears et al, 2000). Given that activated signaling pathways that prevent T58 phosphorylation (and therefore c-Myc degradation) should have the same functional effect on c-Myc as a T58 mutation, we looked for defects in the pathway that regulates T58 phosphorylation, PI3K, and in a negative regulator of the PI3K pathway, PP2A. In some cases we found that signaling through PI3K contributed to high c-Myc levels (Figure 2.4) and in other cases we found dramatic increases in inhibitors of PP2A (*SET* and *CIP2A*, Figure 2.8). Interestingly, there is recent data describing PP2A holoenzymes that negatively regulate PI3K signaling (Padmanabhan et al, 2009; Rodgers et al, 2011), suggesting that activated PI3K signaling and inhibition of PP2A in leukemia could be functionally related. While we did not test whether PP2A inhibition is maintaining the activation of the PI3K pathway in these cell lines and samples, it would be interesting to do so.

The prevalence of PP2A inhibition in leukemia has only recently been explored. Inhibition of PP2A in leukemia development was first demonstrated as a feature of blast crisis progression in chronic myeloid leukemia, in which the PP2A inhibitor SET becomes upregulated during the transition from chronic phase to blast crisis (Neviani et al, 2005). More recently, inhibition of PP2A has been

148

reported in AML. These studies found increased expression of several different PP2A inhibitors, including SET, SETBP1, and CIP2A, and reduced expression of PP2A B regulatory subunits (B56β and B56γ) in both AML cell lines and primary samples (Cristobal et al, 2011; Roberts et al, 2010). Interestingly, a study of CML also reported that the inhibition of PP2A by CIP2A correlated with c-Myc S62 phosphorylation (Lucas et al, 2011), further supporting the role of PP2A inhibition in high S62 phosphorylation. Together, these studies all support the idea that activating PP2A in leukemia could be a useful therapeutic approach for these malignancies. To this end, several compounds exist that may be translated to the clinic in the future. One of these, FTY720, has already shown efficacy in CML (Neviani et al, 2007) and was well tolerated in clinical trials for the treatment of multiple sclerosis (Aktas et al, 2010).

The study of whether PP2A plays a role in the development of T ALL is a recent occurrence, and as such, very little evidence currently exists tying PP2A to T ALL pathogenesis. The first mechanistic description of a role for PP2A in T ALL pathogenesis came from a study that identified concurrent Notch and miR17-92 activation via translocation to the TCRδ locus (Mavrakis et al, 2010). This concurrent activation suggested that increased expression of the miR17-92 locus cooperates with Notch in the development of T ALL, a conclusion supported by mouse modeling of miR17-92 overexpression in Notch-induced T ALL. The authors then employed a genetic screen for shRNAs that could phenocopy miR-19 overexpression (a member of the miR17-92 family) and identified a PP2A B

subunit, B56ε, as one of the critical targets of miR-19's collaborative effect

(Mavrakis et al, 2010). The results from this study suggest an as yet unstudied

role for the inhibition of PP2A in T ALL pathogenesis, which is also supported by

my data in primary T ALL samples showing a correlation between c-Myc S62

phosphorylation and transcriptional upregulation of the PP2A inhibitors *SET* and

CIP2A (Figure 2.8A, 2.8D, 2.8E).

If PP2A is inhibited in some cases of T ALL, then reactivating PP2A could be a

therapeutic strategy for the treatment of those cases of T ALL. To test this idea,

we treated 6 T ALL cell lines with a new PP2A-activating compound, OP449,

which was made available to me through collaboration between our lab and Dale

Christensen at Cognosci, Inc. This compound increases PP2A activity by binding

to the PP2A inhibitor SET ((Christensen et al, 2011) and D. Christensen,

unpublished data), which I found to be upregulated in some primary T ALL

samples (Figure 2.8D). As shown in Figure 5.1, these T ALL cell lines were all

sensitive to OP449 at a lower concentration than that of normal T cells (Figure

5.1), and the cytotoxicity was extremely rapid – depending on the T ALL cell line,

70-90% of cells were dead within 15 minutes of treatment with 1μM OP449 (data

not shown). To test whether this rapid cytotoxicity was dependent on PP2A

activity, I pre-treated these cell lines with okadaic acid (an inhibitor of PP2A

activity) and then measured the cytotoxicity of OP449. In these experiments, the

degree of cytotoxicity did not change, suggesting that inhibiting SET with OP449

is cytotoxic through a PP2A-independent mechanism. SET has been reported to

inhibit a mediator of apoptosis, the nuclease NM23-H1 (Fan et al, 2003), so it is possible that OP449-mediated cytotoxicity is acting through this pathway, but this has not been tested. While these experiments support exploring OP449 as a potential treatment for T ALL, further studies will be required to determine the mechanism of action of OP449 in T ALL.
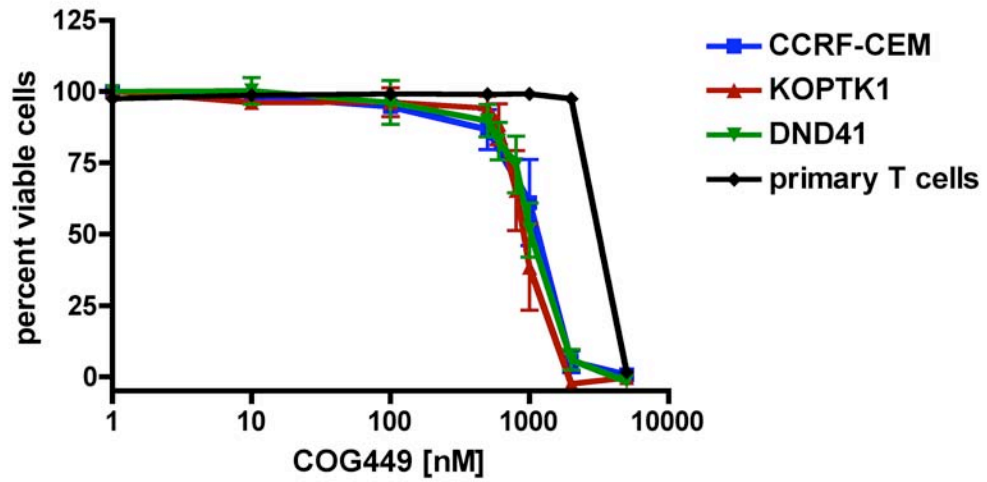
Figure 5.1. OP449 is cytotoxic to T ALL cell lines.

WST assay of cell viability after 72 hr treatment of three T ALL cell lines (CCRF-CEM, KOPTK1, and DND41) and primary T cells with OP449 over a range of concentrations. Other T ALL cell lines tested but not shown: JurkatE6-1, MOLT-3, MOLT-4.

c-Myc is phosphorylated at serine 62 during myeloid differentiation and in acute myeloid leukemia

Proper regulation of c-Myc is critical for both the development and maintenance of the hematopoietic system. Through mouse studies of both *Myc* deletion and overexpression at the mRNA level, it is clear that too little or too much *Myc* expression can have catastrophic effects, including bone marrow failure and tumorigenesis (Dubois et al, 2008; Felsher & Bishop, 1999; Smith et al, 2006; Wilson et al, 2004). While these studies have shown that proper regulation of *Myc* expression in the hematopoietic system is important, it is unknown how *Myc* expression is regulated in this system.

A few recent studies have begun to address how c-Myc levels are regulated in hematopoietic stem and progenitor cells. Examination of *Myc* mRNA expression in HSCs, multipotent progenitors, and myeloid and lymphoid lineage-restricted progenitors revealed that *Myc* expression is roughly equivalent in all of these populations (Laurenti et al, 2008). This result hinted at the idea that c-Myc may instead be dynamically controlled at the protein level in these populations, rather than at the mRNA level. In support of this idea, another group reported that c-Myc protein levels are higher in multipotent progenitors than in hematopoietic stem cells and that this increase in c-Myc protein levels is due to a reduced rate of c-Myc degradation by the E3 ligase Fbw7 (Reavie et al, 2010). In this elegant study, c-Myc protein levels were monitored via GFP levels after the introduction of a *GFP-Myc* transgene into the endogenous *Myc* locus. Together these studies

153

begin to paint a picture where c-Myc levels in stem and progenitor cells are rapidly adjusted through changes in c-Myc protein stability.

Since c-Myc protein stability is controlled in part by phosphorylation at S62 and T58 (Sears et al, 2000; Yeh et al, 2004), and since degradation of c-Myc by Fbw7 is dependent on phosphorylation at T58 (Welcker et al, 2004; Yada et al, 2004), changes in c-Myc protein stability in hematopoietic stem and progenitor cells may be controlled by phosphorylation at S62 and T58. In chapter 3, I demonstrated that in human progenitor cells from the myeloid lineage (progranulocytes), c-Myc is phosphorylated at S62, and that as these cells differentiate into mature granulocytes, S62 phosphorylation decreases, dependent on active GSK3 (Figure 3.2). These results suggest that c-Myc protein stability in granulocytic populations is modulated by the interplay of S62 and T58 phosphorylation, as we have previously shown in normal fibroblasts (Sears et al, 1999; Sears et al, 2000).

The ability to toggle c-Myc protein stability to rapidly affect cellular levels of c-Myc may be a mechanism that is re-used through multiple stages of hematopoiesis. In addition to HSCs, Reavie et al. showed that myeloerythroid progenitors and double-negative T cells also exhibit a dramatic increase in c-Myc levels when Fbw7 is conditionally deleted, implicating a T58-dependent degradation pathway in the control of c-Myc levels in these cell types. However, the conditional Fbw7 knockout approach used by Reavie et al. lacks specificity because Fbw7 has

many substrates (c-Myc, Notch, cyclin E). Instead, specifically investigating c-Myc phosphorylation-dependent degradation in hematopoiesis would require the generation of a mouse with an *LSL-Myc^{T58A}* construct knocked into the endogenous *Myc* locus (similar to the classic *LSL-K-Ras^{G12D}* knock-in mouse model (Jackson et al, 2001)). This tool would allow the excision of endogenous *Myc* with a tissue-specific Cre recombinase and the simultaneous activation of T58A with the endogenous *Myc* locus regulatory controls. Using this system, one could more specifically interrogate the role of c-Myc S62 phosphorylation in the stem cell compartment or in a given hematopoietic lineage.

In chapter 3, I also demonstrated that AMLs with diverse mutations and FAB classifications all have high levels of a high molecular weight form of pS62 c-Myc. This result is intriguing in light of the natural occurrence of high levels of a high molecular weight form of pS62 c-Myc in myeloid progenitor cells. If S62 phosphorylation is a feature of proliferating progenitor cells, then it is reasonable that leukemic cells, which are also undifferentiated and rapidly dividing, likewise express high levels of S62 phosphorylation. However, while proliferating progenitor cells likely stabilize c-Myc in response to the regulated stimulation of signaling pathways, leukemic cells may instead stabilize c-Myc in response to persistent stimulation of these pathways, such as that provided by activating mutations. Mutations in Ras and in receptor tyrosine kinases like FLT3 and c-KIT are common in AML and confer constitutive activation to these molecules. While we found that these activating mutations correlate with the presence of high S62

phosphorylation (Table 3.1 and Figure 3.3A), we were unable to demonstrate

that the presence of this high molecular weight form of pS62 c-Myc was

dependent on activating mutations in FLT3 or Ras, as this form of pS62 c-Myc

appeared to be resistant to short-term inhibition of these pathways. However, we

were able to demonstrate that activating mutations in FLT3 and Ras help

maintain levels of the lower molecular weight form of c-Myc and promote c-Myc

chromatin association (Figure 3.4).

Taken together, my results from chapter 2 and 3 argue that c-Myc S62

phosphorylation is important for promoting increased c-Myc protein stability both

in a regulated fashion in normal hematopoietic progenitor cells and in an

unregulated fashion in the development of both lymphoid and myeloid leukemias.

Integration of c-Myc phosphorylation-dependent degradation and c-Myc transcriptional activity

If phosphorylation of c-Myc at S62 is tightly regulated (Sears et al, 2000; Yeh et

al, 2004), then what is c-Myc S62 phosphorylation doing for the cell? Is there a

functional significance to c-Myc S62 phosphorylation beyond simply promoting

increased c-Myc stability?

Our previous work established S62/T58 phosphorylation as critical regulators of

c-Myc levels in response to growth stimulation, and unpublished data from our

lab now suggests that this regulation not only controls c-Myc levels but also c-

Myc transcriptional activity on at least a subset of c-Myc target genes. We find

that phosphorylation at S62 allows c-Myc to interact with the Pin1 prolyl

isomerase, which binds to phosphorylated serine or threonine residues that are

followed by proline, and subsequent isomerization of S62-phosphorylated c-Myc

by Pin1 increases both c-Myc chromatin association and target gene

transcription (A Farrell, unpublished data). This is supported by sequential ChIP

experiments where we find pS62 c-Myc and Pin1 bound together at c-Myc

transactivated target genes (*E2F2* and *NUCLEOLIN*) (A Farrell, unpublished

data). In addition, we performed RNA-seq experiments to determine whether

Pin1 preferentially affects the expression of some c-Myc target genes. We found

that of the c-Myc target genes that were preferentially upregulated by Pin1, more

than 50% of them were involved in ribosome biogenesis and metabolism (A

Farrell and C. Pelz, unpublished data), suggesting that this mode of regulating c-

Myc transcriptional activity is skewed toward genes that promote cell growth,

though genes involved in cell cycle progression were also represented.

These new results, coupled with our previous results showing that Pin1 promotes

c-Myc degradation (Yeh et al, 2004), suggest that the activity of the Pin1 prolyl

isomerase likely serves as a timing mechanism or extra regulatory step

downstream of S62 phosphorylation by trans-specific kinases like ERK that

allows for the activation and subsequent degradation of c-Myc. This appears to

occur through the assembly of the c-Myc degradation complex on the promoters

of certain target genes, as we are able to detect association of c-Myc, GSK3β,

Pin1, PP2Ac, Fbw7, AXIN1, and the 19S subunit of the proteasome with the c-Myc target gene *NUCLEOLIN* by chromatin IP (A Farrell, unpublished data). In addition, the release of c-Myc from this promoter is blocked by the addition of the proteasome inhibitor MG132, indicating that degradation of c-Myc is required for its release from the DNA.

While these results were obtained in non-cancer cell lines (293s and MCF10As), we also found a strong correlation between the level of pS62 c-Myc and the level of Pin1 in primary breast cancer samples (A. Farrell, unpublished data). These results, along with other reports of S62-phosphorylated c-Myc binding to DNA (Benassi et al, 2006; Hydbring et al, 2010), demonstrate that S62-phosphorylated c-Myc is transcriptionally active. Since I have shown that S62-phosphorylated c-Myc is prevalent in both acute lymphoid and myeloid leukemias, targeting this form of c-Myc, either by inhibiting phosphorylation of S62 or by promoting dephosphorylation of S62, could be a potential therapeutic strategy for these types of leukemia, especially since genes involved in ribosome biogenesis and metabolism are likely supporting the rapid proliferation of these cells.

While c-Myc S62 phosphorylation is prevalent in both leukemia and breast cancer (Zhang et al, 2011), this pathway involving Pin1 is by no means the only modulator of c-Myc transcriptional activity, and other classes of c-Myc target genes may require other post-translational modifications on c-Myc in order to be activated or repressed. For example, we find that S62-phosphorylated c-Myc also

binds to the *P21* promoter, but overexpression or knockdown of Pin1 has no effect (A. Farrell, unpublished data). c-Myc may also function without S62 phosphorylation. An example of this comes from a study in which the PML4 protein binds to c-Myc and destabilizes it, resulting in the release of c-Myc from the repressed target genes *P21* and *P15* and promoting the differentiation of a monocytic leukemia cell line. In this study however, the destabilization of c-Myc by PML4 was both S62- and T58-phosphorylation-independent (Buschbeck et al, 2007).

Hypothetical model for the role of serine 62 phosphorylation in hematopoiesis and leukemia

Based on the results presented in this dissertation and on my survey of the literature, I propose the following general model for the involvement of c-Myc S62 phosphorylation in both hematopoiesis and leukemia. In quiescent hematopoietic stem cells (HSCs), c-Myc protein levels are low due to rapid degradation by the ubiquitin ligase Fbw7, while *MYC* mRNA levels are high. This represents a "poised" state where c-Myc protein levels can be quickly increased by changing c-Myc protein stability. Once the HSC receives signals to leave the stem cell niche, these extracellular signals transiently stabilize c-Myc through the phosphorylation of S62, which promotes cell cycle entry and the subsequent rapid expansion of this population as the HSC becomes a multipotent progenitor. This transient stabilization and S62 phosphorylation persists in both multipotent progenitors and lineage-restricted progenitors as they continue to proliferate.

Once cells of a given lineage commit to terminal differentiation, c-Myc is destabilized through the phosphorylation of T58 by GSK3, dephosphorylation of S62 by Pin1 and PP2A, and ubiquitination by Fbw7, leading to c-Myc degradation. This reduces the level of c-Myc protein as the cell undergoes terminal differentiation, and this is accompanied by a reduction in *MYC* mRNA levels.

In leukemias with high S62 phosphorylation, I propose that the initiating cell has sustained a mutation or other alteration that leads to a disruption of c-Myc degradation. This could include mechanisms that promote S62 phosphorylation, such as the activation of upstream signaling molecules like receptor tyrosine kinases or Ras, or mechanisms that prevent S62 dephosphorylation, such as inactivation of PP2A or activation of the PI3K pathway. These lesions would then maintain a form of c-Myc that is stabilized and S62-phosphorylated, which would help to perpetuate a progenitor-like cell that is no longer able to induce terminal differentiation.

The role of AXIN1 in leukemia development

In chapter 4, I presented results from examining many potential modes of deregulation for AXIN1 in both lymphoid and myeloid leukemia. Collectively, the data presented in chapter 4 do not argue for a major role for AXIN1 in the development of leukemia (Arnold & Sears, 2006; Yeh et al, 2004). While c-Myc is clearly a major player in the development of both lymphoid and myeloid

160

leukemia, and changes in c-Myc phosphorylation and stability are common, it appears that this does not frequently occur through the deregulation of AXIN1.

It is well established that mutations or deregulation of some genes is prevalent in one type of cancer and much less frequent in others. Prominent examples include mutation of *APC* in colorectal cancer (Kinzler & Vogelstein, 1996), mutation of *BRAF* in melanoma (Thomas, 2006), and mutation of *NOTCH1* in T ALL (Weng et al, 2004). *AXIN1* and *AXIN2* are mutated in a handful of solid tumors, including *AXIN1* in ~10% of hepatocellular carcinomas and *AXIN2* in ~20% of mismatch repair-deficient colorectal tumors (Salahshor & Woodgett, 2005). Currently, no single cancer has been reported as having a large fraction of cases carrying AXIN1 mutations.

While I looked at multiple ways that AXIN1 might be deregulated in leukemia (mutation, splicing, mRNA expression, protein levels), it is still possible that AXIN1's function is altered in leukemia, and in solid tumors, through mechanisms such as phosphorylation or changes in subcellular localization. In addition, AXIN1 regulates many pathways (and more are being uncovered), but little is known about how limiting amounts of AXIN1 shuttle between pathways. How deregulation of one pathway could sequester AXIN1 or skew the regulation of other signaling pathways that require AXIN1 may also be a way that AXIN1 could be deregulated in cancer.

Chapter 6. Materials and methods

Cell lines and cell culture

AML cell lines (HL-60, HEL, CTV-1, U937, MOLM-13, MOLM-14, MV4-11, Kasumi-1), a CML cell line (K562), B ALL cell lines (Reh, SupB15), Burkitt's lymphoma cell lines (CA46), T ALL cell lines (Jurkat E6-1, CCRF-CEM, KOPTK1, DND41, MOLT-3, MOLT-4), and an EBV-immortalized B lymphoblastoid cell line (JY) were cultured in Roswell Park Memorial Institute (RPMI) 1640 medium (Invitrogen) supplemented with 10% defined fetal bovine serum (FBS) (Hyclone), 2mM L-glutamine (Invitrogen), and 1X penicillin/streptomycin (Invitrogen), except Kasumi-1 which required 20% FBS. Fresh primary T cells were cultured in RPMI 1640 medium supplemented with 10% defined FBS, 2mM L-glutamine, 1X sodium pyruvate (Invitrogen), 1X penicillin/streptomycin, and 50μM β-mercaptoethanol (Sigma). All cells were cultured in 5% CO_2 in a 37°C humidified incubator. Cell lines were subcultured every 2-3 days by diluting with fresh medium to a density of 5x10^5-7x10e^5 cells/ml, depending on the cell line. Prior to every experiment, cell lines were subcultured on the previous day to ensure healthy, exponentially growing cells as starting material. Cell lines were treated with specific inhibitors (U0126, AC220, IWR-1, LiCl, LY294002, okadaic acid, OP449, MG132, lactacystin) by adding the inhibitor (or its diluent as a negative control) to either asynchronously growing cells or cells that had been starved in media containing 1% FBS for the time indicated in the figure legend (usually 24-48 hours).

Patient Samples

Frozen bone marrow or frozen peripheral blood samples from anonymous patients diagnosed with B ALL, T ALL, or AML were obtained in accordance with OHSU IRB guidelines and were stored by the collector at -150°C prior to recovery. Frozen AML samples collected by apheresis (stored for 0-3 years) were recovered by thawing in a 37°C waterbath followed by slow resuspension in RPMI supplemented with 10% defined FBS, 2mM L-glutamine, and 1X penicillin/streptomycin. Cells were immediately centrifuged at 100 x g for 20 minutes, resuspended in fresh medium, and assessed for 1) cell number by counting on a hemacytometer and 2) cell viability by trypan blue exclusion. Most recovered samples yielded cells with >85% viability. Cells were centrifuged and snap frozen as cell pellets for protein or DNA extraction or were lysed in Trizol reagent (Invitrogen) and snap frozen for RNA extraction. All samples were stored at -80°C until use.

Frozen B ALL and T ALL samples (stored for >15 years) or frozen normal bone marrow samples purchased from Stem Cell Technologies were recovered by thawing in a 37°C waterbath followed by slow resuspension in RPMI supplemented with 10% defined FBS, 2mM L-glutamine, 1X penicillin/streptomycin, and 150 units DNase I and incubation in a 37°C humidified incubator for 4 hours. Cells were centrifuged at 100 x g for 20 minutes, resuspended in fresh medium, and assessed for 1) cell number by

counting on a hemacytometer and 2) cell viability by trypan blue exclusion. Most

recovered B ALL and T ALL samples yielded cells with >80% viability. Normal

bone marrow samples were ~85% viable. Cells were centrifuged and snap frozen

as cell pellets for protein or DNA extraction or were lysed in Trizol reagent and

snap frozen for RNA extraction. All samples were stored at -80°C until use.

Fresh peripheral blood was collected from consented donors in accordance with

OHSU IRB guidelines. Peripheral blood mononuclear cells (PBMCs) were

isolated from peripheral blood by Ficoll density gradient sedimentation by

layering 1:1 blood to buffered salt solution (BSS; 145mM Tris, pH7.6, 126mM

NaCl, 5μM CaCl$_2$, 98μM MgCl$_2$, 540μM KCl, 0.01% D-glucose) over Ficoll-Paque

PLUS (GE Healthcare) and centrifuging at 18-20°C at 400 x g for 40 minutes.

The plasma layer was aspirated and the buffy coat (containing PBMCs) was

collected and washed twice with BSS. PBMCs were resuspended in BSS

supplemented with 2% defined FBS, counted, and assessed for viability by

trypan blue exclusion. PBMC viability was always >95%. PBMCs were either

centrifuged and snap frozen as cell pellets for protein extraction or used for the

isolation of specific leukocyte populations by magnetic bead selection as

described below. Samples were stored at -80°C until use.

Fresh normal bone marrow (NBM) was received from the Hematopoietic Cell

Processing Laboratory (HCPL) as excess clinical material available for research

or from the Bagby lab after collection from consented donors obtained in

accordance with OHSU IRB guidelines. Fresh NBM from the HCPL was washed twice in Red Blood Cell (RBC) Lysis buffer (155mM NH_4Cl, 12mM $NaHCO_3$, 100μM EDTA) for 2 minutes, centrifuged, and resuspended in buffered salt solution supplemented with 2% defined FBS. NBM cells were counted and assessed for viability by trypan blue exclusion. Viability of NBM was ~90%. Cells were centrifuged and snap frozen as cell pellets for protein extraction or were lysed in Trizol reagent and snap frozen for RNA extraction. Alternatively, mononuclear cells from fresh NBM were received from the Bagby lab (with or without removal of red blood cells by dextran sedimentation) after Ficoll-Paque separation and removal of CD34$^+$ cells. In these cases, fresh NBM mononuclear cells (depleted of CD34$^+$ cells) were counted and assessed for viability by trypan blue exclusion. Viability was >95%. Cells were centrifuged and snap frozen as cell pellets for protein extraction. Samples were stored at -80°C until use.

Isolation of specific hematopoietic cell populations

High density neutrophils

High density neutrophils were isolated from fresh normal bone marrow after Ficoll-Paque separation. Neutrophils were counted and then cultured in RPMI supplemented with cytokines (100U/ml GM-CSF, 2U/ml G-CSF, 50ng/ml FLT3L, and 50ng/ml SCF). After 1-2 hours or 24 hours, viability was assessed, which was >95%, and neutrophils were centrifuged and snap frozen as cell pellets for protein extraction and, in parallel, spun onto glass slides for Giemsa staining and morphological examination. Cell pellets were stored at -80°C until use.

Polymorphonuclear cells

Polymorphonuclear (PMN) cells were isolated from peripheral blood by Ficoll density gradient sedimentation by layering 1:1 blood to buffered salt solution (145mM Tris, pH7.6, 126mM NaCl, 5μM CaCl$_2$, 98μM MgCl$_2$, 540μM KCl, 0.01% D-glucose) over Ficoll-Paque PLUS (GE Healthcare) and centrifuging at 18-20°C at 400 x g for 40 minutes. Plasma and Ficoll layers were aspirated, leaving only PMN cells, which sediment to the bottom of the Ficoll gradient just above the erythrocyte layer. PMN cells were enriched by lysing erythrocytes with 2 rounds of RBC lysis buffer and resuspended in BSS, counted, and assessed for viability by trypan blue exclusion. PMN cell viability was always >95%. PMN cells were either centrifuged and snap frozen as cell pellets for protein extraction or lysed in Trizol reagent and snap frozen for RNA extraction. Samples were stored at -80°C until use.

B cells

B cells were isolated from fresh PBMCs by magnetic bead separation using the EasySep Human B Cell Enrichment Kit (Stem Cell Technologies) or EasySep Human CD19 Positive Selection Kit (Stem Cell Technologies) according to manufacturer's instructions. B cells were counted and assessed for viability by trypan blue exclusion, which was always >95%. B cells were then centrifuged and snap frozen as cell pellets for protein extraction or lysed in Trizol reagent and snap frozen for RNA extraction. Samples were stored at -80°C until use.

Monocytes

Monocytes were isolated from fresh PBMCs by magnetic bead separation using the EasySep Human CD14 Positive Selection Kit (Stem Cell Technologies) according to manufacturer's instructions. Monocytes were counted and assessed for viability by trypan blue exclusion, which was always >95%. Monocytes were centrifuged and snap frozen as cell pellets for protein extraction or were lysed in Trizol reagent and snap frozen for RNA extraction. Samples were stored at -80°C until use.

T cells

T cells were isolated from fresh PBMCs by magnetic bead separation using the EasySep Human CD3 Positive Selection Kit (Stem Cell Technologies) according to manufacturer's instructions. T cells were counted and assessed for viability by trypan blue exclusion, which was always >95%. T cells were centrifuged and snap frozen as cell pellets for protein extraction or were lysed in Trizol reagent and snap frozen for RNA extraction. Samples were stored at -80°C until use.

Primary T cell isolation and culture

Fresh peripheral blood was collected from consented donors in accordance with OHSU IRB guidelines. T cells were isolated by negative selection from fresh peripheral blood using the RosetteSep Human T Cell Enrichment Cocktail (Stem Cell Technologies) according to manufacturer's instructions. T cells were washed

with BSS, counted, and assessed for viability by trypan blue exclusion, which was >95%. T cells were either centrifuged and snap frozen as cell pellets for protein extraction or, alternatively, T cells were cultured in the presence or absence of phytohemagglutinin (PHA; Invitrogen), a T cell mitogen, in order to stimulate cell division. After 4 days, cultured T cells were counted and assessed for viability, which was >95%. T cells were then centrifuged and snap frozen as cell pellets for protein extraction. Samples were stored at -80°C until use.

In vitro differentiation of CD34+ cells from normal bone marrow

Fresh normal bone marrow (with or without dextran sedimentation to remove red blood cells) was subjected to Ficoll density gradient sedimentation to isolate bone marrow mononuclear cells. CD34+ cells were isolated from mononuclear cells by magnetic bead separation using the EasySep Human CD34 Positive Selection Kit (Stem Cell Technologies) according to the manufacturer's instructions. CD34+ cells were cultured for up to 12 days in RPMI +10% FBS supplemented with cytokines (100U/ml GM-CSF, 2U/ml G-CSF, 50ng/ml FLT3L, and 50ng/ml SCF), with twice-weekly dilution of cells to a density of 1e6/ml by adding fresh media and cytokines. At the each timepoint, cells were removed from the culture, counted, and assessed for viability by trypan blue exclusion. Viability of these cells was 90-95%. Cells were centrifuged and snap frozen as cell pellets for protein extraction and, in parallel, spun onto glass slides for Giemsa staining and morphological examination.

Antibodies and chemicals

The following antibodies were used for immunoblotting unless otherwise specified. Pan c-Myc antibodies used were N262 (1:1000), C19 (1:100), C33 (1:50) (all from Santa Cruz Biotechnology), C33 (1:500; Calbiochem), and Y69 (1:1000; Abcam). C33-conjugated agarose beads for immunoprecipitation were also from Santa Cruz Biotechnology. c-Myc pS62/pT58 antibody (1:500) was from Cell Signaling, and is made specific for pT58 by blotting in milk. c-Myc pT58 antibody (1:500) was from Abm. c-Myc (thr/ala) polyclonal pS62 antibody was generated as previously described (Escamilla-Powers2007JBC). c-Myc monoclonal pS62 antibody (33A12E10; 1:100) was a gift from Yoichi Taya (National Cancer Center Research Institute, Tokyo, Japan) and the same pS62 antibody is now commercially available (1:500) from Abcam. Myc-tag antibody (71D10; 1:1000) was from Cell Signaling. AXIN1 antibodies were A0481 (1:1000) from Sigma and C76H11 (1:1000) from Cell Signaling. β-actin antibodies were from Santa Cruz Biotechnology (1:1000) and Sigma (1:10 000). α–tubulin antibody (1:2000) was from Sigma. pERK 1/2 (Y204/Y185; 1:200), ERK1 (1:200) were from Santa Cruz Biotechnology. GAPDH antibody (1:10 000) was from Ambion. GSK3β antibody (1:1000) was from Cell Signaling. SET antibody (1:2000) was from Bethyl Labs. Secondary antibodies were goat anti-mouse or goat anti-rabbit conjugated to either AlexaFluor 680 (Invitrogen) or IRDye800 (Rockland) For immunofluorescence, antibodies used were Myc-tag 71D10 (1:50) from Cell Signaling and Y69 (1:1000) from Abcam.

IWR-1 compound was a gift from Lawrence Lum (UT Southwestern) and later available from Sigma. Doxycycline hydrochloride and MG132 were from Sigma. U0126 was from Cell Signaling Technology. AC220 was a gift from Anupriya Agarwal (OHSU) but is available from Selleck Chemicals. Phytohemagglutinin (PHA) was from Invitrogen. Lactacystin was obtained from EJ Corey Lab (Harvard University). LY294002 was from EMD Biosciences. Okadaic acid was from Calbiochem. Cycloheximide was from US Biological. OP449 stapled peptide was a gift from Dale Christensen (Cognosci, Inc.).

Mice

TRE2-Axin-GFP mice (TA32 line) were the kind gift of Frank Costantini, Columbia University; these mice are described in (Hsu et al, 2001). *EµSR-tTa/tet-o-MYC* mice (*tTa* – line 83, *MYC* – line 36) were the kind gift of Dean Felsher, Stanford University; these mice are described in (Felsher & Bishop, 1999). *TRE2-Axin-GFP* mice (mixed 129/C57BL/6 background upon receipt) were housed in the barrier facility at OHSU and maintained by breeding to C57BL/6 mice. *EµSR-tTa/tet-o-MYC* mice (pure FVB/N background upon receipt) were housed in the barrier facility at OHSU and maintained by breeding to FVB/N mice.

To establish cohorts of experimental animals, *EµSR-tTa/tet-o-MYC* males (FVB/N) were bred to *TRE2-Axin-GFP* females (129/BL6). Pups from these breedings were genotyped, and *EµSR-tTa/tet-o-MYC, EµSR-tTa/TRE2-Axin-*

GFP, and *EμSR-tTa/tet-o-MYC/TRE2-Axin-GFP* mice (F1 generation; 50%

FVB/N, 50% 129/BL6) were assigned to cohorts with or without access to

doxycycline water bottles (100μg/ml in H$_2$O, filter sterilized and changed weekly).

Doxycycline administration suppresses expression of both *tet-o-MYC* and *TRE2-*

Axin-GFP. Cohorts were followed for tumor development, and mice were

sacrificed when they became moribund.

To establish the *EμSR-tTa/tet-o-MYC/TRE2-Axin-GFP* homozygous cohort, an

EμSR-tTa/tet-o-MYC/TRE2-Axin-GFP hemizygous male mouse (#861; F1 from

crossing a *EμSR-tTa/tet-o-MYC* FVB/N male and a *TRE2-Axin-GFP* mixed

129/BL6 female) was crossed to a hemizygous *TRE2-Axin-GFP* female (#2043,

129/BL6). This cross did not yield any homozygous offspring, but one of the

EμSR-tTa/tet-o-MYC/TRE2-Axin-GFP hemizygous male offspring (#903) was

used for further breeding because #861 was no longer fertile. #903 was crossed

to two hemizygous *TRE2-Axin-GFP* females (#110 and 105, 129/BL6). The cross

between male #903 and female #110 yielded one *tet-o-MYC/TRE2-Axin-GFP*

homozygous male (#945) and two *EμSR-tTa/TRE2-Axin-GFP* homozygous

females (#944 and 946). The cross between male #903 and female #105 yielded

one additional *EμSR-tTa/TRE2-Axin-GFP* homozygous female (#949). Male

#945 and females #944, 946, and 949 were the founders of the *TRE2-Axin-GFP*

homozygous line and were 3 generations (F3) removed from the pure FVB/N

line, with an approximate mixture of 12% FVB/N and 88% 129/BL6. All *EμSR-*

tTa/tet-o-MYC/TRE2-Axin-GFP homozygous experimental animals were derived

from crossing male #945 and females #944, 946, and 949 or from backcrossing progeny of these crosses with male #945.

In all cases, experimental animals were hemizygous for the *EμSR-tTa* transgene.

Genotyping

Tail tips were removed from mice between the ages of 10-14 days, and mice were labeled by ear tagging. DNA was isolated from tail tips by digesting tails with 100μg/ml proteinase K in Tail Buffer (100mM Tris HCl, pH 8.5, 200mM NaCl, 0.2% SDS, 5mM EDTA), followed by precipitation of DNA with isopropanol. DNA pellets were dried and resuspended in TE buffer. Genotyping of tail DNA was performed by PCR amplification using the primers listed in Table 6.1. Mice carrying *EμSR-tTa, tet-o-MYC*, or one copy of *TRE2-Axin-GFP* (hemizygous) were genotyped by traditional PCR using the primers listed in Table 6.1. PCR reactions contained 1μl DNA, 0.5μl forward primer, 0.5μl reverse primer, and 10μl 2X ImmoMix Red (Bioline) in a total volume of 20μl. PCR reactions were heated to 95°C for 10 minutes to activate the DNA polymerase followed by 35 cycles of amplification (95°C for 30 sec, 55-59°C for 30 sec (depending on primer pair; see Table 6.1), 72°C for 30 sec) and a 10 minute extension at 72°C. Products were analyzed by agarose gel electrophoresis for presence/absence of bands. For genotyping homozygous *TRE2-Axin-GFP* mice, DNA was isolated from tails using Qiagen Blood and Tissue DNA kit according to manufacturer's instructions followed by quantitative real time PCR using the primers listed in

Table 6.1. PCR reactions contained 1μl DNA, 0.5μl forward primer, 0.5μl reverse primer, and 10μl 2X PerfeCTa SYBR Green SuperMix (Quanta Biosciences) in a total volume of 20μl. PCR reactions were heated to 95°C for 20 seconds to activate the DNA polymerase followed by 40 cycles of amplification (95°C for 15 sec, 60°C for 60 sec; alternatively, 95°C for 3 sec, 60°C for 30 sec using PerfeCTa SYBR Green FastMix (Quanta Biosciences)) on a StepOne Real-Time PCR System machine (Applied Biosystems). *TRE2-Axin-GFP* transgene copy number was analyzed by using the $2^{\Delta\Delta Ct}$ method with *IL2* as a reference gene. To score animals as hemizygous or homozygous, the sample with the lowest relative copy number value was set to 1, and animals were scored as hemizygous if they were within 1.5 fold of the sample with the lowest expression. Animals with a copy number value greater than 3 fold were scored as homozygous. Animals with a copy number value between 1.5 fold and 3 fold were thrown out as ambiguous. This protocol was developed because genotyping by quantitative real time PCR does not yield clean results of 1:1 and 2:1 transgene to reference gene amplification, like one might expect (Annie Powell, personal communication). Once homozygotes were established unambiguously, homozygotes were crossed together to propagate the homozygous line.

Table 6.1. Genotyping primers.

primer name	primer sequence (5'->3')	type of PCR	annealing temp	reference
tet-o-MYC 1	TAG TGA ACC GTC AGA TCG CCT G	traditional	59°	(Felsher & Bishop, 1999)
tet-o-MYC 2	TTT GAT GAA GGT CTC GTC GTC C	traditional	59°	(Felsher & Bishop, 1999)
Eμ-tTA 1	AGG CCT GTA CGG AAG TGT	traditional	59°	(Felsher & Bishop, 1999)
Eμ-tTA 2	CTC TGC ACC TTG GTG ATC	traditional	59°	(Felsher & Bishop, 1999)
TRE2–Axin–GFP Fwd	ACG GCA AGC TGA CCC TGA AGT	traditional	55°	(Hsu et al, 2001)
TRE2–Axin–GFP Rev	GCT TCT CGT TGG GGT CTT TGC	traditional	55°	(Hsu et al, 2001)
mouse Axin1 Fwd	ACG GTA CAA CGA AGC AGA GAG CT	quantitative	60°	(Dao et al, 2007)
mouse Axin1 Rev	CGG ATC TCC TTT GGC ATT CGG TAA	quantitative	60°	(Dao et al, 2007)
IL2 Fwd	CTA GGC CAC AGA ATT GAA AGA TCT	quantitative	60°	Jackson Labs protocol
IL2 Rev	GTA GGT GGA AAT TCT AGC ATC ATC C	quantitative	60°	Jackson Labs protocol

Tissue preservation

To analyze tissues and tumors from experimental animals, mice were sacrificed and tissues were dissected. Tissues and tumors were preserved by fixing in 10% formalin overnight followed by incubation in 70% ethanol until paraffin embedding. Tissues and tumors were also preserved by snap freezing in liquid nitrogen and storing at -150°C. Single cell suspensions from tumors were prepared by crushing tumors in PBS and passing the tissue slurry through a 70 micron filter. Single cells were preserved by resuspending in 10% DMSO and 90% FBS, followed by controlled-rate freezing and storage at -150°C.

Histology

Formalin-fixed tissue was embedded in paraffin blocks, sectioned, and stained with hematoxylin and eosin by Carolyn Gendron in the OHSU Histopathology Shared Resource.

Immunofluorescence

Paraffin sections were de-paraffined by soaking in xylene and rehydrated through an ethanol series (100%, 95%, 70%, 50%). Sections were then washed with PBS and blocked in 5% BSA/PBS for 1 hour at room temperature. Sections were incubated overnight with primary antibody in 3% BSA/PBS. Antibody complexes were detected with AlexaFluor 488 goat anti-rabbit IgG secondary antibodies, and DNA was stained with 4',6-diamidino-2-phenylindole (DAPI).

Fluorescence in situ hybridization

Proliferating HL-60, K562, REH, and SupB15 cells or primary patient samples

stimulated with phytohemagglutinin were used for FISH. At the time of harvest,

colcemid was added at a final concentration of 150 ng/ml. After 4–6 h, cells were

trypsinized, placed in hypotonic media consisting of 5% FBS and 75mM KCl, and

fixed to slides. The slides were baked for 6 min at 90°C in PBS, washed with 2x

SSC at 37°C for 30 min, dehydrated through graded alcohols and then air-dried.

Probes for *MYC* (fluorescein isothiocyanate) and the centromeric region of

chromosome 8 (CEP8) (Aqua) (Abbott Laboratories) were mixed, denatured at

75°C for 10 min and pre-annealed at 37°C for 30 min. The probes were then

added onto the slides, and hybridization was carried out using HYBrite (Vysis;

72°C denaturation temperature, 2 min denaturation time and reannealing at 37°C

overnight). The next day, the slides were washed with 0.4x SSC/0.1% NP-40 at

73°C for 2 min, with 2x SSC/0.1% NP-40 at room temperature for 1 min, and

then counterstained with 125 mg/ml 4',6-diamidino-2-phenylindole II (Vysis).

Cells were observed using a Nikon E800 fluorescence microscope, and captured

using CytoVision software from Applied Imaging.

Gene mutation testing by Sequenom MassARRAY

DNA was extracted and purified from peripheral blood apheresis samples from

patients with myeloid leukemia. Multiplex mutation screening was performed

using Sequenom MassARRAY system. Assay Designer software was used to

design multiplexes targeting point mutations in genes known to be associated with leukemia. Assays were carried out using Sequenom according to manufacturer's instructions. Initial PCR reactions used 10ng DNA per multiplex in a total volume of 5μL, with 100nmol/L primers, 2mmol/L MgCl2, 500μmol/L dNTPs and 0.1 units Taq polymerase. Amplification included one cycle of 94°C for 4 min, followed by 45 cycles of 94°C for 20 sec, 56°C for 30 sec, and 72°C for 1 min, and one final cycle of 72°C for 3 min. Unincorporated nucleotides were inactivated by addition of 0.3 units shrimp alkaline phosphatase (SAP) and incubation at 37°C for 40 min, followed by heat inactivation of SAP at 85°C for 5 min. Single base primer extension reactions were carried out with 0.625-1.25 μmol/L extension primer, and 1.35 units TypePLEX thermosequenase DNA polymerase. Extension cycling included one cycle of 94°C for 30 sec, 40 cycles of 94°C for 5 sec, with 5 cycles of 52°C for 5 sec and 80°C for 5 sec, followed by one cycle of 72°C for 3 min. Extension products were purified with an ion exchange resin, and approximately 10nL of product was spotted onto SpectroChip II matrices. A Bruker matrix-assisted laser desorption/ionization time of flight (MALDI-TOF) mass spectrometer (MassARRAY Compact, Sequenom) was used to resolve extension products. MassARRAY Typer Analyzer software (Sequenom) was used for automated data analysis, accompanied by visual inspection of extension products. Mutations detected by mass spectrometry were confirmed by conventional bi-directional sequencing.

Genes tested for mutations known to be associated with leukemia were as follows, listed by functional category. Receptor tyrosine kinases: FLT3, c-KIT, FMS, PDGFRB, FGFR4, NTRK1, MET; cytoplasmic tyrosine kinases: JAK1, JAK2, JAK3, FES, ABL1; signaling molecules: CBL, CBLB, NRAS, KRAS, HRAS, SOS1; serine/threonine kinases: AKT1, AKT2, AKT3, BRAF; cytokine receptors: MPL; receptors: NOTCH; phosphatases: PTPN1; metabolic pathways: IDH1, IDH2; Ubiquitin ligase: FBXW7; transcription factors: PAX5, NPM1, GATA1.

AXIN1 sequencing from genomic DNA

Genomic DNA was isolated from leukemia patient samples using the Qiagen Blood and Tissue Kit according to manufacturer's instructions. All 11 exons of *AXIN1* were amplified by PCR using 1μl of genomic DNA, 12.5μl of 2X Immomix Red (Bioline), 0.5μl forward primer, and 0.5μl reverse primer in a total volume of 25μl. PCR reactions were heated to 95°C for 10 minutes to activate the DNA polymerase followed by 35 cycles of amplification (95°C for 30 sec, 55-65°C for 30 sec (depending on primer pair; see Table 6.2), 72°C for 30 sec) and a 10 minute extension at 72°C. Products were analyzed by agarose gel electrophoresis to verify the amplification of a single band. Products were cleaned up using ExoSAP-IT exonuclease (Affymetrix) according to manufacturer's instructions and directly sequenced using traditional Sanger sequencing by Clive Woffendin in the OCTRI core laboratory. Sequence data was analyzed with Mutation Surveyor software (Softgenetics).

Table 6.2. Annealing temperatures for primers used to sequence *AXIN1*.

primer pair	*annealing temp*
AX02	55°
AX03	55°
AX04	55°
AX05	55°
AX06	55°
AX07	60°
AX08	55°
AX09	65°
AX10	60°
AX11	55°
AX12	55°
AX13	60°
AX14	55°
AX15	65°
AX16	55°
AX17	55°

Primers are from (Webster et al, 2000).

RNA isolation

Samples from leukemia cell lines were homogenized in Trizol reagent (Invitrogen), snap frozen in liquid nitrogen, and frozen at -80°C until needed. RNA was isolated from cell lines according to manufacturer's instructions. Alternatively, samples from mouse tissue, mouse tumors, mouse tumor cell suspensions, and primary human AML, ALL, normal bone marrow, and peripheral blood-derived cell populations were subjected to a modified version of the Trizol RNA extraction protocol as follows. Samples were thawed and rotated at room temperature for 75 minutes and then centrifuged at 12,000 x g for 10 minutes to remove insoluble material. Supernatant was combined with chloroform, vigorously mixed, allowed to stand for 10 minutes, and then centrifuged at 12,000 x g for 10 minutes. Aqueous phases were combined with isopropanol and precipitated overnight at -20°C. Precipitated RNA was centrifuged at 12,000 x g for 30 minutes, washed with 75% ethanol, and air-dried for 10 minutes. RNA was resuspended in nuclease-free water and placed at 65°C for 10 minutes to solubilize RNA. To remove genomic DNA, RNA was DNase-treated by incubation in Incubation Buffer (40mM Tris-HCl, 10mM NaCl, 6mM $MgCl_2$, 1mM $CaCl_2$, pH 7.9), 10 units RNase inhibitor, and 10 units DNase I (Roche) at 37°C for 20 minutes. DNase was heat inactivated by incubating DNase-treated RNA at 75°C for 10 minutes. RNA cleanup was performed on all samples, regardless of Trizol protocol, using RNeasy Mini Kit (Qiagen). For primary AML, ALL, NBM, and peripheral blood-derived samples, RNA cleanup protocol contained a modification to retain miRNAs and other small RNAs, where

buffer RLT was diluted with 3.5 volumes of 100% ethanol instead of 1 volume of 100% ethanol as in the standard clean-up protocol. Purified RNA was stored at -80°C.

cDNA generation

cDNA was made from DNase-treated RNA (generally 1ug total RNA but not less than 500ng) using the High Capacity cDNA Reverse Transcription kit (Applied Biosystems) and random primers according to manufacturer's instructions. For RT-PCR from mouse tissues and for cloning *AXIN1* from HL-60, Reh, and SupB15 cell lines, cDNA was made using MMLV reverse transcriptase (Invitrogen) and oligo dT according to manufacturer's instructions.

Cloning AXIN1

To clone *AXIN1* from the HL-60, Reh, and SupB15 cell lines, *AXIN1* was amplified from cDNA from each cell line by PCR using Pfu Ultra (Stratagene) and *AXIN1* forward primer 5'- C ACC ATG AAT ATC CAA GAG CAG GGT TTC C-3' and reverse primer 5'-TCA GTC CAC CTT CTC CAC TTT GC-3'. PCR products were cloned into pENTR/D-TOPO (Invitrogen) according to manufacturer's instructions. TOPO reactions were used to transform chemically competent α-Select Gold Efficiency cells (Bioline), and colonies were miniprepped using Wizard miniprep kit (Promega) and sequenced.

RT-PCR

To detect expression of *Axin1* and *MYC* in tissues from young transgenic mice, RT-PCR was performed using primers specific for human *MYC* (hMyc898/1007), the *GFP* portion of the *TRE2-Axin-GFP* transgene (TRE2-Axin-GFP Fwd and Rev; see Table 6.1), and mouse *Gapdh* (Fwd 5'- ACG GCC GCA TCT TCT TGT GC -3' and Rev 5'- GTG CAG GAT GCA TTG CTG AC -3'). PCR reactions contained 1μl cDNA (2.5ng), 0.5μl forward primer, 0.5μl reverse primer, and 2X Immomix Red (Bioline) in 25μl. PCR reactions were heated to 95°C for 5 minutes to activate the DNA polymerase followed by 35 cycles of amplification (95°C for 30 sec, 53°C for 30 sec, 72°C for 30 sec) and a final extension of 72°C for 5 minutes. Products were analyzed by agarose gel electrophoresis.

Quantitative real time PCR

qRT-PCR was carried out in triplicate reactions using 5ng cDNA, Taqman primers for the gene of interest, and PerfeCta qPCR FastMix (Quanta Biosciences) on a StepOne Real-Time PCR System machine (Applied Biosystems). Taqman primer/probe sets were pre-designed by Applied Biosystems for the following genes: *MYC* (Hs00905030_m1), *AXIN1* (total; Hs00394718_m1), *AXIN1V1* (Hs00394723_m1), *AXIN1V2* (Hs01558063_m1), *PPP2R5A* (PP2A-B56α; Hs00196542_m1), *CIP2A* (Hs00405413_m1), *SET* (Hs00853870_g1), *18S* (Hs99999901_s1), *ACTIN* (Hs99999903_m1), *GAPDH* (Hs02786624_g1). For gene expression analysis in leukemia patient samples,

normal bone marrow, and terminally differentiated hematopoietic cells, gene of interest expression was analyzed using the $2^{\Delta\Delta Ct}$ method and *18S* as the reference gene. In early experiments, I tested *ACTIN* and *GAPDH* and found them to be highly variable between samples and therefore poor reference genes for analyzing gene expression in leukemia samples.

For detection of ectopic *Axin1* expression in mouse lymphomas, qRT-PCR was carried out in triplicate reactions using 5ng cDNA and primers for the gene of interest. To detect ectopic *Axin1*, primers that amplify the GFP sequence were used: 5'- GGA GCG CAC GAT CTT CTT CA -3' and 5'- AGG GTG TCG CCC TCG AA -3' (from (Geraerts et al, 2006)). Primers that amplify mouse *Actin* were also used: 5'- AGG TGA CAG CAT TGC TTC TG -3' and 5'- GCT GCC TCA ACA CCT CAA C -3'. PCR reactions contained 1μl DNA, 0.5μl forward primer, 0.5μl reverse primer, and 10μl 2X PerfeCTa SYBR Green FastMix (Quanta Biosciences) in a total volume of 20μl. PCR reactions were heated to 95°C for 20 seconds to activate the DNA polymerase followed by 40 cycles of amplification (95°C for 3 sec, 60°C for 30 sec) on a StepOne Real-Time PCR System machine (Applied Biosystems). Ectopic *Axin1* expression was analyzed using the $2^{\Delta\Delta Ct}$ method and *Actin* as the reference gene.

PCR

To detect the *TRE2-Axin1-GFP* transgene in the DNA of mouse lymphomas,
PCR was used. Genomic DNA was isolated using Qiagen Blood and Tissue DNA
kit according to manufacturer's instructions, and the transgene was amplified
using primers directed against the GFP portion of the transgene (TRE2-Axin1-
GFP Fwd and Rev; see Table 6.1). PCR reactions contained 1μl DNA, 0.5μl
forward primer, 0.5μl reverse primer, and 10μl 2X ImmoMix Red (Bioline) in a
total volume of 20μl. PCR reactions were heated to 95°C for 10 minutes to
activate the DNA polymerase followed by 35 cycles of amplification (95°C for 30
sec, 55°C for 30 sec, 72°C for 30 sec) and a 10 minute extension at 72°C.
Products were analyzed by agarose gel electrophoresis.

Transfections and luciferase assay

See (Arnold et al, 2009) for full details.

Co-immunoprecipitation

For Figure 2.4B, equal cell numbers were lysed in 10x cell volumes of Co-
immunoprecipitation (Co-IP) buffer (20mM Tris, pH 7.5, 12.5% glycerol, 0.2%
NP-40, 200mM NaCl, 1mM EDTA, 1mM ethylene glycol tetraacetate (EGTA),
1mM dithiothreitol (DTT), 10mM sodium fluoride, 100mM sodium vanadate,
1μg/ml aprotinin, 1μg/ml pepstatin, 0.5μg/ml leupeptin, 0.2 mg/ml AEBSF and 1.6
mg/ml iodoacetamide) and pre-cleared with protein A+G agarose (Calbiochem).

Samples were then incubated with either 1:50 dilution of anti-c-Myc (C33)-conjugated beads (Santa Cruz Biotechnology) or control protein A+G agarose. Precipitated proteins were washed three times in 10x cell volumes of Co-IP buffer and released by boiling in SDS sample buffer.

For Figure 4.1B, 293 cells transfected with the indicated constructs were lysed in 10x cell pellet volumes of Co-IP buffer. Lysates were incubated on ice for 20 min, sonicated 10 pulses (output=1 and 10% duty), and cleared by centrifugation at 20K rcf for 10 min at 4°C. Cleared lysate volumes were adjusted for transfection efficiency by b-gal assay. Immunoprecipitations were carried out with a 1:750 dilution of V5 antibody (Invitrogen) conjugated to either protein A or G beads. Precipitated proteins were washed three times in 10x cell volumes of co-IP buffer, with a 1-min incubation during each wash, and released by boiling in SDS sample buffer.

Immunoblotting

Protein lysates were prepared for immunoblotting in two different ways. For Figure 2.1A, 2.3, 2.4A, 3.1C&D, 4.6B, 4.7B, 4.9A&B, and 4.10A, cells were lysed in cold Ab lysis buffer (20mM Tris, pH 7.5, 50mM NaCl, 0.5% NP-40, 0.5% deoxycholate, 0.5% SDS, 1μM EDTA) supplemented with protease inhibitors (0.2mg/ml AEBSF, 1μg/ml aprotinin, 0.5μg/ml leupeptin, 1.6mg/ml iodoacetamide, 1μg/ml pepstatin) and phosphatase inhibitors (10mM sodium fluoride, 100mM sodium vanadate, 10mM β-glycerolphosphate disodium

pentahydrate), sonicated, and clarified by centrifugation. Protein concentration of supernatants was determined by BioRad Protein Assay (BioRad) or BCA kit (Sigma and Pierce). Prior to loading, 5X SDS Sample Buffer (0.3M Tris pH 6.8, 48% glycerol, 24% β-ME, 9.6% SDS) was added to samples to achieve a final concentration of 1.5X. Alternatively, for all other immunoblotting figures, cells were lysed in hot 1.5X SDS Sample Buffer. Samples were boiled for 10 minutes and separated by SDS-PAGE followed by transfer to Immobilon-FL (Millipore). Membrane was blocked in Aquablock (East Coast Biosciences) and incubated in primary antibodies at the indicated dilutions. Antibodies were diluted into a solution of 1:1 Aquablock to PBS plus 0.1% Tween-20, unless indicated otherwise. Primary antibodies were detected using secondary antibodies (goat anti-mouse, goat anti-rabbit) conjugated to near-infrared fluorescent dyes Alexa Fluor 680 (Molecular Probes) or IRDye800 (Rockland) diluted 1:10,000 in 1:1 Aquablock to PBS plus 0.1% Tween-20. Immunoblots were scanned using a LI-COR Odyssey Infrared Imager to visualize proteins, which allows for simultaneous dual wavelength detection when using secondary antibodies directed against two different species. Antibody signals were quantified using LI-COR Odyssey Infrared Imager software version 1.2, which allows for linear signal quantitation over four orders of magnitude.

Metabolic labeling and determination of c-Myc half-life

Exponentially growing leukemia cells were starved in methionine/cysteine-free DMEM (Invitrogen) supplemented with 10% dialyzed FBS for 20 minutes then

labeled with ^{35}S-methionine/cysteine (Perkin-Elmer) in methionine/cysteine-free

DMEM supplemented with 10% dialyzed FBS. Leukemia cell lines and JY cells

were labeled for 20-30 minutes; primary leukemia bone marrow cells, ficolled

normal bone marrow cells, and PBMCs were labeled for 2-4 hours due to their

slow metabolic rate. Cells were washed once with 'chase' medium (RPMI with

10% FBS, 5mM L-methionine, and 3mM L-cysteine) and then incubated in chase

media for the indicated times. To harvest cells at each time point, equal cell

numbers were washed in ice-cold PBS and snap frozen. Cell pellets were lysed

in 1ml Ab lysis buffer, sonicated, pre-cleared for 30 min with protein A+G beads

(Calbiochem) and incubated overnight with C33-conjugated protein A+G beads

(Santa Cruz Biotechnology) to immunoprecipitate c-Myc. The following day,

additional protein A+G beads were added to each IP, and beads were washed 4

times with cold Ab lysis buffer before adding 1.5x SB and boiling for 10 minutes.

Immunoprecipitated proteins were separated by SDS-PAGE, and gels were fixed

in 45:45:10 methanol/glacial acetic acid/water for 30 minutes, followed by a 30

minute incubation in Amplify Fluorographic Reagent (Amersham) for signal

intensification. Gels were dried overnight on a heated gel dryer under vacuum

and the following day were exposed to film at -80°C to visualize bands or

exposed to a phosphorimager screen for quantitation. For quantitation, the

phosphorimager screen was read on a STORM phosphorimager, and

background-subtracted band intensities were used to plot the rate of decay of c-

Myc by setting the zero timepoint to 100%. c-Myc half-life was calculated from

the equation of the line of best fit through all timepoints (Microsoft Excel).

Chromatin immunoprecipitation

AML cells were crosslinked with formaldehyde to a final concentration of 0.5% in media and incubated at room temperature for 6 minutes, followed by centrifugation at 1000rpm for 8 minutes for a total crosslinking time of 14 minutes. Cells were washed 3 times in ice-cold 1X PBS-1mM EDTA and centrifuged for 8 minutes at 1000prm. Cells were resuspended in 1.5 ml of Impey ChIP lysis buffer (0.1% SDS, 0.5% Triton X-100, 20mM Tris-HCl (pH 8.1), 150mM NaCl and protease inhibitors). Cell lysates were sonicated 4X (output = 3.5, 30% duty, 15 pulses; 15 min incubation on ice between rounds of sonication) and then cleared by centrifugation at 14K rpm for 10 min at 4ºC. Cell lysates were pre-cleared with 50 μl 50% slurry of protein A beads (IPA 300) for 1 hr with rotation at 4ºC. Lysates were cleared by centrifugation at 4000 rpm for 1.5 min. Immunoprecipitations were performed with 2 μg of each antibody overnight at 4ºC. 2 μg of normal rabbit IgG (Santa Cruz Biotechnology) was used as a negative control. Immunoprecipitates were bound by adding 60μl protein A beads and incubating for 1 hr at 4ºC. Immunoprecipitates were washed six times with ChIP lysis buffer and twice with 1X TE, pH 8. Samples were rotated 15 min at 4ºC for the first 6 washes, 30 min at 4ºC for the 7th wash, and 5 min at 4ºC for the 8th wash. Immunoprecipitates were eluted from the beads with elution buffer (0.1 M NaHCO$_3$ and 1% SDS) by rotating for 15 min at room temperature. Elution products were transferred to new tubes and 4M NaCl was added to a final concentration of 0.2 M and samples were incubated at 65ºC overnight. DNA was

188

purified with the QIAquick PCR purification Kit (Qiagen) and used for quantitative

PCR analysis (as described above) with specified primers. For quantitative ChIP

experiments, primers to the promoter regions of c-Myc target genes, as well as

internal GAPDH primers were used to amplify DNA. The internal GAPDH

primers were used as a negative control. Quantitative PCR was used to measure

signals in 1% of the input material, as well as in each immunoprecipitation (IP).

The percentage of input was then calculated for each IP (control IgG and

specific) as the IP signal above the input signal using the formula: $100 \times 2^{(input\ Ct\ -\ IP\ Ct)}$. Relative level of bound DNA was then graphed as the percent input of the

specific IP relative to the percent input of the mock IgG control using GraphPad

Prism.

WST assay

WST assay was used to determine proliferation and viability of T ALL cell lines

and primary T cells treated with OP449. T ALL cell lines were seeded in 96 well

plates at 12,500 cells/well (or 70,000 cells/well for unstimulated primary T cells)

in complete media (RPMI + 10% defined FBS, 2mM L-glutamine, and pen/strep)

with increasing doses of OP449 (from 10nM to 5μM). PBS treatment served as a

negative control and cycloheximide treatment (400μg/ml) served as a positive

control. For each dose, cells were seeded in quadruplicate. Cells were incubated

at 37ºC for 68 hours, followed by the addition of 10μl WST-1/ECS solution

(Millipore) per well and 4 hours additional incubation at 37ºC (total time of

exposure to OP449 = 72 hours). Plates were read on a plate reader at 440nM

absorbance. WST assay was repeated 4-6 times for each T ALL cell line (3 times for unstimulated primary T cells). Unstimulated primary T cells were not able to metabolize the WST-1 reagent to a level above background (at least at the cell number we used), and so after reading the WST assay on the plate reader, unstimulated primary T cell viability was determined by staining cells with trypan blue and counting live versus dead cells in duplicate from 3 separate 96 well plates.

Appendix 1. List of publications

Arnold HK, Zhang X, Daniel CJ, **Tibbitts D**, Escamilla-Powers J, Farrell A, Tokarz S, Morgan C, Sears RC. 2009. The Axin1 scaffold protein promotes formation of a degradation complex for c-Myc. *EMBO Journal* 28(5):500-12.

O'neil J, Grim J, Strack P, Rao S, **Tibbitts D**, Winter C, Hardwick J, Welcker M, Meijerink JP, Pieters R, Draetta G, Sears R, Clurman BE, Look AT. 2007. FBW7 mutations in leukemic cells mediate NOTCH pathway activation and resistance to (Tesio et al)-secretase inhibitors. *Journal of Experimental Medicine* 204(8):1813-24.

Malempati S, **Tibbitts D**, Cunningham M, Akkari Y, Olson S, Fan G, Sears RC. 2006. Aberrant stabilization of c-Myc protein in some lymphoblastic leukemias. *Leukemia* 20(9):1572-81.

Appendix 2. Figure contributions

Chapter 2

Figure 2.1. Immunoblot (Figure 2.1A, left) and sequencing (Figure 2.1C) were performed by Suman Malempati. FISH (Figure 2.1B) was performed by Yassmine Akkari.

Figure 2.2. Pulse-chase experiments on SupB15, Reh, HL-60, PBMC samples were performed by Suman Malempati.

Figure 2.3. Immunoblotting and quantitation was performed by Suman Malempati.

Figure 2.4. Cell treatments and immunoblotting (Figure 2.4A) were performed by Suman Malempati. Co-immunoprecipitation and immunoblotting (Figure 2.4B) was performed by Melissa Cunningham.

Figure 2.5. Pulse-chase experiments were performed by Suman Malempati.

Figure 2.7. Pulse-chase experiments on pediatric T ALL samples (Figure 2.7C) were performed by Suman Malempati.

Table 2.1. FISH was performed by Yassmine Akkari.

Chapter 3

Figure 3.2. Bone marrow fractionation, CD34+ cell isolation, and *in vitro* myeloid differentiation were performed by Keaney Rathbun.

Figure 3.4. Cell treatments and immunoblotting were performed by Karyn Taylor.

Figure 3.5. Cell treatments and chromatin immunoprecipitation were performed by Colin Daniel.

Table 3.1. Mutation detection by Sequenom MassARRAY was performed by Chris Corless.

Chapter 4

Figure 4.1. CoIP (Figure 4.1B) and luciferase (Figure 4.1C) experiments were performed by Hugh Arnold.

Figure 4.7. Immunofluorescence (Figure 4.7C) was performed by Xiaoyan Wang.

Figure 4.9. Immunofluorescence (Figure 4.9C) was performed by Xiaoyan Wang.

Figure 4.10. Immunofluorescence (Figure 4.9D, E) was performed by Xiaoyan Wang.

Table 4.1. AXIN1 sequencing was performed by Arun Kumar Krishnamoorthy.

References

Adams JM, Harris AW, Pinkert CA, Corcoran LM, Alexander WS, Cory S, Palmiter RD, Brinster RL (1985) The c-myc oncogene driven by immunoglobulin enhancers induces lymphoid malignancy in transgenic mice. *Nature* **318**(6046)**:** 533-538

Adams MR, Sears R, Nuckolls F, Leone G, Nevins JR (2000) Complex transcriptional regulatory mechanisms control expression of the E2F3 locus. *Molecular and Cellular Biology* **20**(10)**:** 3633-3639

Adhikary S, Eilers M (2005) Transcriptional regulation and transformation by Myc proteins. *Nature Reviews Molecular Cell Biology* **6**(8)**:** 635-645

Adhikary S, Marinoni F, Hock A, Hulleman E, Popov N, Beier R, Bernard S, Quarto M, Capra M, Goettig S, Kogel U, Scheffner M, Helin K, Eilers M (2005) The ubiquitin ligase HectH9 regulates transcriptional activation by Myc and is essential for tumor cell proliferation. *Cell* **123**(3)**:** 409-421

Aktas O, Kury P, Kieseier B, Hartung H-P (2010) Fingolimod is a potential novel therapy for multiple sclerosis. *Nature Reviews Neurology* **6**(7)**:** 373-382

Amanullah A, Liebermann DA, Hoffman B (2000) p53-independent apoptosis associated with c-Myc-mediated block in myeloid cell differentiation. *Oncogene* **19**(26)**:** 2967-2977

Andjelkovic M, Jakubowicz T, Cron P, Ming XF, Han JW, Hemmings BA (1996) Activation and phosphorylation of a pleckstrin homology domain containing protein kinase (RAC-PK/PKB) promoted by serum and protein phosphatase inhibitors. *Proceedings of the National Academy of Sciences of the United States of America* **93**(12)**:** 5699-5704

Arnold HK, Sears RC (2006) Protein phosphatase 2A regulatory subunit B56alpha associates with c-Myc and negatively regulates c-Myc accumulation. *Molecular and Cellular Biology* **26**(7)**:** 2832-2844

Arnold HK, Zhang X, Daniel CJ, Tibbitts D, Escamilla-Powers J, Farrell A, Tokarz S, Morgan C, Sears RC (2009) The Axin1 scaffold protein promotes formation of a degradation complex for c-Myc. *The EMBO Journal* **28**(5)**:** 500-512

Askew DS, Ashmun RA, Simmons BC, Cleveland JL (1991) Constitutive c-myc expression in an IL-3-dependent myeloid cell line suppresses cell cycle arrest and accelerates apoptosis. *Oncogene* **6**(10)**:** 1915-1922

Ayer DE, Eisenman RN (1993) A switch from Myc:Max to Mad:Max heterocomplexes accompanies monocyte/macrophage differentiation. *Genes & Development* **7**(11)**:** 2110-2119

Ayer DE, Kretzner L, Eisenman RN (1993) Mad: a heterodimeric partner for Max that antagonizes Myc transcriptional activity. *Cell* **72**(2)**:** 211-222

Ayer DE, Lawrence QA, Eisenman RN (1995) Mad-Max transcriptional repression is mediated by ternary complex formation with mammalian homologs of yeast repressor Sin3. *Cell* **80**(5)**:** 767-776

Bahram F, von der Lehr N, Cetinkaya C, Larsson LG (2000) c-Myc hot spot mutations in lymphomas result in inefficient ubiquitination and decreased proteasome-mediated turnover. *Blood* **95**(6)**:** 2104-2110

Barnes T, Kim W-C, Mantha A, Kim S-E, Izumi T, Mitra S, Lee C (2009) Identification of Apurinic/apyrimidinic endonuclease 1 (APE1) as the endoribonuclease that cleaves c-myc mRNA. *Nucleic Acids Research* **37**(12)**:** 3946-3958

Baudino T, McKay C, Pendeville-Samain H, Nilsson J, Maclean K, White E, Davis A, Ihle J, Cleveland J (2002) c-Myc is essential for vasculogenesis and angiogenesis during development and tumor progression. *Genes & Development* **16**(19)**:** 2530-2543

Benassayag C, Montero L, Colombie N, Gallant P, Cribbs D, Morello D (2005) Human c-Myc isoforms differentially regulate cell growth and apoptosis in Drosophila melanogaster. *Molecular and Cellular Biology* **25**(22)**:** 9897-9909

Benassi B, Fanciulli M, Fiorentino F, Porrello A, Chiorino G, Loda M, Zupi G, Biroccio A (2006) c-Myc Phosphorylation Is Required for Cellular Response to Oxidative Stress. *Molecular Cell* **21**(4)**:** 509-519

Berns K, Hijmans EM, Koh E, Daley GQ, Bernards R (2000) A genetic screen to identify genes that rescue the slow growth phenotype of c-myc null fibroblasts. *Oncogene* **19**(29)**:** 3330-3334

Bernstein PL, Herrick DJ, Prokipcak RD, Ross J (1992) Control of c-myc mRNA half-life in vitro by a protein capable of binding to a coding region stability determinant. *Genes & Development* **6**(4)**:** 642-654

Bhatia K, Huppi K, Spangler G, Siwarski D, Iyer R, Magrath I (1993) Point mutations in the c-Myc transactivation domain are common in Burkitt's lymphoma and mouse plasmacytomas. *Nature Genetics* **5**(1)**:** 56-61

Blackwell TK, Kretzner L, Blackwood EM, Eisenman RN, Weintraub H (1990) Sequence-specific DNA binding by the c-Myc protein. *Science* **250**(4984)**:** 1149-1151

Blackwood EM, Eisenman RN (1991) Max: a helix-loop-helix zipper protein that forms a sequence-specific DNA-binding complex with Myc. *Science* **251**(4998)**:** 1211-1217

Bonetti P, Davoli T, Sironi C, Amati B, Pelicci PG, Colombo E (2008) Nucleophosmin and its AML-associated mutant regulate c-Myc turnover through Fbw7 gamma. *The Journal of Cell Biology* **182**(1)**:** 19-26

Bouchard C, Dittrich O, Kiermaier A, Dohmann K, Menkel A, Eilers M, L√ºscher B (2001) Regulation of cyclin D2 gene expression by the Myc/Max/Mad network: Myc-dependent TRRAP recruitment and histone acetylation at the cyclin D2 promoter. *Genes & Development* **15**(16)**:** 2042-2047

Boxer LM, Dang CV (2001) Translocations involving c-myc and c-myc function. *Oncogene* **20**(40)**:** 5595-5610

Brewer G, Ross J (1988) Poly(A) shortening and degradation of the 3' A+U-rich sequences of human c-myc mRNA in a cell-free system. *Molecular and Cellular Biology* **8**(4)**:** 1697-1708

Bruyere H, Sutherland H, Chipperfield K, Hudoba M (2010) Concomitant and successive amplifications of MYC in APL-like leukemia. *Cancer Genetics and Cytogenetics* **197**(1)**:** 75-80

Buschbeck M, Uribesalgo I, Ledl A, Gutierrez A, Minucci S, Muller S, Di Croce L (2007) PML4 induces differentiation by Myc destabilization. *Oncogene* **26**(23)**:** 3415-3422

Chen B, Dodge ME, Tang W, Lu J, Ma Z, Fan CW, Wei S, Hao W, Kilgore J, Williams NS, Roth MG, Amatruda JF, Chen C, Lum L (2009) Small molecule-mediated disruption of Wnt-dependent signaling in tissue regeneration and cancer. *Nature Chemical Biology* **5**(2)**:** 100-107

Choi SH, Wright JB, Gerber SA, Cole MD (2010) Myc protein is stabilized by suppression of a novel E3 ligase complex in cancer cells. *Genes & Development* **24**(12)**:** 1236-1241

Christensen DJ, Ohkubo N, Oddo J, Van Kanegan MJ, Neil J, Li F, Colton CA, Vitek MP (2011) Apolipoprotein E and peptide mimetics modulate inflammation by binding the SET protein and activating protein phosphatase 2A. *Journal of Immunology* **186**(4)**:** 2535-2542

References

Ciraolo E, Morello F, Hirsch E (2011) Present and Future of PI3K Pathway Inhibition in Cancer: Perspectives and Limitations. *Current Medicinal Chemistry* **18**(18): 2674-2685

Clark HM, Yano T, Otsuki T, Jaffe ES, Shibata D, Raffeld M (1994) Mutations in the coding region of c-MYC in AIDS-associated and other aggressive lymphomas. *Cancer Research* **54**(13): 3383-3386

Coppola JA, Cole MD (1986) Constitutive c-myc oncogene expression blocks mouse erythroleukaemia cell differentiation but not commitment. *Nature* **320**(6064): 760-763

Cristobal I, Garcia-Orti L, Cirauqui C, Alonso MM, Calasanz MJ, Odero MD (2011) PP2A impaired activity is a common event in acute myeloid leukemia and its activation by forskolin has a potent anti-leukemic effect. *Leukemia* **25**(4): 606-614

Cross DA, Alessi DR, Cohen P, Andjelkovich M, Hemmings BA (1995) Inhibition of glycogen synthase kinase-3 by insulin mediated by protein kinase B. *Nature* **378**(6559): 785-789

Dalla-Favera R, Wong-Staal F, Gallo RC (1982) Onc gene amplification in promyelocytic leukaemia cell line HL-60 and primary leukaemic cells of the same patient. *Nature* **299**(5878): 61-63

Dani C, Blanchard JM, Piechaczyk M, El Sabouty S, Marty L, Jeanteur P (1984) Extreme instability of myc mRNA in normal and transformed human cells. *Proceedings of the National Academy of Sciences of the United States of America* **81**(22): 7046-7050

Dao DY, Yang X, Chen DI, Zuscik M, O'Keefe RJ (2007) Axin1 and Axin2 Are Regulated by TGF- and Mediate Cross-talk between TGF- and Wnt Signaling Pathways. *Annals of the New York Academy of Sciences* **1116**: 82-99

David C, Manley J (2010) Alternative pre-mRNA splicing regulation in cancer: pathways and programs unhinged. *Genes & Development* **24**(21): 2343-2364

Davis AC, Wims M, Spotts GD, Hann SR, Bradley A (1993) A null c-myc mutation causes lethality before 10.5 days of gestation in homozygotes and reduced fertility in heterozygous female mice. *Genes & Development* **7**(4): 671-682

Delgado D, Leon J (2010) Myc Roles in Hematopoiesis and Leukemia. *Genes & Cancer* **1**(6): 605-616

Derksen PW, de Gorter DJ, Meijer HP, Bende RJ, van Dijk M, Lokhorst HM, Bloem AC, Spaargaren M, Pals ST (2003) The hepatocyte growth factor/Met pathway controls proliferation and apoptosis in multiple myeloma. *Leukemia* **17**(4): 764-774

Ding VW, Chen RH, McCormick F (2000) Differential regulation of glycogen synthase kinase 3beta by insulin and Wnt signaling. *Journal of Biological Chemistry* **275**(42): 32475-32481

Dominguez-Sola D, Ying C, Grandori C, Ruggiero L, Chen B, Li M, Galloway D, Gu W, Gautier J, Dalla-Favera R (2007) Non-transcriptional control of DNA replication by c-Myc. *Nature* **448**(7152): 445-451

Downs KM, Martin GR, Bishop JM (1989) Contrasting patterns of myc and N-myc expression during gastrulation of the mouse embryo. *Genes & Development* **3**(6): 860-869

Doyle GA, Betz NA, Leeds PF, Fleisig AJ, Prokipcak RD, Ross J (1998) The c-myc coding region determinant-binding protein: a member of a family of KH domain RNA-binding proteins. *Nucleic Acids Research* **26**(22): 5036-5044

Dubois N, Adolphe C, Ehninger A, Wang R, Robertson E, Trumpp A (2008) Placental rescue reveals a sole requirement for c-Myc in embryonic erythroblast survival and hematopoietic stem cell function. *Development* **135**(14): 2455-2465

Eilers M, Schirm S, Bishop JM (1991) The MYC protein activates transcription of the alpha-prothymosin gene. *The EMBO Journal* **10**(1): 133-141

Eischen CM, Weber JD, Roussel MF, Sherr CJ, Cleveland JL (1999) Disruption of the ARF-Mdm2-p53 tumor suppressor pathway in Myc-induced lymphomagenesis. *Genes & Development* **13**(20): 2658-2669

Eischen CM, Woo D, Roussel MF, Cleveland JL (2001) Apoptosis triggered by Myc-induced suppression of Bcl-X(L) or Bcl-2 is bypassed during lymphomagenesis. *Molecular and Cellular Biology* **21**(15): 5063-5070

Erikson J, Finger L, Sun L, ar-Rushdi A, Nishikura K, Minowada J, Finan J, Emanuel BS, Nowell PC, Croce CM (1986) Deregulation of c-myc by translocation of the alpha-locus of the T-cell receptor in T-cell leukemias. *Science* **232**(4752): 884-886

Evan GI, Wyllie AH, Gilbert CS, Littlewood TD, Land H, Brooks M, Waters CM, Penn LZ, Hancock DC (1992) Induction of apoptosis in fibroblasts by c-myc protein. *Cell* **69**(1): 119-128

Falini B, Martelli M, Bolli N, Sportoletti P, Liso A, Tiacci E, Haferlach T (2011) Acute myeloid leukemia with mutated nucleophosmin (NPM1): is it a distinct entity? *Blood* **117**(4)**:** 1109-1120

Falini B, Mecucci C, Tiacci E, Alcalay M, Rosati R, Pasqualucci L, La Starza R, Diverio D, Colombo E, Santucci A, Bigerna B, Pacini R, Pucciarini A, Liso A, Vignetti M, Fazi P, Meani N, Pettirossi V, Saglio G, Mandelli F, Lo-Coco F, Pelicci P-G, Martelli M (2005) Cytoplasmic nucleophosmin in acute myelogenous leukemia with a normal karyotype. *The New England Journal of Medicine* **352**(3)**:** 254-266

Fan Z, Beresford P, Oh D, Zhang D, Lieberman J (2003) Tumor suppressor NM23-H1 is a granzyme A-activated DNase during CTL-mediated apoptosis, and the nucleosome assembly protein SET is its inhibitor. *Cell* **112**(5)**:** 659-672

Felsher D (2010) MYC Inactivation Elicits Oncogene Addiction through Both Tumor Cell-Intrinsic and Host-Dependent Mechanisms. *Genes & Cancer* **1**(6)**:** 597-604

Felsher DW, Bishop JM (1999) Reversible tumorigenesis by MYC in hematopoietic lineages. *Molecular Cell* **4**(2)**:** 199-207

Fernandez P, Frank S, Wang L, Schroeder M, Liu S, Greene J, Cocito A, Amati B (2003) Genomic targets of the human c-Myc protein. *Genes & Development* **17**(9)**:** 1115-1129

Flinn EM, Busch CM, Wright AP (1998) myc boxes, which are conserved in myc family proteins, are signals for protein degradation via the proteasome. *Molecular and Cellular Biology* **18**(10)**:** 5961-5969

Frank S, Parisi T, Taubert S, Fernandez P, Fuchs M, Chan H-M, Livingston D, Amati B (2003) MYC recruits the TIP60 histone acetyltransferase complex to chromatin. *EMBO reports* **4**(6)**:** 575-580

Frank SR, Schroeder M, Fernandez P, Taubert S, Amati B (2001) Binding of c-Myc to chromatin mediates mitogen-induced acetylation of histone H4 and gene activation. *Genes & Development* **15**(16)**:** 2069-2082

Geraerts M, Willems S, Baekelandt V, Debyser Z, Gijsbers R (2006) Comparison of lentiviral vector titration methods. *BMC Biotechnol* **6:** 34

Gilliland DG, Griffin JD (2002) The roles of FLT3 in hematopoiesis and leukemia. *Blood* **100**(5)**:** 1532-1542

Ginisty H, Amalric F, Bouvet P (1998) Nucleolin functions in the first step of ribosomal RNA processing. *The EMBO Journal* **17**(5)**:** 1476-1486

Gomez-Roman N, Grandori C, Eisenman R, White R (2003) Direct activation of RNA polymerase III transcription by c-Myc. *Nature* **421**(6920)**:** 290-294

Gowda SD, Koler RD, Bagby GC (1986) Regulation of C-myc expression during growth and differentiation of normal and leukemic human myeloid progenitor cells. *The Journal of Clinical Investigation* **77**(1)**:** 271-278

Grandori C, Gomez-Roman N, Felton-Edkins Z, Ngouenet C, Galloway D, Eisenman R, White R (2005) c-Myc binds to human ribosomal DNA and stimulates transcription of rRNA genes by RNA polymerase I. *Nature Cell Biology* **7**(3)**:** 311-318

Gregory M, Qi Y, Hann S (2003) Phosphorylation by Glycogen Synthase Kinase-3 Controls c-Myc Proteolysis and Subnuclear Localization. *Journal of Biological Chemistry* **278**(51)**:** 51606-51612

Gregory MA, Hann SR (2000) c-Myc proteolysis by the ubiquitin-proteasome pathway: stabilization of c-Myc in Burkitt's lymphoma cells. *Molecular and Cellular Biology* **20**(7)**:** 2423-2435

Gstaiger M, Jordan R, Lim M, Catzavelos C, Mestan J, Slingerland J, Krek W (2001) Skp2 is oncogenic and overexpressed in human cancers. *Proceedings of the National Academy of Sciences of the United States of America* **98**(9)**:** 5043-5048

Guo X, Ramirez A, Waddell D, Li Z, Liu X, Wang X-F (2008) Axin and GSK3-control Smad3 protein stability and modulate TGF- signaling. *Genes & Development* **22**(1)**:** 106-120

Gusse M, Ghysdael J, Evan G, Soussi T, Mechali M (1989) Translocation of a store of maternal cytoplasmic c-myc protein into nuclei during early development. *Molecular and Cellular Biology* **9**(12)**:** 5395-5403

Hann SR (2006) Role of post-translational modifications in regulating c-Myc proteolysis, transcriptional activity and biological function. *Seminars in Cancer Biology* **16**(4)**:** 288-302

Hann SR, Eisenman RN (1984) Proteins encoded by the human c-myc oncogene: differential expression in neoplastic cells. *Molecular and Cellular Biology* **4**(11)**:** 2486-2497

Hann SR, Sloan-Brown K, Spotts GD (1992) Translational activation of the non-AUG-initiated c-myc 1 protein at high cell densities due to methionine deprivation. *Genes & Development* **6**(7)**:** 1229-1240

He C, Hu H, Braren R, Fong S-Y, Trumpp A, Carlson T, Wang R (2008) c-myc in the hematopoietic lineage is crucial for its angiogenic function in the mouse embryo. *Development* **135**(14)**:** 2467-2477

Hemann MT, Bric A, Teruya-Feldstein J, Herbst A, Nilsson JA, Cordon-Cardo C, Cleveland JL, Tansey WP, Lowe SW (2005) Evasion of the p53 tumour surveillance network by tumour-derived MYC mutants. *Nature* **436**(7052)**:** 807-811

Henriksson M, Bakardjiev A, Klein G, Luscher B (1993) Phosphorylation sites mapping in the N-terminal domain of c-myc modulate its transforming potential. *Oncogene* **8**(12)**:** 3199-3209

Hermeking H, Rago C, Schuhmacher M, Li Q, Barrett JF, Obaya AJ, O'Connell BC, Mateyak MK, Tam W, Kohlhuber F, Dang CV, Sedivy JM, Eick D, Vogelstein B, Kinzler KW (2000) Identification of CDK4 as a target of c-MYC. *Proceedings of the National Academy of Sciences of the United States of America* **97**(5)**:** 2229-2234

Hoang AT, Lutterbach B, Lewis BC, Yano T, Chou TY, Barrett JF, Raffeld M, Hann SR, Dang CV (1995) A link between increased transforming activity of lymphoma-derived MYC mutant alleles, their defective regulation by p107, and altered phosphorylation of the c-Myc transactivation domain. *Molecular and Cellular Biology* **15**(8)**:** 4031-4042

Holt JT, Redner RL, Nienhuis AW (1988) An oligomer complementary to c-myc mRNA inhibits proliferation of HL-60 promyelocytic cells and induces differentiation. *Molecular and Cellular Biology* **8**(2)**:** 963-973

Hsu W, Shakya R, Costantini F (2001) Impaired mammary gland and lymphoid development caused by inducible expression of Axin in transgenic mice. *The Journal of Cell Biology* **155**(6)**:** 1055-1064

Huang SM, Mishina YM, Liu S, Cheung A, Stegmeier F, Michaud GA, Charlat O, Wiellette E, Zhang Y, Wiessner S, Hild M, Shi X, Wilson CJ, Mickanin C, Myer V, Fazal A, Tomlinson R, Serluca F, Shao W, Cheng H, Shultz M, Rau C, Schirle M, Schlegl J, Ghidelli S, Fawell S, Lu C, Curtis D, Kirschner MW, Lengauer C, Finan PM, Tallarico JA, Bouwmeester T, Porter JA, Bauer A, Cong F (2009) Tankyrase inhibition stabilizes axin and antagonizes Wnt signalling. *Nature* **461**(7264)**:** 614-620

Hung C-Y, Yu J-J, Seshan K, Reichard U, Cole G (2002) A parasitic phase-specific adhesin of Coccidioides immitis contributes to the virulence of this respiratory Fungal pathogen. *Infection and Immunity* **70**(7)**:** 3443-3456

Hurlin P, Huang J (2006) The MAX-interacting transcription factor network. *Seminars in Cancer Biology* **16**(4)**:** 265-274

Hydbring P, Bahram F, Su Y, Tronnersjo S, Hogstrand K, von der Lehr N, Sharifi HR, Lilischkis R, Hein N, Wu S, Vervoorts J, Henriksson M, Grandien A, Luscher B, Larsson L-G (2010) Phosphorylation by Cdk2 is required for Myc to repress Ras-induced senescence in cotransformation. *Proceedings of the National Academy of Sciences of the United States of America* **107**(1)**:** 58-63

Ikeda S, Kishida S, Yamamoto H, Murai H, Koyama S, Kikuchi A (1998) Axin, a negative regulator of the Wnt signaling pathway, forms a complex with GSK-3beta and beta-catenin and promotes GSK-3beta-dependent phosphorylation of beta-catenin. *The EMBO Journal* **17**(5)**:** 1371-1384

Iritani BM, Eisenman RN (1999) c-Myc enhances protein synthesis and cell size during B lymphocyte development. *Proceedings of the National Academy of Sciences of the United States of America* **96**(23)**:** 13180-13185

Jackson EL, Willis N, Mercer K, Bronson RT, Crowley D, Montoya R, Jacks T, Tuveson DA (2001) Analysis of lung tumor initiation and progression using conditional expression of oncogenic K-ras. *Genes & Development* **15**(24)**:** 3243-3248

Jacobsen KA, Prasad VS, Sidman CL, Osmond DG (1994) Apoptosis and macrophage-mediated deletion of precursor B cells in the bone marrow of E mu-myc transgenic mice. *Blood* **84**(8)**:** 2784-2794

Jayapal SR, Lee KL, Ji P, Kaldis P, Lim B, Lodish H (2010) Down-regulation of Myc is essential for terminal erythroid maturation. *The Journal of Biological Chemistry* **285**(51)**:** 40252-40265

Jones TR, Cole MD (1987) Rapid cytoplasmic turnover of c-myc mRNA: requirement of the 3' untranslated sequences. *Molecular and Cellular Biology* **7**(12)**:** 4513-4521

Junttila M, Puustinen P, Niemela M, Ahola R, Arnold H, Bottzauw T, Ala-aho R, Nielsen C, Ivaska J, Taya Y, Lu S-L, Lin S, Chan E, Wang X-J, Grenman R, Kast J, Kallunki T, Sears R, Kahari V-M, Westermarck J (2007) CIP2A inhibits PP2A in human malignancies. *Cell* **130**(1)**:** 51-62

Kelly K, Cochran BH, Stiles CD, Leder P (1983) Cell-specific regulation of the c-myc gene by lymphocyte mitogens and platelet-derived growth factor. *Cell* **35**(3 Pt 2)**:** 603-610

Kim HH, Kuwano Y, Srikantan S, Lee EK, Martindale J, Gorospe M (2009) HuR recruits let-7/RISC to repress c-Myc expression. *Genes & Development* **23**(15)**:** 1743-1748

Kim K-T, Baird K, Ahn J-Y, Meltzer P, Lilly M, Levis M, Small D (2005) Pim-1 is up-regulated by constitutively activated FLT3 and plays a role in FLT3-mediated cell survival. *Blood* **105**(4)**:** 1759-1767

Kim S, Li Q, Dang CV, Lee LA (2000) Induction of ribosomal genes and hepatocyte hypertrophy by adenovirus-mediated expression of c-Myc in vivo. *Proceedings of the National Academy of Sciences of the United States of America* **97**(21)**:** 11198-11202

Kim SY, Herbst A, Tworkowski KA, Salghetti SE, Tansey WP (2003) Skp2 regulates Myc protein stability and activity. *Molecular Cell* **11**(5)**:** 1177-1188

Kinzler KW, Vogelstein B (1996) Lessons from hereditary colorectal cancer. *Cell* **87**(2)**:** 159-170

Kirkland TN, Finley F, Orsborn KI, Galgiani JN (1998) Evaluation of the proline-rich antigen of Coccidioides immitis as a vaccine candidate in mice. *Infection and Immunity* **66**(8)**:** 3519-3522

Kiyoi H, Towatari M, Yokota S, Hamaguchi M, Ohno R, Saito H, Naoe T (1998) Internal tandem duplication of the FLT3 gene is a novel modality of elongation mutation which causes constitutive activation of the product. *Leukemia* **12**(9)**:** 1333-1337

Kumar M, Lu J, Mercer K, Golub T, Jacks T (2007) Impaired microRNA processing enhances cellular transformation and tumorigenesis. *Nature Genetics* **39**(5)**:** 673-677

Kurihara T, Ikeda S, Ishizaki Y, Fujimori M, Tokumoto N, Hirata Y, Ozaki S, Okajima M, Sugino K, Asahara T (2004) Immunohistochemical and sequencing analyses of the Wnt signaling components in Japanese anaplastic thyroid cancers. *Thyroid : official journal of the American Thyroid Association* **14**(12)**:** 1020-1029

Larsson LG, Ivhed I, Gidlund M, Pettersson U, Vennstrom B, Nilsson K (1988) Phorbol ester-induced terminal differentiation is inhibited in human U-937 monoblastic cells expressing a v-myc oncogene. *Proceedings of the National Academy of Sciences of the United States of America* **85**(8)**:** 2638-2642

Larsson LG, Pettersson M, Oberg F, Nilsson K, Luscher B (1994) Expression of mad, mxi1, max and c-myc during induced differentiation of hematopoietic cells: opposite regulation of mad and c-myc. *Oncogene* **9**(4)**:** 1247-1252

Latres E, Chiarle R, Schulman BA, Pavletich NP, Pellicer A, Inghirami G, Pagano M (2001) Role of the F-box protein Skp2 in lymphomagenesis. *Proceedings of the National Academy of Sciences of the United States of America* **98**(5)**:** 2515-2520

Laurenti E, Varnum-Finney B, Wilson A, Ferrero I, Blanco-Bose WE, Ehninger A, Knoepfler PS, Cheng PF, MacDonald HR, Eisenman RN, Bernstein ID, Trumpp A (2008) Hematopoietic stem cell function and survival depend on c-Myc and N-Myc activity. *Cell Stem Cell* **3**(6)**:** 611-624

Lee CM, Reddy EP (1999) The v-myc oncogene. *Oncogene* **18**(19)**:** 2997-3003

Lee E, Salic A, Kruger R, Heinrich R, Kirschner MW (2003) The roles of APC and Axin derived from experimental and theoretical analysis of the Wnt pathway. *PLoS Biol* **1**(1)

Lee J, Soung Y, Kim S, Nam S, Park W, Lee J, Yoo N, Lee S (2006) Mutational analysis of MYC in common epithelial cancers and acute leukemias. *APMIS* **114**(6)**:** 436-439

Lee S, Kim M, Lim J, Kim Y, Han K, Kim HJ, Cho SG, Min WS (2009) Acute myeloid leukemia with MYC amplification in the homogeneous staining regions and double minutes. *Cancer Genetics and Cytogenetics* **192**(2)**:** 96-98

Leone G, DeGregori J, Sears R, Jakoi L, Nevins JR (1997) Myc and Ras collaborate in inducing accumulation of active cyclin E/Cdk2 and E2F. *Nature* **387**(6631)**:** 422-426

Li J, Lin Q, Wang W, Wade P, Wong J (2002) Specific targeting and constitutive association of histone deacetylase complexes during transcriptional repression. *Genes & Development* **16**(6)**:** 687-692

Li M, Makkinje A, Damuni Z (1996) The myeloid leukemia-associated protein SET is a potent inhibitor of protein phosphatase 2A. *The Journal of Biological Chemistry* **271**(19)**:** 11059-11062

Li Q, Lin S, Wang X, Lian G, Lu Z, Guo H, Ruan K, Wang Y, Ye Z, Han J, Lin SC (2009) Axin determines cell fate by controlling the p53 activation threshold after DNA damage. *Nature Cell Biology* **11**(9)**:** 1128-1134

Li Z, Boone D, Hann S (2008) Nucleophosmin interacts directly with c-Myc and controls c-Myc-induced hyperproliferation and transformation. *Proceedings of the National Academy of Sciences of the United States of America* **105**(48)**:** 18794-18799

Li Z, Van Calcar S, Qu C, Cavenee W, Zhang M, Ren B (2003) A global transcriptional regulatory role for c-Myc in Burkitt's lymphoma cells. *Proceedings of the National Academy of Sciences of the United States of America* **100**(14)**:** 8164-8169

Liu W, Rui H, Wang J, Lin S, He Y, Chen M, Li Q, Ye Z, Zhang S, Chan SC, Chen Y-G, Han J, Lin S-C (2006) Axin is a scaffold protein in TGF-beta signaling that promotes degradation of Smad7 by Arkadia. *The EMBO Journal* **25**(8)**:** 1646-1658

Lowenberg B, Downing JR, Burnett A (1999) Acute myeloid leukemia. *The New England Journal of Medicine* **341**(14)**:** 1051-1062

Lucas C, Harris R, Giannoudis A, Copland M, Slupsky J, Clark R (2011) Cancerous inhibitor of PP2A (CIP2A) at diagnosis of chronic myeloid leukemia is a critical determinant of disease progression. *Blood* **117**(24)**:** 6660-6668

Lutterbach B, Hann SR (1994) Hierarchical phosphorylation at N-terminal transformation-sensitive sites in c-Myc protein is regulated by mitogens and in mitosis. *Molecular and Cellular Biology* **14**(8)**:** 5510-5522

Maggi L, Kuchenruether M, Dadey D, Schwope R, Grisendi S, Townsend R, Pandolfi PP, Weber J (2008) Nucleophosmin serves as a rate-limiting nuclear export chaperone for the Mammalian ribosome. *Molecular and Cellular Biology* **28**(23)**:** 7050-7065

Malempati S, Tibbitts D, Cunningham M, Akkari Y, Olson S, Fan G, Sears RC (2006) Aberrant stabilization of c-Myc protein in some lymphoblastic leukemias. *Leukemia* **20**(9)**:** 1572-1581

Malynn BA, de Alboran IM, O'Hagan RC, Bronson R, Davidson L, DePinho RA, Alt FW (2000) N-myc can functionally replace c-myc in murine development, cellular growth, and differentiation. *Genes & Development* **14**(11)**:** 1390-1399

Mao J, Wang J, Liu B, Pan W, Farr GH, Flynn C, Yuan H, Takada S, Kimelman D, Li L, Wu D (2001) Low-density lipoprotein receptor-related protein-5 binds to Axin and regulates the canonical Wnt signaling pathway. *Molecular Cell* **7**(4)**:** 801-809

Marhin WW, Chen S, Facchini LM, Fornace AJ, Penn LZ (1997) Myc represses the growth arrest gene gadd45. *Oncogene* **14**(23)**:** 2825-2834

Martelli MP, Pettirossi V, Thiede C, Bonifacio E, Mezzasoma F, Cecchini D, Pacini R, Tabarrini A, Ciurnelli R, Gionfriddo I, Manes N, Rossi R, Giunchi L, Oelschlagel U, Brunetti L, Gemei M, Delia M, Specchia G, Liso A, Di Ianni M, Di Raimondo F, Falzetti F, Del Vecchio L, Martelli M, Falini B (2010) CD34+ cells

from AML with mutated NPM1 harbor cytoplasmic mutated nucleophosmin and generate leukemia in immunocompromised mice. *Blood* **116**(19)**:** 3907-3922

Mateyak MK, Obaya AJ, Adachi S, Sedivy JM (1997) Phenotypes of c-Myc-deficient rat fibroblasts isolated by targeted homologous recombination. *Cell Growth & Differentiation* **8**(10)**:** 1039-1048

Mathew S, Lorsbach RB, Shearer P, Sandlund JT, Raimondi SC (2000) Double minute chromosomes and c-MYC amplification in a child with secondary myelodysplastic syndrome after treatment for acute lymphoblastic leukemia. *Leukemia* **14**(7)**:** 1314-1315

Matsuoka Y, Nagahara Y, Ikekita M, Shinomiya T (2003) A novel immunosuppressive agent FTY720 induced Akt dephosphorylation in leukemia cells. *British Journal of Pharmacology* **138**(7)**:** 1303-1312

Mavrakis K, Wolfe A, Oricchio E, Palomero T, de Keersmaecker K, McJunkin K, Zuber J, James T, Khan A, Leslie C, Parker J, Paddison P, Tam W, Ferrando A, Wendel H-G (2010) Genome-wide RNA-mediated interference screen identifies miR-19 targets in Notch-induced T-cell acute lymphoblastic leukaemia. *Nature Cell Biology* **12**(4)**:** 372-379

McMahon SB, Wood MA, Cole MD (2000) The essential cofactor TRRAP recruits the histone acetyltransferase hGCN5 to c-Myc. *Molecular and Cellular Biology* **20**(2)**:** 556-562

McManus EJ, Sakamoto K, Armit LJ, Ronaldson L, Shpiro N, Marquez R, Alessi DR (2005) Role that phosphorylation of GSK3 plays in insulin and Wnt signalling defined by knockin analysis. *The EMBO Journal* **24**(8)**:** 1571-1583

Meyer N, Penn LZ (2008) Reflecting on 25 years with MYC. *Nature Reviews Cancer* **8**(12)**:** 976-990

Muller-Tidow C, Steffen B, Cauvet T, Tickenbrock L, Ji P, Diederichs S, Sargin B, Kohler G, Stelljes M, Puccetti E, Ruthardt M, deVos S, Hiebert S, Koeffler P, Berdel W, Serve H (2004) Translocation products in acute myeloid leukemia activate the Wnt signaling pathway in hematopoietic cells. *Molecular and cellular biology* **24**(7)**:** 2890-2904

Murphy MJ, Wilson A, Trumpp A (2005) More than just proliferation: Myc function in stem cells. *Trends in Cell Biology* **15**(3)**:** 128-137

Nakajima M, Fukuchi M, Miyazaki T, Masuda N, Kato H, Kuwano H (2003) Reduced expression of Axin correlates with tumour progression of oesophageal squamous cell carcinoma. *British Journal of Cancer* **88**(11)**:** 1734-1739

Nesbit CE, Tersak JM, Prochownik EV (1999) MYC oncogenes and human neoplastic disease. *Oncogene* **18**(19)**:** 3004-3016

Neviani P, Santhanam R, Oaks JJ, Eiring AM, Notari M, Blaser BW, Liu S, Trotta R, Muthusamy N, Gambacorti-Passerini C, Druker BJ, Cortes J, Marcucci G, Chen CS, Verrills NM, Roy DC, Caligiuri MA, Bloomfield CD, Byrd JC, Perrotti D (2007) FTY720, a new alternative for treating blast crisis chronic myelogenous leukemia and Philadelphia chromosome-positive acute lymphocytic leukemia. *The Journal of Clinical Investigation* **117**(9)**:** 2408-2421

Neviani P, Santhanam R, Trotta R, Notari M, Blaser B, Liu S, Mao H, Chang JS, Galietta A, Uttam A, Roy D, Valtieri M, Bruner-Klisovic R, Caligiuri M, Bloomfield C, Marcucci G, Perrotti D (2005) The tumor suppressor PP2A is functionally inactivated in blast crisis CML through the inhibitory activity of the BCR/ABL-regulated SET protein. *Cancer Cell* **8**(5)**:** 355-368

Nguyen HQ, Selvakumaran M, Liebermann DA, Hoffman B (1995) Blocking c-Myc and Max expression inhibits proliferation and induces differentiation of normal and leukemic myeloid cells. *Oncogene* **11**(11)**:** 2439-2444

Niklinski J, Claassen G, Meyers C, Gregory MA, Allegra CJ, Kaye FJ, Hann SR, Zajac-Kaye M (2000) Disruption of Myc-tubulin interaction by hyperphosphorylation of c-Myc during mitosis or by constitutive hyperphosphorylation of mutant c-Myc in Burkitt's lymphoma. *Molecular and Cellular Biology* **20**(14)**:** 5276-5284

Novershtern N, Subramanian A, Lawton LN, Mak RH, Haining WN, McConkey ME, Habib N, Yosef N, Chang CY, Shay T, Frampton GM, Drake AC, Leskov I, Nilsson B, Preffer F, Dombkowski D, Evans JW, Liefeld T, Smutko JS, Chen J, Friedman N, Young RA, Golub TR, Regev A, Ebert BL (2011) Densely interconnected transcriptional circuits control cell states in human hematopoiesis. *Cell* **144**(2)**:** 296-309

O'Neil J, Grim J, Strack P, Rao S, Tibbitts D, Winter C, Hardwick J, Welcker M, Meijerink J, Pieters R, Draetta G, Sears R, Clurman B, Look T (2007) FBW7 mutations in leukemic cells mediate NOTCH pathway activation and resistance to gamma-secretase inhibitors. *The Journal of Experimental Medicine* **204**(8)**:** 1813-1824

Orian A, van Steensel B, Delrow J, Bussemaker H, Li L, Sawado T, Williams E, Loo L, Cowley S, Yost C, Pierce S, Edgar B, Parkhurst S, Eisenman R (2003) Genomic binding by the Drosophila Myc, Max, Mad/Mnt transcription factor network. *Genes & Development* **17**(9)**:** 1101-1114

Padmanabhan S, Mukhopadhyay A, Narasimhan SD, Tesz G, Czech M, Tissenbaum H (2009) A PP2A regulatory subunit regulates C. elegans

insulin/IGF-1 signaling by modulating AKT-1 phosphorylation. *Cell* **136**(5): 939-951

Patschinsky T, Jansen HW, Blocker H, Frank R, Bister K (1986) Structure and transforming function of transduced mutant alleles of the chicken c-myc gene. *Journal of Virology* **59**(2): 341-353

Paulsson K, Lassen C, Kuric N, Billstrom R, Fioretos T, Tanke HJ, Johansson B (2003) MYC is not overexpressed in a case of chronic myelomonocytic leukemia with MYC-containing double minutes. *Leukemia* **17**(4): 813-815

Perez-Roger I, Solomon DL, Sewing A, Land H (1997) Myc activation of cyclin E/Cdk2 kinase involves induction of cyclin E gene transcription and inhibition of p27(Kip1) binding to newly formed complexes. *Oncogene* **14**(20): 2373-2381

Peukert K, Staller P, Schneider A, Carmichael G, Hanel F, Eilers M (1997) An alternative pathway for gene regulation by Myc. *The EMBO Journal* **16**(18): 5672-5686

Popov N, Schulein C, Jaenicke L, Eilers M (2010) Ubiquitylation of the amino terminus of Myc by SCF(beta-TrCP) antagonizes SCF(Fbw7)-mediated turnover. *Nature cell biology* **12**(10): 973-981

Popov N, Wanzel M, Madiredjo M, Zhang D, Beijersbergen R, Bernards R, Moll R, Elledge S, Eilers M (2007) The ubiquitin-specific protease USP28 is required for MYC stability. *Nature Cell Biology* **9**(7): 765-774

Proft T, Hilbert H, Layh-Schmitt G, Herrmann R (1995) The proline-rich P65 protein of Mycoplasma pneumoniae is a component of the Triton X-100-insoluble fraction and exhibits size polymorphism in the strains M129 and FH. *Journal of Bacteriology* **177**(12): 3370-3378

Pulverer BJ, Fisher C, Vousden K, Littlewood T, Evan G, Woodgett JR (1994) Site-specific modulation of c-Myc cotransformation by residues phosphorylated in vivo. *Oncogene* **9**(1): 59-70

Rao PH, Houldsworth J, Dyomina K, Parsa NZ, Cigudosa JC, Louie DC, Popplewell L, Offit K, Jhanwar SC, Chaganti RS (1998) Chromosomal and gene amplification in diffuse large B-cell lymphoma. *Blood* **92**(1): 234-240

Reavie L, Della Gatta G, Crusio K, Aranda-Orgilles B, Buckley SM, Thompson B, Lee E, Gao J, Bredemeyer AL, Helmink BA, Zavadil J, Sleckman BP, Palomero T, Ferrando A, Aifantis I (2010) Regulation of hematopoietic stem cell differentiation by a single ubiquitin ligase-substrate complex. *Nature Immunology* **11**(3): 207-215

References

Renneville A, Roumier C, Biggio V, Nibourel O, Boissel N, Fenaux P, Preudhomme C (2008) Cooperating gene mutations in acute myeloid leukemia: a review of the literature. *Leukemia* **22**(5)**:** 915-931

Rice K, Hormaeche I, Doulatov S, Flatow J, Grimwade D, Mills K, Leiva M, Ablain J, Ambardekar C, McConnell M, Dick J, Licht J (2009) Comprehensive genomic screens identify a role for PLZF-RARalpha as a positive regulator of cell proliferation via direct regulation of c-MYC. *Blood* **114**(27)**:** 5499-5511

Roberts K, Smith A, McDougall F, Carpenter H, Horan M, Neviani P, Powell J, Thomas D, Guthridge M, Perrotti D, Sim A, Ashman L, Verrills N (2010) Essential requirement for PP2A inhibition by the oncogenic receptor c-KIT suggests PP2A reactivation as a strategy to treat c-KIT+ cancers. *Cancer Research* **70**(13)**:** 5438-5447

Rodgers JT, Vogel RO, Puigserver P (2011) Clk2 and B56beta mediate insulin-regulated assembly of the PP2A phosphatase holoenzyme complex on Akt. *Molecular Cell* **41**(4)**:** 471-479

Salahshor S, Woodgett JR (2005) The links between axin and carcinogenesis. *Journal of Clinical Pathology* **58**(3)**:** 225-236

Salghetti SE, Kim SY, Tansey WP (1999) Destruction of Myc by ubiquitin-mediated proteolysis: cancer-associated and transforming mutations stabilize Myc. *The EMBO Journal* **18**(3)**:** 717-726

Sarid J, Halazonetis TD, Murphy W, Leder P (1987) Evolutionarily conserved regions of the human c-myc protein can be uncoupled from transforming activity. *Proceedings of the National Academy of Sciences of the United States of America* **84**(1)**:** 170-173

Schlosser I, Holzel M, Murnseer M, Burtscher H, Weidle U, Eick D (2003) A role for c-Myc in the regulation of ribosomal RNA processing. *Nucleic Acids Research* **31**(21)**:** 6148-6156

Schmitt CA, McCurrach ME, de Stanchina E, Wallace-Brodeur RR, Lowe SW (1999) INK4a/ARF mutations accelerate lymphomagenesis and promote chemoresistance by disabling p53. *Genes & Development* **13**(20)**:** 2670-2677

Schreiber-Agus N, Chin L, Chen K, Torres R, Rao G, Guida P, Skoultchi AI, DePinho RA (1995) An amino-terminal domain of Mxi1 mediates anti-Myc oncogenic activity and interacts with a homolog of the yeast transcriptional repressor SIN3. *Cell* **80**(5)**:** 777-786

Schuhmacher M, Kohlhuber F, Holzel M, Kaiser C, Burtscher H, Jarsch M, Bornkamm GW, Laux G, Polack A, Weidle UH, Eick D (2001) The transcriptional

program of a human B cell line in response to Myc. *Nucleic Acids Research* **29**(2)**:** 397-406

Schuhmacher M, Staege MS, Pajic A, Polack A, Weidle UH, Bornkamm GW, Eick D, Kohlhuber F (1999) Control of cell growth by c-Myc in the absence of cell division. *Current Biology* **9**(21)**:** 1255-1258

Sears R, Leone G, DeGregori J, Nevins JR (1999) Ras enhances Myc protein stability. *Molecular Cell* **3**(2)**:** 169-179

Sears R, Nuckolls F, Haura E, Taya Y, Tamai K, Nevins JR (2000) Multiple Ras-dependent phosphorylation pathways regulate Myc protein stability. *Genes & Development* **14**(19)**:** 2501-2514

Sears R, Ohtani K, Nevins JR (1997) Identification of positively and negatively acting elements regulating expression of the E2F2 gene in response to cell growth signals. *Molecular and Cellular Biology* **17**(9)**:** 5227-5235

Seoane J, Pouponnot C, Staller P, Schader M, Eilers M, Massague J (2001) TGFbeta influences Myc, Miz-1 and Smad to control the CDK inhibitor p15INK4b. *Nature Cell Biology* **3**(4)**:** 400-408

Shima EA, Le Beau MM, McKeithan TW, Minowada J, Showe LC, Mak TW, Minden MD, Rowley JD, Diaz MO (1986) Gene encoding the alpha chain of the T-cell receptor is moved immediately downstream of c-myc in a chromosomal 8;14 translocation in a cell line from a human T-cell leukemia. *Proceedings of the National Academy of Sciences of the United States of America* **83**(10)**:** 3439-3443

Smith DP, Bath ML, Metcalf D, Harris AW, Cory S (2006) MYC levels govern hematopoietic tumor type and latency in transgenic mice. *Blood* **108**(2)**:** 653-661

Soucek L, Whitfield J, Martins C, Finch A, Murphy D, Sodir N, Karnezis A, Swigart LB, Nasi S, Evan G (2008) Modelling Myc inhibition as a cancer therapy. *Nature* **455**(7213)**:** 679-683

Staller P, Peukert K, Kiermaier A, Seoane J, Lukas J, Karsunky H, Moroy T, Bartek J, Massague J, Hanel F, Eilers M (2001) Repression of p15INK4b expression by Myc through association with Miz-1. *Nature Cell Biology* **3**(4)**:** 392-399

Stanton BR, Perkins AS, Tessarollo L, Sassoon DA, Parada LF (1992) Loss of N-myc function results in embryonic lethality and failure of the epithelial component of the embryo to develop. *Genes & Development* **6**(12A)**:** 2235-2247

Stasik CJ, Nitta H, Zhang W, Mosher CH, Cook JR, Tubbs RR, Unger JM, Brooks TA, Persky DO, Wilkinson ST, Grogan TM, Rimsza LM (2010) Increased MYC gene copy number correlates with increased mRNA levels in diffuse large B-cell lymphoma. *Haematologica* **95**(4)**:** 597-603

Steiger D, Furrer M, Schwinkendorf D, Gallant P (2008) Max-independent functions of Myc in Drosophila melanogaster. *Nature Genetics* **40**(9)**:** 1084-1091

Storlazzi CT, Fioretos T, Surace C, Lonoce A, Mastrorilli A, Strombeck B, D'Addabbo P, Iacovelli F, Minervini C, Aventin A, Dastugue N, Fonatsch C, Hagemeijer A, Jotterand M, Muhlematter D, Lafage-Pochitaloff M, Nguyen-Khac F, Schoch C, Slovak M, Smith A, Sole F, Van Roy N, Johansson B, Rocchi M (2006) MYC-containing double minutes in hematologic malignancies: evidence in favor of the episome model and exclusion of MYC as the target gene. *Human Molecular Genetics* **15**(6)**:** 933-942

Strasser A, Harris AW, Bath ML, Cory S (1990) Novel primitive lymphoid tumours induced in transgenic mice by cooperation between myc and bcl-2. *Nature* **348**(6299)**:** 331-333

Switzer CH, Cheng RY, Vitek TM, Christensen DJ, Wink DA, Vitek MP (2011) Targeting SET/I(2)PP2A oncoprotein functions as a multi-pathway strategy for cancer therapy. *Oncogene* **30**(22)**:** 2504-2513

Symonds G, Hartshorn A, Kennewell A, O'Mara MA, Bruskin A, Bishop JM (1989) Transformation of murine myelomonocytic cells by myc: point mutations in v-myc contribute synergistically to transforming potential. *Oncogene* **4**(3)**:** 285-294

Takayama N, Nishimura S, Nakamura S, Shimizu T, Ohnishi R, Endo H, Yamaguchi T, Otsu M, Nishimura K, Nakanishi M, Sawaguchi A, Nagai R, Takahashi K, Yamanaka S, Nakauchi H, Eto K (2010) Transient activation of c-MYC expression is critical for efficient platelet generation from human induced pluripotent stem cells. *The Journal of Experimental Medicine* **207**(13)**:** 2817-2830

Tallman MS, Gilliland DG, Rowe JM (2005) Drug therapy for acute myeloid leukemia. *Blood* **106**(4)**:** 1154-1163

Tesio M, Gammaitoni L, Gunetti M, Leuci V, Pignochino Y, Jordaney N, Capellero S, Cammarata C, Caione L, Migliaretti G, Fagioli F, Tabilio A, Aglietta M, Piacibello W (2008) Sustained Long-Term Engraftment and Transgene Expression of Peripheral Blood CD34+ Cells Transduced with Third-Generation Lentiviral Vectors. *Stem Cells* **26**(6)**:** 1620-1627

Thomas NE (2006) BRAF somatic mutations in malignant melanoma and melanocytic naevi. *Melanoma Research* **16**(2)**:** 97-103

Thompson B, Buonamici S, Sulis ML, Palomero T, Vilimas T, Basso G, Ferrando A, Aifantis I (2007) The SCFFBW7 ubiquitin ligase complex as a tumor suppressor in T cell leukemia. *The Journal of Experimental Medicine* **204**(8)**:** 1825-1835

Trumpp A, Refaeli Y, Oskarsson T, Gasser S, Murphy M, Martin GR, Bishop JM (2001) c-Myc regulates mammalian body size by controlling cell number but not cell size. *Nature* **414**(6865)**:** 768-773

Vennstrom B, Sheiness D, Zabielski J, Bishop JM (1982) Isolation and characterization of c-myc, a cellular homolog of the oncogene (v-myc) of avian myelocytomatosis virus strain 29. *Journal of Virology* **42**(3)**:** 773-779

Vita M, Henriksson M (2006) The Myc oncoprotein as a therapeutic target for human cancer. *Seminars in Cancer Biology* **16**(4)**:** 318-330

von der Lehr N, Johansson S, Wu S, Bahram F, Castell A, Cetinkaya C, Hydbring P, Weidung I, Nakayama K, Nakayama KI, Suderberg O, Kerppola TK, Larsson LG (2003) The F-box protein Skp2 participates in c-Myc proteosomal degradation and acts as a cofactor for c-Myc-regulated transcription. *Molecular Cell* **11**(5)**:** 1189-1200

Wall M, Poortinga G, Hannan K, Pearson R, Hannan R, McArthur G (2008) Translational control of c-MYC by rapamycin promotes terminal myeloid differentiation. *Blood* **112**(6)**:** 2305-2317

Webster MT, Rozycka M, Sara E, Davis E, Smalley M, Young N, Dale TC, Wooster R (2000) Sequence variants of the axin gene in breast, colon, and other cancers: an analysis of mutations that interfere with GSK3 binding. *Genes, Chromosomes & Cancer* **28**(4)**:** 443-453

Welcker M, Orian A, Jin J, Grim J, Harper W, Eisenman R, Clurman B (2004) The Fbw7 tumor suppressor regulates glycogen synthase kinase 3 phosphorylation-dependent c-Myc protein degradation. *Proceedings of the National Academy of Sciences of the United States of America* **101**(24)**:** 9085-9090

Weng A, Ferrando A, Lee W, Morris J, Silverman L, Sanchez-Irizarry C, Blacklow S, Look T, Aster J (2004) Activating Mutations of NOTCH1 in Human T Cell Acute Lymphoblastic Leukemia. *Science* **306**(5694)**:** 269-271

Weng A, Millholland J, Yashiro-Ohtani Y, Arcangeli M, Lau A, Wai C, del Bianco C, Rodriguez C, Sai H, Tobias J, Li Y, Wolfe M, Shachaf C, Felsher D, Blacklow S, Pear W, Aster J (2006) c-Myc is an important direct target of Notch1 in T-cell

acute lymphoblastic leukemia/lymphoma. *Genes & Development* **20**(15)**:** 2096-2109

Wierstra I, Alves J (2008) The c-myc promoter: still MysterY and challenge. *Advances in Cancer Research* **99:** 113-333

Williamson MP (1994) The structure and function of proline-rich regions in proteins. *The Biochemical Journal* **297 (Pt 2):** 249-260

Wilson A, Laurenti E, Oser G, van der Wath R, Blanco-Bose W, Jaworski M, Offner S, Dunant C, Eshkind L, Bockamp E, Lio P, Macdonald R, Trumpp A (2008) Hematopoietic stem cells reversibly switch from dormancy to self-renewal during homeostasis and repair. *Cell* **135**(6)**:** 1118-1129

Wilson A, Murphy M, Oskarsson T, Kaloulis K, Bettess M, Oser G, Pasche A-C, Knabenhans C, Macdonald R, Trumpp A (2004) c-Myc controls the balance between hematopoietic stem cell self-renewal and differentiation. *Genes & Development* **18**(22)**:** 2747-2763

Wu S, Cetinkaya C, Munoz-Alonso M, von der Lehr N, Bahram F, Beuger V, Eilers M, Leon J, Larsson L-G (2003) Myc represses differentiation-induced p21CIP1 expression via Miz-1-dependent interaction with the p21 core promoter. *Oncogene* **22**(3)**:** 351-360

Xu HT, Wang L, Lin D, Liu Y, Liu N, Yuan XM, Wang EH (2006) Abnormal beta-catenin and reduced axin expression are associated with poor differentiation and progression in non-small cell lung cancer. *American Journal of Clinical Pathology* **125**(4)**:** 534-541

Yada M, Hatakeyama S, Kamura T, Nishiyama M, Tsunematsu R, Imaki H, Ishida N, Okumura F, Nakayama K, Nakayama K (2004) Phosphorylation-dependent degradation of c-Myc is mediated by the F-box protein Fbw7. *The EMBO Journal* **23**(10)**:** 2116-2125

Yeh E, Cunningham M, Arnold H, Chasse D, Monteith T, Ivaldi G, Hahn WC, Stukenberg PT, Shenolikar S, Uchida T, Counter CM, Nevins JR, Means AR, Sears R (2004) A signalling pathway controlling c-Myc degradation that impacts oncogenic transformation of human cells. *Nature Cell Biology* **6**(4)**:** 308-318

Zarrinkar P, Gunawardane R, Cramer M, Gardner M, Brigham D, Belli B, Karaman M, Pratz K, Pallares G, Chao Q, Sprankle K, Patel H, Levis M, Armstrong R, James J, Bhagwat S (2009) AC220 is a uniquely potent and selective inhibitor of FLT3 for the treatment of acute myeloid leukemia (AML). *Blood* **114**(14)**:** 2984-2992

References

Zeller K, Zhao X, Lee C, Chiu KP, Yao F, Yustein J, Ooi HS, Orlov Y, Shahab A, Yong HC, Fu Y, Weng Z, Kuznetsov V, Sung W-K, Ruan Y, Dang C, Wei C-L (2006) Global mapping of c-Myc binding sites and target gene networks in human B cells. *Proceedings of the National Academy of Sciences of the United States of America* **103**(47)**:** 17834-17839

Zeller KI, Haggerty TJ, Barrett JF, Guo Q, Wonsey DR, Dang CV (2001) Characterization of nucleophosmin (B23) as a Myc target by scanning chromatin immunoprecipitation. *The Journal of Biological Chemistry* **276**(51)**:** 48285-48291

Zhang X, Farrell AS, Daniel CJ, Arnold H, Scanlan C, Laraway BJ, Janghorban M, Lum L, Chen D, Troxell M, Sears R (2011) Breast Cancer Special Feature: Mechanistic insight into Myc stabilization in breast cancer involving aberrant Axin1 expression. *Proceedings of the National Academy of Sciences of the United States of America*

Zhang Y, Wang Z, Li X, Magnuson NS (2008) Pim kinase-dependent inhibition of c-Myc degradation. *Oncogene* **27**(35)**:** 4809-4819